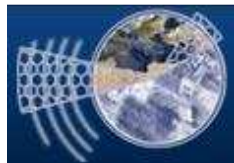




**Technological Educational Institute of
Crete**

School of Applied Technology

Department of Applied Informatics & Multimedia



Final Paper

Title:

Non-linear Dynamics and Chaos

Nikos Kounalakis (1403)

Supervisor Professor: G. Papadourakis

Abstract

The purpose of this study is the presentation of the basic concepts, techniques and approaches to problems of nonlinear dynamics theory or better known as chaos theory. The approach is more theoretical but can be applied to a big variety of systems, most of them found in nature, that may in first sight have no relation or similarity. Understanding the dynamics of those systems is very important in many sciences like biology, chemistry, signal processing, telecommunications and many more in order to make conclusions about the behavior of the system. Most of the examples presented here are real applications and often famous systems due to their founders like the Lorenz equation and the logistic map. Specifically, the first 2 chapters are introductory and include some history on the field and its pioneers and the second is about system representation and also some terminology is provided in order to continue the study. The third chapter is about stability and bifurcation theory adjusted to nonlinear systems. It provides definitions and the standard methods to determine stability and bifurcations. The 4th chapter is about fractal geometry developed to study chaotic attractors which can be viewed as geometrical objects. Euclidean geometry is not enough to characterize these objects. In this chapter the fractal geometry and dimension are introduced. In chapters 5 and 6 the aforementioned concepts are organized in an analytical and statistical way in order to be used to make conclusions about real systems. Chaos theory is a relatively new field of science and although very interesting, it is also complicated in many ways. Although the theory can be applied to almost any system in nature, it remains bounded to complicated mathematical analysis and may discourage people from science fields not close to mathematics or physics to use it. Beside the knowledge gained from this study, learning the basic terms and concepts is a good start for anyone interested taking the first step so hopefully this study will help.

Σύνοψη

Ο σκοπός της εργασίας είναι η παρουσίαση βασικών εννοιών και προσεγγίσεων σε προβλήματα μη γραμμικών συστημάτων ή όπως είναι ευρύτερα γνωστά, χαοτικά συστήματα. Η προσέγγιση είναι περισσότερο θεωρητική αλλά μπορεί να εφαρμοστεί σε μεγάλη ποικιλία συστημάτων, που τα περισσότερα από αυτά είναι φυσικά συστήματα και μπορεί να μην δείχνουν να έχουν τόσες ομοιότητες με την πρώτη ματιά. Η κατανόηση της δυναμικής αυτών των συστημάτων είναι σημαντική για πολλές επιστήμες όπως η βιολογία, η χημεία, τηλεπικοινωνίες κ .α. ούτως ώστε να κατανοήσουμε την συμπεριφορά αυτών των συστημάτων. Τα περισσότερα παραδείγματα που παρουσιάζονται εδώ είναι παραδείγματα τέτοιων φυσικών συστημάτων όπως το μοντέλο του Lorenz για τον καιρό που είναι και ένα διάσημο σύστημα μιας και ήταν από τα πρώτα που μελετήθηκαν. Πιο συγκεκριμένα, τα πρώτα δυο κεφάλαια είναι εισαγωγικά, το πρώτο περιλαμβάνει μια ιστορική αναδρομή στο πεδίο και τους πρωτοπόρους του και το δεύτερο ασχολείται με την αναπαράσταση δυναμικών συστημάτων και παρέχεται επίσης κάποια ορολογία. Στο τρίτο κεφάλαιο παρουσιάζονται οι θεωρίες ευστάθειας και διακλαδώσεων προσαρμοσμένες στην μη γραμμική δυναμική. Παρέχονται θεωρία και τεχνικές για εύρεση και εξέταση της ευσταθείας και των διακλαδώσεων των λύσεων. Στο πέμπτο κεφάλαιο παρουσιάζεται η γεωμετρία των fractal η οποία αναπτύχθηκε και χρησιμοποιήθηκε για την μελέτη των περίεργων ελκυστών, οι οποίοι μπορούν να χαρακτηριστούν σαν γεωμετρικά αντικείμενα. Η ευκλείδεια γεωμετρία δεν είναι αρκετή για να περιγράψει τέτοια αντικείμενα. Στο πέμπτο και το έκτο κεφάλαιο οι παραπάνω έννοιες οργανώνονται ε ένα αναλυτικό τρόπο για να μελετηθούν πραγματικά πειραματικά δεδομένα τα οποία θα δώσουν στοιχεία για την συμπεριφορά του συστήματος. Η θεωρία του χάους είναι ένα σχετικά καινούργιο πεδίο της επιστήμης. Είναι αρκετά ενδιαφέρον αλλά ταυτόχρονα πολύπλοκο. Παρόλο που η θεωρία μπορεί να εφαρμοστεί σε πολλά φυσικά συστήματα, περιορίζεται από την περίπλοκη μαθηματική ανάλυση και μπορεί να αποθαρρύνει πολλούς, από πεδία όχι άμεσα συνδεδεμένα με τα μαθηματικά, να ασχοληθούν με αυτήν. Πέρα από την απόκτηση των γνώσεων που είναι απαραίτητες για περαιτέρω μελέτη τέτοιων συστημάτων, η εκμάθηση των βασικών προσεγγίσεων και τεχνικών είναι μια καλή αρχή για κάποιον που ενδιαφέρεται να κάνει τα πρώτα βήματα σε αυτήν την επιστήμη και ελπίζω αυτή η μελέτη να βοηθήσει.

| Table of Contents | |
|---|--------------|
| Chapter 1 – Introduction | |
| 1.1 History | <i>p. 6</i> |
| 1.2 Random and chaotic data | <i>p. 10</i> |
| 1.3 Applications | <i>p. 11</i> |
| Chapter 2 - Dynamical systems | |
| 2.1 Basic Definitions | <i>p. 12</i> |
| 2.2 Equilibrium Points | <i>p. 14</i> |
| 2.3 Stretching & folding | <i>p. 16</i> |
| 2.4 Local Linearization | <i>p. 17</i> |
| 2.5 Poincare section | <i>p. 22</i> |
| Chapter 3 - Stability & Bifurcations | |
| 3.1 Stability | <i>p. 24</i> |
| 3.1.1 Lyapunov function | <i>p. 25</i> |
| 3.2 Bifurcations | <i>p. 28</i> |
| 3.2.1 Bifurcation Diagrams | <i>p. 28</i> |
| 3.2.2 Local Bifurcations | <i>p. 30</i> |
| 3.2.3 Global Bifurcations | <i>p. 35</i> |
| 3.2.4 Non smooth Bifurcations | <i>p. 38</i> |
| 3.3 Examples | <i>p. 39</i> |
| Chapter 4 - Fractals | |
| 4.1 Introduction | <i>p. 49</i> |
| 4.2 Dimension | <i>p. 51</i> |
| 4.3 Mandelbrot & Julia sets | <i>p. 54</i> |
| 4.4 Cantor & Sierpinsky sets | <i>p. 56</i> |
| Chapter 5 - Statistical analysis of attractors | |
| 5.1 Introduction | <i>p. 59</i> |
| 5.2 Density | <i>p. 59</i> |
| 5.3 Dimension | <i>p. 63</i> |
| 5.4 Lyapunov exponent | <i>p. 63</i> |
| Chapter 6 - Analysis of chaotic time series | |
| 6.1 Introduction | <i>p. 68</i> |
| 6.2 Probability density function | <i>p. 68</i> |
| 6.3 Auto Correlation function | <i>p. 69</i> |
| 6.4 Contained Frequency (Taurus | <i>p. 69</i> |
| 6.5 Phase space reconstruction (Delay Coordinate embedding) | <i>p. 70</i> |
| 6.6 Chaos control | <i>p. 70</i> |
| Chapter 7 – Nonlinear System Representation | |
| 7.1 Introduction | <i>p. 74</i> |
| 7.2 Input-Output System representation | <i>p. 74</i> |
| 7.2 Nonlinear Differentiable algebraic representation | <i>p. 75</i> |
| 7.4 State-Space representation | <i>p. 76</i> |
| 7.5 Nonlinear representation using neural networks | <i>p. 76</i> |
| Bibliography | <i>p. 81</i> |
| Solution of linear differential equations | <i>p. 84</i> |

Chapter 1 - Introduction

1.1 History of system dynamics

The advent of computers in the last decades made it possible to tackle unsolvable nonlinear problems. This possibility led to a completely different view onto dynamical systems and in association with it to a new language about dynamical systems.

The basic terms of this language are more geometrically oriented. In linear dynamics, one seeks the fundamental solutions from which one can build all other solutions. Instead of quantitative solutions (which can be obtained only numerically in nearly all cases), qualitative aspects are of greater interest like the type of solutions, the stability of solutions, and the bifurcation of new solutions.

Nonlinear dynamics became famous because of the possibility of deterministic chaos, i.e., irregular solutions even though the equation of motion is deterministic. This is impossible in linear dynamics.

Outside the scientific community, nonlinear dynamics is therefore often called chaos theory, even though not all nonlinear systems behave chaotically.

The main catalyst for the development of chaos theory was the electronic computer. Much of the mathematics of chaos theory involves the repeated iteration of simple mathematical formulas, which would be impractical to do by hand. Electronic computers made these repeated calculations practical, while figures and images made it possible to visualize these systems.

Nature is essentially nonlinear and the idea that natural processes have regular behavior is a consequence of linear paradigms. The excessive use of linear analysis had limited the comprehension of natural processes for many years. One of these paradigms is the strict determinism, clearly illustrated by the Laplace thinking: *"If we conceive of an intelligence which at a given instant comprehends of all the relations of the entities of this universe, it could state the respect positions, motions, and general effects of all these entities at any time in the past or future"*. In the end of the XIX century, Poincaré studied the dynamical response of the three-body problem. Poincaré tries to analyze the stability of the universe, studying a complicated problem compared with the two-body problem, usually employed in that time. Figure 1 presents some orbits of the third body, showing complex responses (Stewart, 1991).

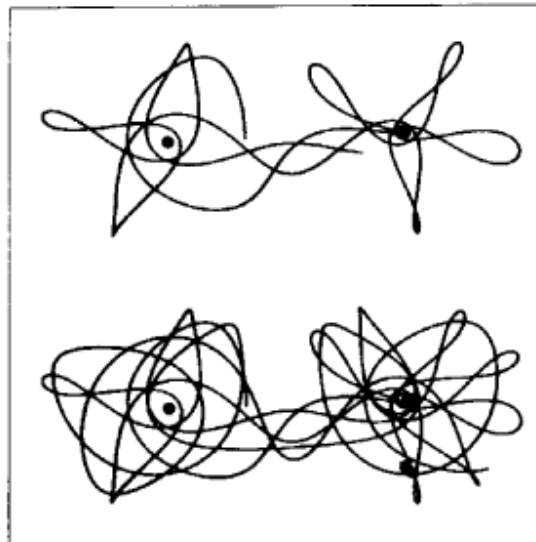


Figure 1 - Orbits related to the three body problem

The analysis of Poincaré includes the chance in contrast of the strict determinism of Laplace: "*Even if the case that the natural laws had no longer secret for us, ... it may happen that small differences in initial conditions produce very great ones in the final phenomena*".

Although Poincaré has an absolutely clear vision with respect to chaos (as it is understood nowadays), only in 1963, when Lorenz developed studies about meteorology, the idea of chance related to dynamical systems is taken again. Lorenz studied the classical problem of Rayleigh-Benard for fluid convection, which contemplates two parallel plates, separated by a fluid, where the upper plate has a lower temperature when compared with the lower plate. The Lorenz's analysis shows that small variations on initial conditions may cause great changes in the system response, being identified as the start of the modern study of chaos. This phenomenon represents sensitive dependence on initial conditions, being a characteristic feature of chaos. Colloquially, it became famous as the *butterfly effect*, which means that if a butterfly flaps its wings in China, then it may cause a hurricane in Brazil. Figure 2 shows different response patterns related to the Lorenz's problem (Van Dyke, 1982).

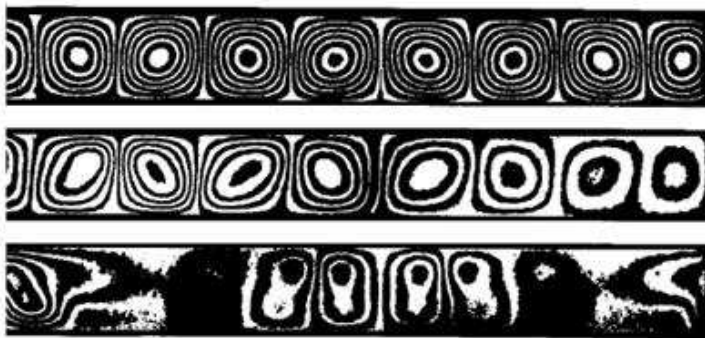


Figure 2 - Natural Convection

In 1898 Jacques Hadamard published an influential study of the chaotic motion of a free particle gliding frictionlessly on a surface of constant negative curvature. In the system studied, "Hadamard's billiards," Hadamard was able to show that all trajectories are unstable in that all particle trajectories diverge exponentially from one another, with a positive Lyapunov exponent.

Despite initial insights in the first half of the twentieth century, chaos theory became formalized as such only after mid-century, when it first became evident for some scientists that linear theory, the prevailing system theory at that time, simply could not explain the observed behaviour of certain experiments like that of the logistic map. What had been beforehand excluded as measure imprecision and simple "noise" was considered by chaos theories as a full component of the studied systems.

Much of the earlier theory was developed almost entirely by mathematicians, under the name of argotic theory. Later studies, also on the topic of nonlinear differential equations, were carried out by G.D. Birkhoff, A. N. Kolmogorov, M.L. Cartwright and J.E. Littlewood and Stephen Smale. Except for Smale, these studies were all directly inspired by physics: the three-body problem in the case of Birkhoff, turbulence and astronomical problems in the case of Kolmogorov, and radio engineering in the case of Cartwright and Littlewood.

Studies of the critical point beyond which a system creates turbulence was important for Chaos theory, analyzed for example by the Soviet physicist Lev Landau who developed the Landau-Hopf theory of turbulence. David Ruelle and Floris Takens later predicted, against Landau, that fluid turbulence could develop through a strange attractor, a main concept of chaos theory.

An early pioneer of the theory was Edward Lorenz whose interest in chaos came about accidentally through his work on weather prediction in 1961. Lorenz was using a simple digital computer, a Royal McBee LGP-30, to run his weather simulation. He wanted to see a sequence of data again and to save time he started the simulation in the middle of its course. He was able to do this by entering a printout of the data corresponding to conditions in the middle of his simulation which he had calculated last time.

To his surprise the weather that the machine began to predict was completely different from the weather calculated before. Lorenz tracked this down to the computer printout. The computer worked with 6-digit precision, but the printout rounded variables off to a 3-digit number, so a value like 0.506127 was printed as 0.506. This difference is tiny and the consensus at the time would have been that it should have had practically no effect. However Lorenz had discovered that small changes in initial conditions produced large changes in the long-term outcome. Lorenz's discovery, which gave its name to Lorenz attractors, proved that meteorology could not reasonably predict weather beyond a weekly period (at most).

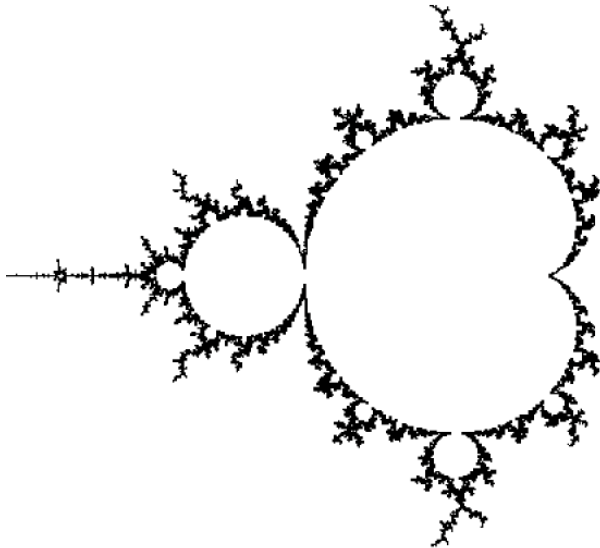


Figure 3 - Mandelbrot set

The year before, Benoît Mandelbrot found recurring patterns at every scale in data on cotton prices. Beforehand, he had studied information theory and concluded noise was patterned like a Cantor set: on any scale the proportion of noise-containing periods to error-free periods was a constant – thus errors were inevitable and must be planned for by incorporating redundancy. Mandelbrot described both the "Noah effect" (in which sudden discontinuous changes can occur, e.g., in a stock's prices after bad news, thus challenging normal distribution theory in statistics, aka Bell Curve) and the "Joseph effect" (in which persistence of a value can occur for a while, yet suddenly change afterwards). In 1967, he published "How long is the coast of Britain? Statistical self-similarity and fractional dimension," showing that a coastline's length varies with the scale of the measuring instrument, resembles itself at all scales, and is infinite in length for an infinitesimally small measuring device. Arguing that a ball of twine appears to be a point when viewed from far away (0-dimensional), a ball when viewed from fairly near (3-dimensional), or a curved strand (1-dimensional), he argued that the dimensions of an object are relative to the observer and may be fractional. An object whose irregularity is constant over different scales ("self-similarity") is a fractal (for example, the Koch curve or "snowflake", which is infinitely long yet encloses a finite space and has fractal dimension equal to circa 1.2619, the Menger sponge and the Sierpiński gasket). In 1975 Mandelbrot published *The Fractal Geometry of Nature*, which became a classic of chaos theory. Biological systems such as the branching of the circulatory and bronchial systems proved to fit a fractal model.

Chaos was observed by a number of experimenters before it was recognized; e.g., in 1927 by van der Poland in 1958 by R.L. Ives. However, as a graduate student in Chihiro Hayashi's laboratory at Kyoto University, Yoshisuke Ueda was experimenting with analog computers (that is, vacuume tubes) and noticed, on Nov. 27, 1961, what he called "randomly transitional phenomena". Yet his advisor did not agree with his conclusions at the time, and did not allow him to report his findings until 1970.

In December 1977 the New York Academy of Sciences organized the first symposium on Chaos, attended by David Ruelle, Robert May, James A. Yorke (coiner of the term "chaos" as used in mathematics), Robert Shaw (a physicist, part of the Eudemons group with J. Doyne Farmer and Norman Packard who tried to find a mathematical method to beat roulette, and then created with them the Dynamical Systems Collective in Santa Cruz, California), and the meteorologist Edward Lorenz.

The following year, Mitchell Feigenbaum published the noted article "Quantitative Universality for a Class of Nonlinear Transformations", where he described logistic maps. Feigenbaum had applied fractal geometry to the study of natural forms such as coastlines. Feigenbaum notably discovered the universality in chaos, permitting an application of chaos theory to many different phenomena.

In 1979, Albert J. Libchaber, during a symposium organized in Aspen by Pierre Hohenberg, presented his experimental observation of the bifurcation cascade that leads to chaos and turbulence in convective Rayleigh–Benard systems. He was awarded the Wolf Prize in Physics in 1986 along with Mitchell J. Feigenbaum "for his brilliant experimental demonstration of the transition to turbulence and chaos in dynamical systems".

Then in 1986 the New York Academy of Sciences co-organized with the National Institute of Mental Health and the Office of Naval Research the first important conference on Chaos in biology and medicine. There, Bernardo Huberman presented a mathematical model of the eye tracking disorder among schizophrenics. This led to a renewed of physiology in the 1980s through the application of chaos theory, for example in the study of pathological cardiac cycles.

In 1987, Per Bak, Chao Tang and Kurt Wiesenfeld published a paper in *Physical Review Letters* describing for the first time self-organized criticality (SOC), considered to be one of the mechanisms by which complexity arises in nature. Alongside largely lab-based approaches such as the Bak–Tang–Wiesenfeld sandpile, many other investigations have centered around large-scale natural or social systems that are known (or suspected) to display scale-invariant behaviour. Although these approaches were not always welcomed (at least initially) by specialists in the subjects examined, SOC has nevertheless become established as a strong candidate for explaining a number of natural phenomena, including: earthquakes (which, long before SOC was discovered, were known as a source of scale-invariant behaviour such as the Gutenberg–Richter law describing the statistical distribution of earthquake sizes, and the Omori law describing the frequency of aftershocks); solar flares; fluctuations in economic systems such as financial markets (references to SOC are common in econophysics); landscape formation; forest fires; landslides; epidemics; and biological evolution (where SOC has been invoked, for example, as the dynamical mechanism behind the theory of "punctuated equilibria" put forward by Niles Eldredge and Stephen Jay Gould). Worryingly, given the implications of a scale-free distribution of event sizes, some researchers have suggested that another phenomenon that should be considered an example of SOC is the occurrence of wars. These "applied" investigations of SOC have included both attempts at modelling (either developing new models or adapting existing ones to the specifics of a given natural system), and extensive data analysis to determine the existence and/or characteristics of natural scaling laws.

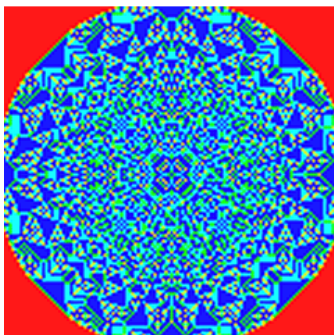


Figure 4 - The Bak–Tang–Wiesenfeld sandpile model is the first discovered example of a dynamical system displaying self-organized criticality and is named after Per Bak, Chao Tang and Kurt Wiesenfeld. The model is a cellular automaton. At each site on the lattice there is a value that corresponds to the slope of the pile.

This slope builds up as grains of sand are randomly placed onto the pile, until the slope exceeds a specific threshold value at which time that site collapses transferring sand into the adjacent sites, increasing their slope.

The same year, James Gleick published *Chaos: Making a New Science*, which became a best-seller and introduced general principles of chaos theory as well as its history to the broad public. At first the domains of work of a few, isolated individuals, chaos theory progressively emerged as a transdisciplinary and institutional discipline, mainly under the name of nonlinear systems analysis. Alluding to Thomas Kuhn's concept of a paradigm shift exposed in *The Structure of Scientific Revolutions* (1962), many "chaologists" (as some self-nominated themselves) claimed that this new theory was an example of such a shift, a thesis upheld by J. Gleick.

The availability of cheaper, more powerful computers broadens the applicability of chaos theory. Currently, chaos theory continues to be a very active area of research, involving many different disciplines (mathematics, topology, physics, population biology, biology, meteorology, astrophysics, information theory, etc.).

1.2 Random and chaotic data

When a non-linear deterministic system is attended by external fluctuations, its trajectories present serious and permanent distortions. Furthermore, the noise is amplified due to the inherent non-linearity and reveals totally new dynamical properties. Statistical tests attempting to separate noise from the deterministic skeleton or inversely isolate the deterministic part risk failure. Things become worse when the deterministic component is a non-linear feedback system. In presence of interactions between nonlinear deterministic components and noise, the resulting nonlinear series can display dynamics that traditional tests for nonlinearity are sometimes not able to capture.

It can be difficult to tell from data whether a physical or other observed process is random or chaotic, because in practice no time series consists of pure 'signal.' There will always be some form of corrupting noise, even if it is present as round-off or truncation error. Thus any real time series, even if mostly deterministic, will contain some randomness.

All methods for distinguishing deterministic and stochastic processes rely on the fact that a deterministic system always evolves in the same way from a given starting point. Thus, given a time series to test for determinism, one can:

- pick a test state;
- search the time series for a similar or 'nearby' state; and
- compare their respective time evolutions.
- Define the error as the difference between the time evolution of the 'test' state and the time evolution of the nearby state. A deterministic system will have an error that either remains small (stable, regular solution) or increases exponentially with time (chaos). A stochastic system will have a randomly distributed error.

When we try to define the position of a point in a space with some type of coordinate system there will always be an error in our measurements. If that error is x then around the point we are measuring there will be a sphere (in case of 3-dimensional space), with $r=x$ and centre that point, within infinite points would exist. So we cannot really say that we defined a point but we can say that we measured an area with a factor of accuracy, within which that point will exist. That sphere is called error ball

If the system is stable starting from Initial conditions within the error ball the deviations of the orbits will decay as the system evolves. Thus the error ball will shrink. It can be shown that the eigenvectors at that point are contracting and that the direction of contraction is along the eigenvectors.

If the system is unstable the error balls will expand leading orbits to infinity. Again the direction of the expansion would be along the eigenvectors.

In the case of chaotic orbits the error ball will shrink into the one direction and expand to the other. So distance between 2 initial conditions will keep growing without orbits going to infinity. This is due to the folding of state space.

Essentially all measures of determinism taken from time series rely upon finding the closest states to a given 'test' state (i.e., correlation dimension, Lyapunov exponents, etc.). To define the state of a system one typically relies on phase space embedding methods. Typically one chooses an embedding dimension, and investigates the propagation of the error between two nearby states. If the error looks random, one increases the dimension. If you can increase the dimension to obtain a deterministic looking error, then you are done. Though it may sound simple it is not really. One complication is that as the dimension increases the search for a nearby state requires a lot more computation time and a lot of data (the amount of data required increases exponentially with embedding dimension) to find a suitably close candidate. If the embedding dimension (number of measures per state) is chosen too small (less than the 'true' value) deterministic data can appear to be random but in theory there is no problem choosing the dimension too large – the method will work.

1.3 Applications

Chaos theory is applied in many scientific disciplines: mathematics, biology, computer science, economics, engineering, finance, philosophy, physics, politics, population dynamics, psychology, and robotics. . In this context, Briggs & Peat (2000) say that "*chaos reveals that, we need to use all uncertainties of life instead of resist to them*".

Chaotic behavior has been observed in the laboratory in a variety of systems including electrical circuits, lasers, oscillating chemical reactions, fluid dynamics, and mechanical and magneto-mechanical devices. Observations of chaotic behavior in nature include the dynamics of satellites in the solar system, the time evolution of the magnetic field of celestial bodies, population growth in ecology, the dynamics of the action potentials in neurons, and molecular vibrations. There is some controversy over the existence of chaotic dynamics in plate tectonics and in economics.

One of the most successful applications of chaos theory has been in ecology, where dynamical systems such as the Ricker model have been used to show how population growth under density dependence can lead to chaotic dynamics.

Chaos theory is also currently being applied to medical studies of epilepsy, specifically to the prediction of seemingly random seizures by observing initial conditions.

A related field of physics called quantum chaos theory investigates the relationship between chaos and quantum mechanics. Recently, another field, called relativistic chaos, has emerged to describe systems that follow the laws of general relativity.

Although chaotic planetary motion had not been observed, experimentalists had encountered turbulence in fluid motion and nonperiodic oscillation in radio circuits without the benefit of a theory to explain what they were seeing.

Dynamics - A Capsule History

| | | |
|-----------|--|--|
| 1666 | Newton | Invention of calculus, explanation of planetary motion |
| 1700s | | Flourishing of calculus and classical mechanics |
| 1800s | | Analytical studies of planetary motion |
| 1890s | Poincaré | Geometric approach, nightmares of chaos |
| 1920–1950 | | Nonlinear oscillators in physics and engineering, invention of radio, radar, laser |
| 1920–1960 | Birkhoff Kolmogorov Arnol'd Moser | Complex behavior in Hamiltonian mechanics |
| 1963 | Lorenz | Strange attractor in simple model of convection |
| 1970s | Ruelle & Takens | Turbulence and chaos |
| | May | Chaos in logistic map |
| | Feigenbaum | Universality and renormalization, connection between chaos and phase transitions |
| | | Experimental studies of chaos |
| | Winfrey | Nonlinear oscillators in biology |
| | Mandelbrot | Fractals |
| 1980s | | Widespread interest in chaos, fractals, oscillators, and their applications |

Figure 5 - Brief History of dynamical systems theory

Chapter 2 - Dynamical systems

2.1 Basic Definitions

A dynamical system is a part of the world which can be seen as a self-contained entity with some temporal behaviour. In mathematics it is a concept where a fixed rule describes the time dependence of a point in a geometrical space. In nonlinear dynamics, speaking about a dynamical system usually means to speak about an abstract mathematical system which is a model for such an entity. Mathematically, a dynamical system is defined by its state and by its dynamics. A pendulum is an example for a dynamical system.

A state of the system is A number or a vector (i.e., a list of numbers usually variables) defining the state of the dynamical system uniquely. An initial condition is a state from which an orbit starts in the state space.

Dynamics or Equations of motion is the causal relation between the present state and the next state. It is a *deterministic rule* which tells us what happens in the next time step. In the case of a continuous time, the time step is infinitesimally small. Thus, the equation of motion is a differential equation or a system of differential equations where x is the state and t is the time variable:

$$\frac{dx}{dt} = f(x)$$

In the case of a discrete time, the time steps are nonzero and the dynamics is a map with the discrete time n :

$$x_{n+1} = f(x_n)$$

The dynamics is linear if the causal relation between the present state and the next state is linear. Otherwise it is nonlinear.

Orbit is a solution of the equation of motion. In the case of continuous time, it is a curve in phase space. In the case of a discrete system, it is an ordered set of points in the phase space.

The mapping of the whole state space of a continuous dynamical system onto itself for a given time step t is called **vector field**. If t is an infinitesimal time step dt , the flow is just given by the right side of the equation of motion. In general, the flow for a finite time step is not known analytically because this would be equivalent to have a solution of the equation of motion. Given an Initial condition somewhere the orbit will follow the flow.

On this basis, a dynamical system may be understood as a transformation f that is imposed to a vector field x . The space of dependent variables, x , called *state space* or *phase space*, may have different topologies. Topology is the science that studies continuous transformations and furnishes the tools to understand global aspects related to dynamical systems. Essentially, it is possible to define geometrical properties of objects under transformations (Singer & Thorpe, 1967).

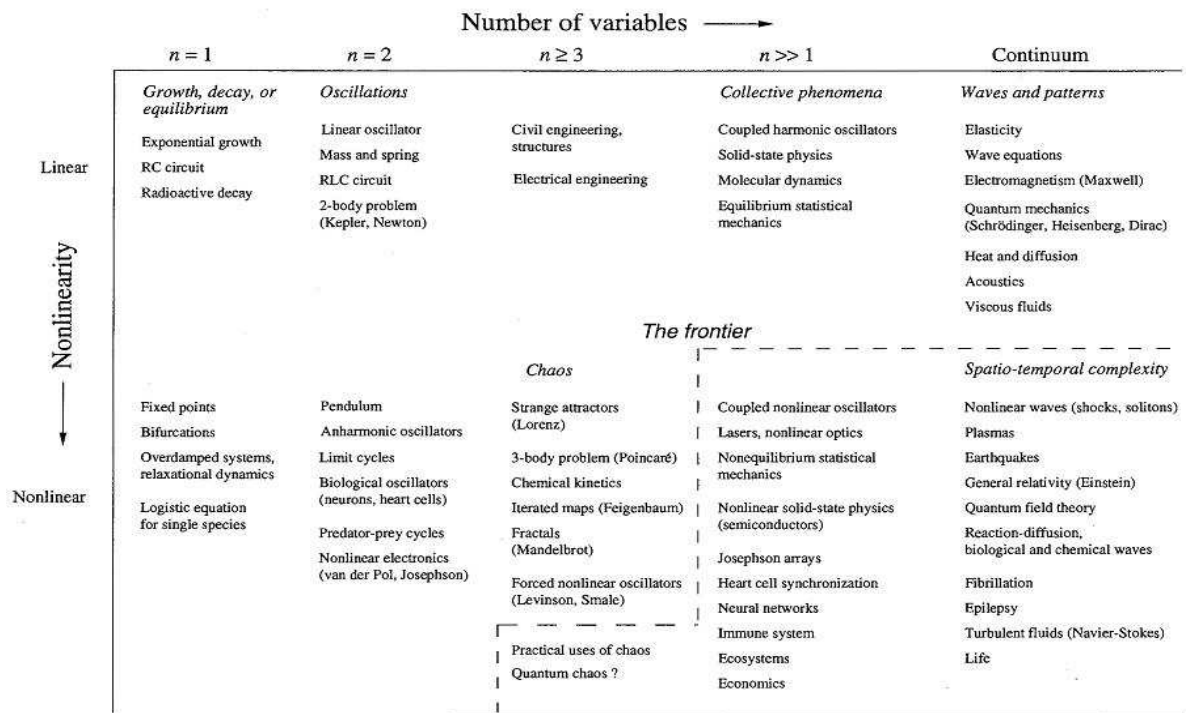


Figure 6 - The frontier where chaos rises. It is a unique characteristic of non-linear systems.

2.2 Equilibrium points or fixed points:

An equilibrium point (or fixed point) is a special point of the state space where the system may stay stationary, which means that the solution does not vary with time. Therefore, if x_n^* is an equilibrium point of the system, hence $(\dot{x}_n^*) = 0$.

Fixed points are coming in four flavors geometrically:

- Points: Stationary solutions.
- Limit cycles: Periodic solutions (of period - n from 0 to infinity).
- Quasiperiodic orbits: Periodic solutions with at least two incommensurable frequencies (the ratio of the frequencies is an irrational number – Torus state space).
- Chaotic orbits: Bound non-periodic solutions.

The first three types can also occur in linear dynamics. The fourth type appears only in nonlinear systems. Its possibility was first anticipated by Henri Poincaré. In the seventies, this irregular behaviour was termed deterministic chaos. A fixed point can be either stable or unstable. Changing a parameter of the system can change the stability of a fixed point. This is accompanied by a change of the *number* of fixed points called bifurcation. Chaotic solutions are the more interesting because they lead to attractors that can have great detail and complexity.

Chaotic behaviour can only arise in a continuous dynamical system if it has three or more dimensions. However, no such restriction applies to discrete systems, which can exhibit chaotic behaviour in two or even one dimensional systems. (Poincaré-Bendixson)

Simple systems can also produce chaos without relying on differential equations. An example is the logistic map, which is a difference equation (recurrence relation) that describes population growth over time. Another example is the Ricker model of population dynamics.

Other examples are the Lorenz system which is generated by a system of three differential equations with a total of seven terms on the right hand side, five of which are linear terms and two of which are quadratic (and therefore nonlinear). Another well-known chaotic system is generated by the Rossler equations with seven terms on the right hand side, only one of which is (quadratic) nonlinear. Sprott found a three dimensional system with just five terms on the right hand side, and with just one quadratic nonlinearity, which exhibits chaos for certain parameter values. Zhang and Heidel showed that, at least for dissipative and conservative quadratic systems, three dimensional quadratic systems with only three or four terms on the right hand side cannot exhibit chaotic behaviour. The reason is, simply put, that solutions to such systems are asymptotic to a two dimensional surface and therefore solutions are well behaved.

Even the evolution of simple discrete systems, such as cellular automata, can heavily depend on initial conditions. Stephen Wolfram has investigated a cellular automaton with this property, termed by him *rule 30*.

Sharkovskii's theorem is the basis of the Li and Yorke (1975) proof that any one-dimensional system which exhibits a regular cycle of period three will also display regular cycles of every other length as well as completely chaotic orbits.

Systems that experience chaotic behaviour under certain conditions have some common properties:
 Sensitive dependence on Initial conditions. This means that little perturbation on initial condition will lead to completely different orbits in the state space as the system evolves

There will be some kind of periodicity

The orbits remain bounded to certain geometry

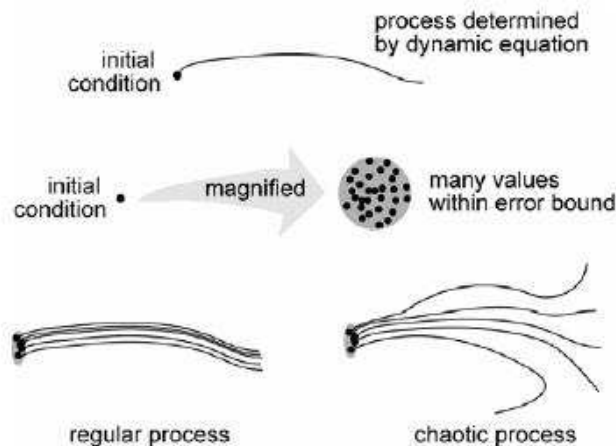


Figure 7 - Error balls and orbits evolving in time

Classical dynamics does not generalize over initial condition, whose value for each case is assigned “from outside.” Modern dynamics generalizes over initial conditions by making it a *theoretical variable* internal to the state-space representation. This broadened theoretical framework enables scientists to introduce new concepts for dynamical processes with various initial conditions. Chaos and attractors are such novel concepts.

By internalizing initial conditions instead of receiving them “from outside,” dynamical theory attains a higher level of generality. Its scope expands from individual processes to processes with all possible initial conditions.

2.3 Stretching and Folding

Sensitivity on the initial conditions leads to chaos only if the trajectories are bound. That is that the system cannot go to infinity. With linear dynamics, there is either sensitivity on the initial conditions or bound trajectories, but not both. With nonlinearity, both can exist. The figure shows why this is possible. The phase space of the system is stretching and folding, thus the distance between 2 Initial conditions that were close after infinite steps goes to infinity. Yet the phase space remains bounded. Stretching and folding are responsible for deterministic chaos And folding occurs only in nonlinear systems.

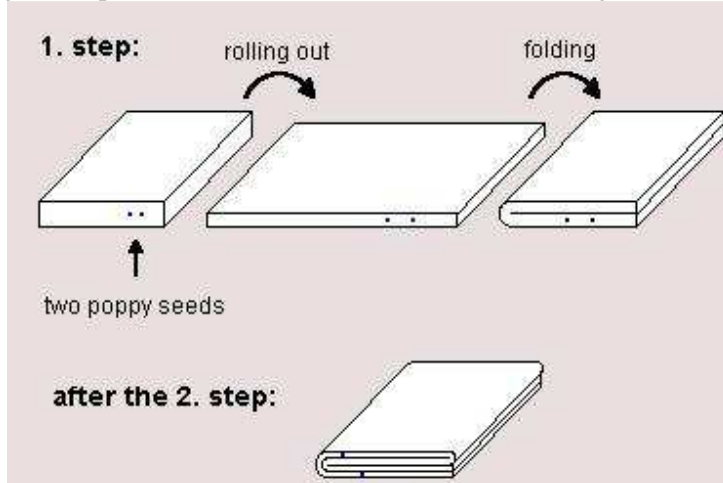


Figure 8 - Continuous separation of nearby initial conditions due to the stretching and folding mechanism

Chaos may be geometrically understood considering some characteristics related to dynamical system transformations. On this basis, let a unitary square Q , subject to f such that one direction is contracted while the other is expanded. This transformation is considered to be the positive part of a more general transformation. Analogously, it is possible to think in the reverse transformation (the negative part of transformation), where contraction and expansion of Q is taken in a different way.

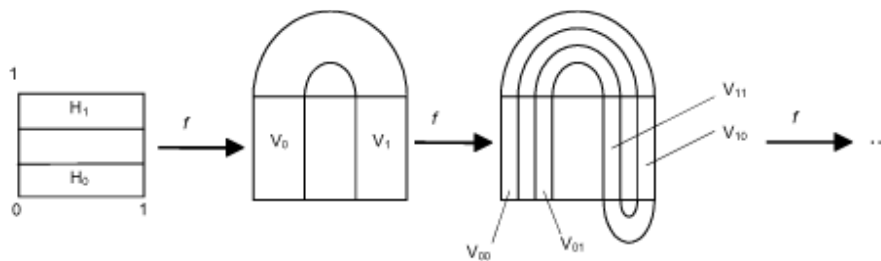


Figure 5. Sequence of transformations subjected to the square Q for the function f .

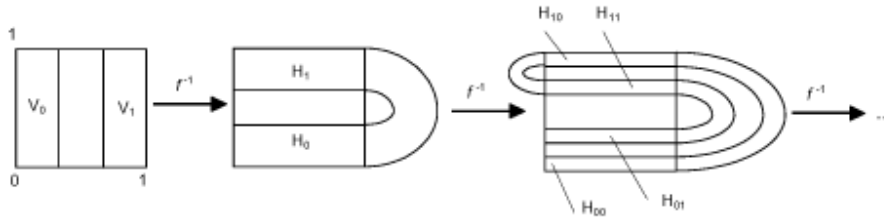


Figure 6. Sequence of transformations subjected to the square Q for the inverse of function f .

Figure 9 - Smalle's Horseshoe, a famous example of this kind of transformation named after S. Smale

Because of the form of the transformed square and also as a tribute to the mathematician Steve Smale, this kind of transformation became known as the *Smale horseshoe*. A dynamical system subjected to this kind of transformation has some special characteristics. This transformation implies that, to a general point of Q , p , it is possible to associate a neighbor, e , which may be too small, where it can be chosen another point \tilde{p} . It does not matter the size of the neighbor e , there is a number of iterations imposed by f such as p and \tilde{p} are separated by a finite distance. Therefore, the system presents a sensitive dependence on initial condition, as shown in Figure 8 (Wiggins, 1990; Strogatz, 1994). This property characterizes the chaotic behavior of a dynamical system. This sensitive dependence represents the butterfly effect described in Lorenz's work.

2.4 Local linearization

In nonlinear dynamics, the main questions are: What is the qualitative behaviour of the system? Which and how many non-wandering sets (i.e. a fixed point, a limit cycle, a quasi-periodic or chaotic orbit) occur? Which of them are stable? How does the number of non-wandering sets change while changing a parameter of the system (called control parameter)?

The basic approach to such situations is to locally observe the systems state space at the fixed points to see local behaviour and then try to extend that conclusions to the whole state space.

Linearization makes it possible to use tools for studying linear systems to analyze the behavior of a nonlinear function near a given point. The linearization of a function is the first order term of its Taylor expansion around the point of interest.

Here we are not trying to solve the equations to find the exact orbit(that might be impossible) but we are trying to estimate the qualitative character of the orbit by looking at the fixed points.

The Jacobean matrix is the matrix of all first-order partial derivatives of a vector- or scalar-valued function with respect to another vector. The Jacobean of a function describes the orientation of a tangent plane to the function at a given point. Likewise, the Jacobean can also be thought of as describing the amount of "stretching" that a transformation imposes. The importance of the Jacobean lies in the fact that it represents the best linear approximation to a differentiable function near a given point. In this sense, the Jacobean is the derivative of a multivariate function. For a function of n variables, $n > 1$, the derivative of a numerical function must be matrix-valued, or a partial derivative.

In stability analysis, one can use the eigenvalues of the Jacobean matrix evaluated at an equilibrium point to determine the nature of that equilibrium. If any of the eigenvalues are positive, the equilibrium is unstable. if they are all negative the equilibrium is stable; and if the values are of mixed signs, the equilibrium is possibly a saddle point. Any complex eigenvalues will appear in complex conjugate pairs and indicate a spiral.

In general the procedure is:

- Finding the fixed points
- Local linearization using the Jacobean (or slope in case of 1D)
- Obtaining Eigenvectors and Eigenvalues (n for n-dimensional systems)
- Evaluate eigenvalues to estimate local stability (contracting or expanding Behaviour)

- Estimate the Character of the Vector field based on the character around those points.

This procedure is similar for flows and maps. The evaluation of eigenvalues leads to conclusion about the behavior around the fixed point:

- For real and negative \rightarrow contracting behavior
- For real and pos \rightarrow expanding behavior
- For real, one pos one ne ($n=2$) \rightarrow contracting and expanding behavior or saddle (chaotic)
- For pure complex Conjugate \rightarrow Sinusoidal behaviour (closed orbits)
- For complex conjugate with ne real part \rightarrow decaying sinusoidal behaviour (Spiral orbits for $n>2$)
- For complex conjugate with positive real part \rightarrow increasing sinusoidal behaviour (Spiral orbits for $n>2$)

The frequency of the oscillation depends on the Imaginary part. In the case of complex eigenvalues the eigenvectors will rotate in addition (Spiral motion). The behaviour can be visualized in some cases and enables us to make general conclusions easier. In 3 dimensions for example, two stable manifolds form a surface with the same properties as an 1-dimensional stable manifold.

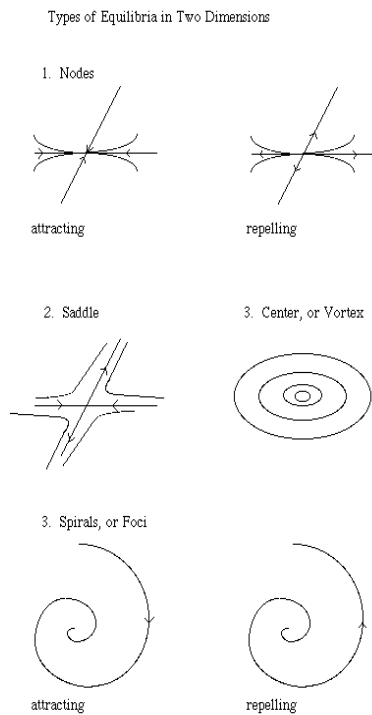


Figure 10 - Classification of fixed points based on their behavior for 2-dimensional systems

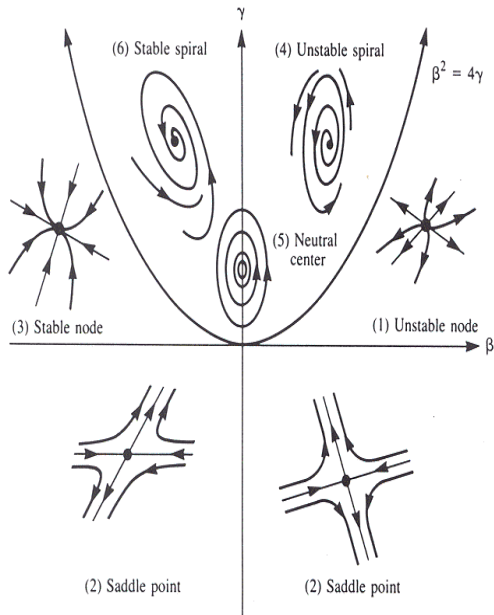


Figure 11 – Types of fixed points placed in the parameter space for 3-dimensional systems

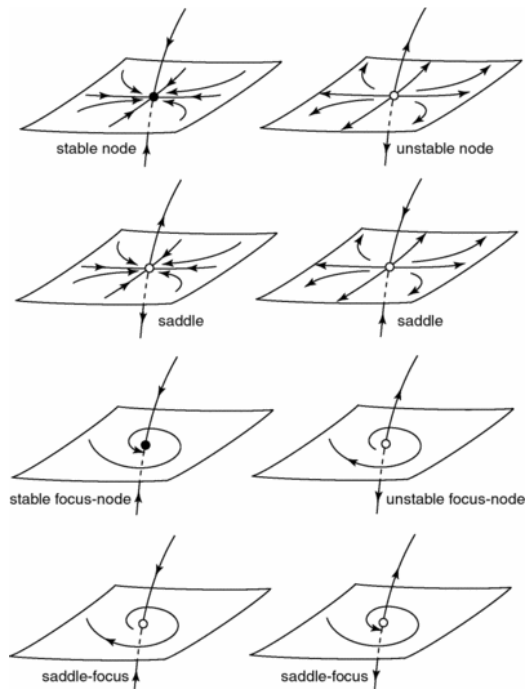


Figure 12 - Different types of behavior and their common used names

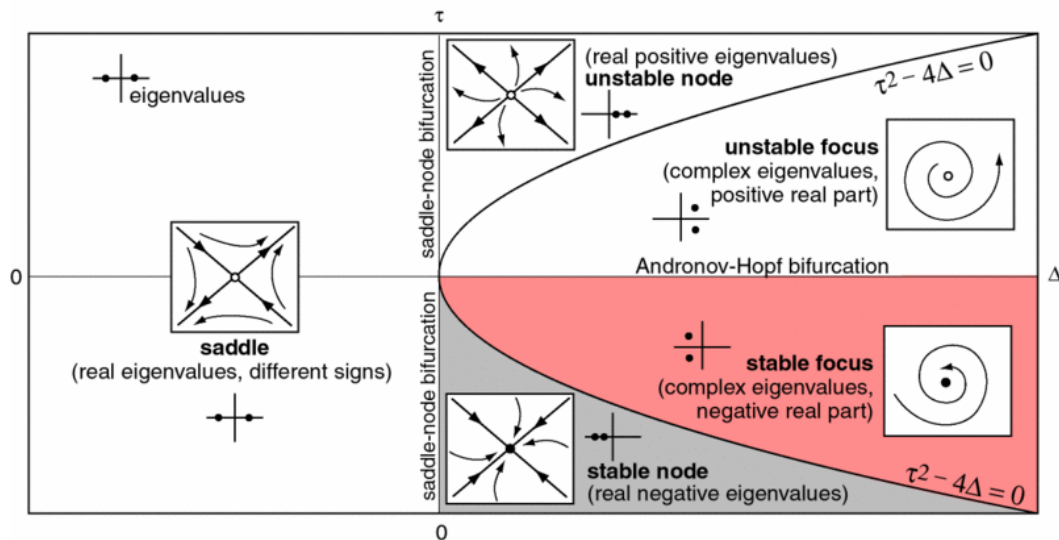


Figure 13 - Relations with stability and bifurcation theory

The notion spiral and node are inspired by the flow near the fixed point. A pair of conjugated complex eigenvalues lead to a spiral, whereas a node is caused by two real eigenvalues of the same sign. Real eigenvalues of different sign lead to a saddle. In general, a saddle is a fixed point where at least one eigenvalue has a positive real part but also at least one eigenvalue has a negative real part. Near a saddle, an orbit is usually attracted at first but repelled later on. There are points in the phase space which approach the fixed point for $t \rightarrow \infty$. They form the stable manifold. The Eigenspace for the eigenvalues with negative real part is tangential to the stable manifold. The unstable manifold are built by all points approaching the fixed point for $t \rightarrow \infty$.

Calculating the roots of a polynomial analytically is impossible if its order is greater than five, and tedious if the order is greater than two. For time-continuous system, the question on stability can be answered without explicitly calculating the eigenvalues, thanks to the theorem of Routh and Hurwitz. This theorem says that the real parts of all roots of a polynomial are negative if and only if certain conditions are fulfilled which can be easily calculated. This theorem is useful even in the case of a two-dimensional phase space where the characteristic polynomial is quadratic: Both eigenvalues have negative real part if and only if the determinant $Df(u_0)$ is positive and the trace of $Df(u_0)$ is negative.

The extension of these conclusions to the whole vector field is based around the following two concepts:

- The vector fields are smooth (same set of equations everywhere)
- The moment the Differential Equations are defined, there is a unique vector for each point of the field leading to the conclusion that vectors do not interfere one another (only at equilibrium points) and ultimately that Initial Conditions that are close have similar behaviour.

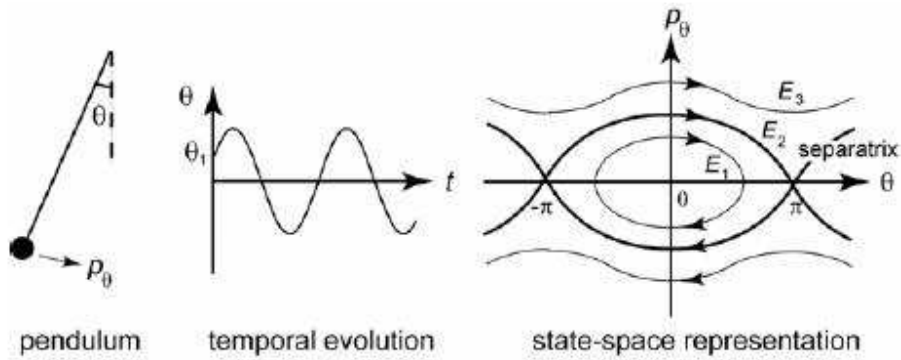


Figure 14 - Different approaches for analysis, the state space representation is the most common used to extract the behavior of the system starting from different initial conditions.

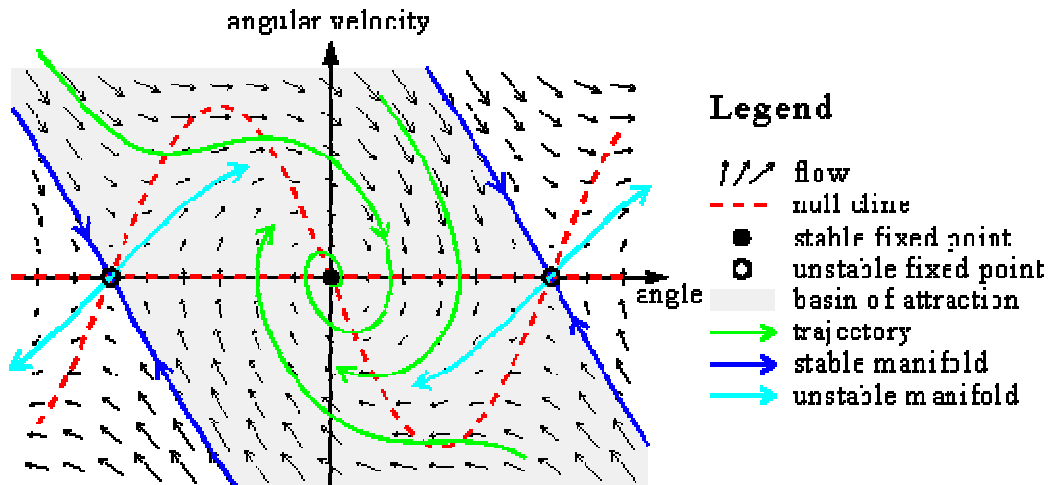


Figure 15 - Construction of the flow diagram, starting from the local behavior around the equilibria the generalization to the whole field is easier

2.5 Poincare section

In many cases representation and mathematical analysis of flows of higher dimensions is difficult. Poincare invented a technique to transform a continuous map into a discrete one by using the Poincare section. This creates a map that has 1 dimension less and also can be analysed easier by using discrete time techniques and represented.

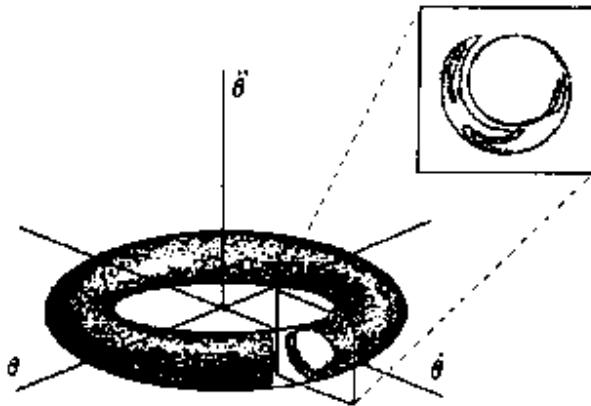


Figure 16 - A Poincaré section placed on a torus state space system. This helps reducing the dimensions of the system by one and also discretizes it.

$$\dot{x} = f(x) \rightarrow x_{n+1} = f(x_n)$$

It can be proved that the qualitative behaviour of the two maps is the same so Poincaré map represents the system fully.

Poincaré section mathematically is a plane of 1 dimension less than the state space of the given system. In general, it is considered as a surface that transversely intersects a given orbit. For systems subjected to periodic forcing, Poincaré section may be represented by a surface that corresponds to a specific phase of the driving force. On this basis, one has a stroboscopically sample of the system response (Figure 9).

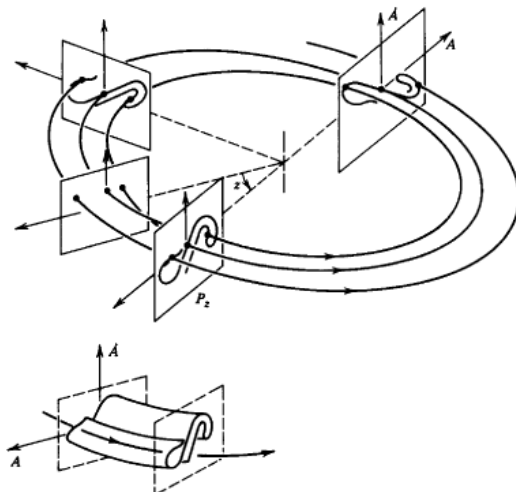


Figure 9. Poincaré section (Modified from Moon, 1992).

Figure 17 - The Poincaré section is placed with certain rules and must cover almost all orbits. When the orbit crosses the section, it leaves a dot that can be treated as a point on a discrete map.

It is placed based on specific rules defined by Poincaré in order to intersect with the orbit of a fixed point. If it is placed correctly no qualitative behaviour is lost and the map represents the system correctly.

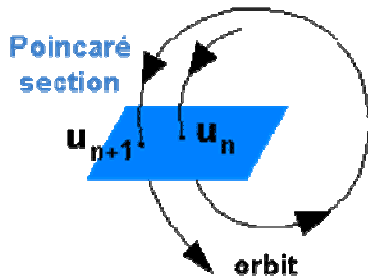


Figure 18 - The iterations create sequences of points (discrete jumps)

If the Poincaré section is carefully chosen no information is lost concerning the qualitative behaviour of the dynamics. Poincaré maps are invertible maps because one gets u_n from u_{n+1} by following the orbit backwards. In the Poincaré map, limit cycles become fixed points. A non-wandering set can be either stable or unstable. Changing a parameter of the system can change the stability of a Equilibrium point. This is accompanied by a change of the *number* of attractors due to a bifurcation. In the Poincaré map, limit cycles become fixed points

In the Poincaré map we can see the period-1 orbit as a fixed point, period-2 orbit as a set of points etc. then by watching the mapping of different initial conditions as the system evolves we can conclude if the fixed point is stable or not.

After this is done we can make conclusions about the qualitative behavior of the system by studying the Poincaré map of the original system.

this is done by using local linearization as described but using the Poincaré map as the state space and with some modifications applied to discrete maps. The convergence is determined by the slope at the fixed point for 1-dimensional maps and by the Jacobean at the fixed point for 2-dimensional and higher order maps.

Chapter 3 - Stability & Bifurcations

3.1 Stability

Stability theory addresses the stability of solutions of differential equations and of trajectories of dynamical systems under small perturbations of initial condition.

Various criteria have been developed to prove stability or instability of an orbit. Under favorable circumstances, the question may be reduced to a well-studied problem involving eigenvalues of matrices. A more general method involves Lyapunov functions.

There are two types of stability:

- **Lyapunov stability:** Every orbit starting in a neighbourhood of the fixed point remains in a neighbourhood.
- **Asymptotic stability:** In addition to the Lyapunov stability, every orbit in a neighbourhood converges to the fixed point asymptotically.

The mathematical definition would be:

Suppose a system:

$$\dot{x} = f(x)$$

The equilibrium point $x = 0$ would be

- **Stable:**
If for each $V > 0$ exists $\delta = \delta(V) > 0$ such that $\|x(0)\| < \delta$ for $\|x(V)\| < V \forall V \geq 0$
This implies that starting from a neighborhood of the equilibrium point ($x=0$) that is enclosed within a ball of radius δ , then for all t (time) in the future, a function $\delta(V)$ can be defined which will always be contained in a ball of radius V .
- **Asymptotically stable:**
If it is stable and δ can be chosen such that $\|x(0)\| < \delta$ for $\lim_{t \rightarrow \infty} x(t) = 0$
This implies that a radius δ can be defined such that if the Initial condition is in that radius, then asymptotically the state will converge to the equilibrium point.

This characterizes the fixed points as marginally stable, asymptotically stable or unstable. Asymptotically stable fixed points are also called attractors. The basin of attraction is the set of all initial states approaching the attractor in the long time limit. V is called Lyapunov function.

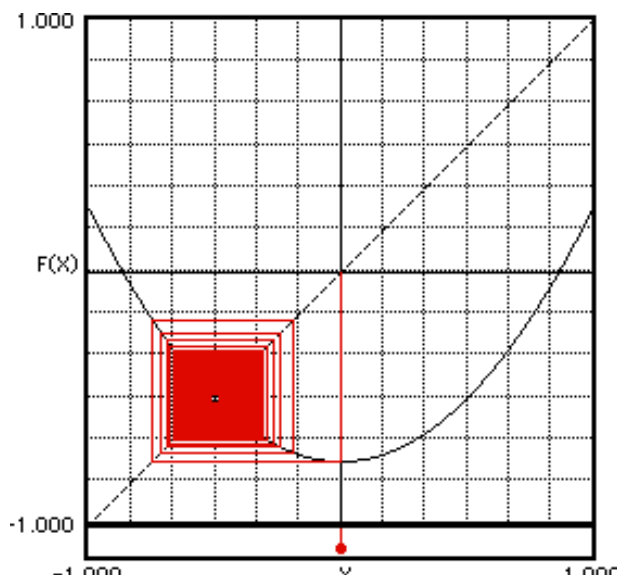


Figure 19 - Orbits converging to the fixed point asymptotically, approaching from both sides

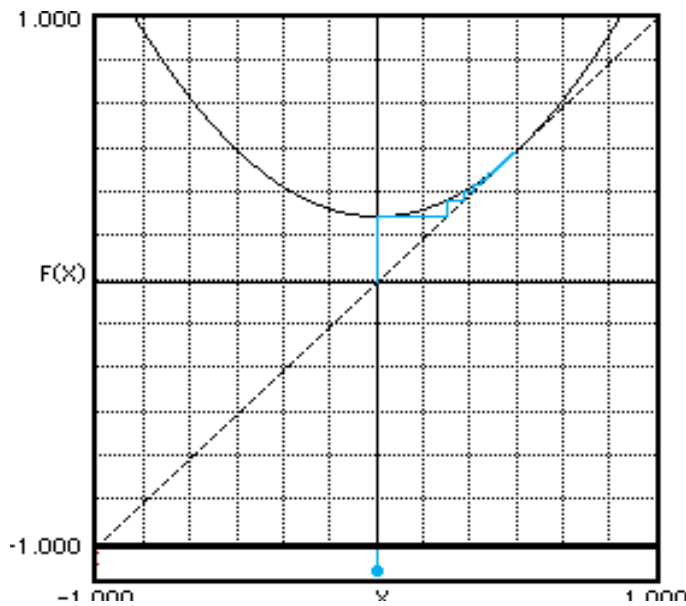


Figure 20 - orbits converging and approaching from one side to a stable fixed point

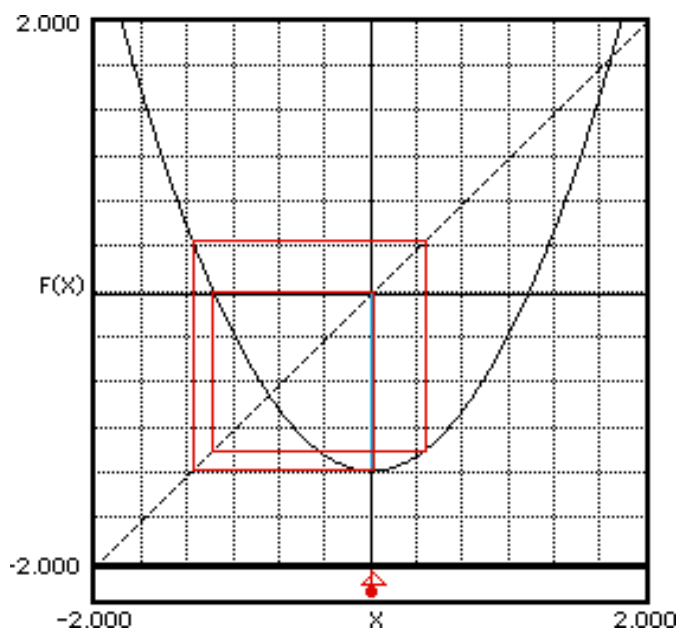


Figure 21 - Orbit diverting from the unstable fixed point

3.1.1 Lyapunov function

Lyapunov functions are functions which can be used to prove the stability of a certain fixed point in a dynamical system or autonomous differential equation without actually solving the equations. This is inspired by considering the total energy of the system. Looking at its equation and its derivative we can make conclusions about the qualitative behavior of the system. The total energy is unknown in most cases but Lyapunov showed that we don't need the total energy function but if instead we can define a function with the following properties, then the Eq. point will be stable .

- V is always positive
- \dot{V} always negative or zero

The definition would be:

Let $x = 0$ be an Eq.Point. Let V be a continuously differentiable function on a neighborhood D of $x = 0$ such that:

$$V(0) = 0 \text{ and } V(x) > 0 \text{ in } D \setminus \{0\} \text{ and}$$

$$\dot{V}(x) \leq 0 \text{ in } D$$

Then the Equilibrium Point is Stable if $\dot{V}(x) < 0$ and asymptotically stable if $\dot{V}(x) = 0$.

In general $V(x)$ is defined as:

$$V(x) = x^T P x = \sum_{i=1}^n \sum_{j=1}^n P_{ij} x_i x_j$$

We chose P as a symmetric matrix and if it is chosen properly (all eigenvalues positive), then V is always positive. Then for the derivative $\dot{V}(x)$ we can use the matrix $-P$.

Pendulum Example

The above can be shown in the pendulum system which exhibits both stable (simple pendulum) and asymptotically stable behavior for different values of the parameter. For this system we know the total energy function and we can compare it to the calculated Lyapunov function.

The equations of this system are:

$$\dot{x}_1 = x_2$$

$$\dot{x}_2 = -\frac{g}{l} \sin x_1 \left(-\frac{R}{m} x_2\right)$$

Where x_1 is the position parameter and x_2 is the velocity parameter. The part inside the brackets is the friction part. If R is 0, there is no friction so the system will be stable. If R greater than 0, it will be asymptotically stable. This can be extracted from the total energy function expressed as a sum of the potential and the kinetic energy:

$$E(x) = \int_0^{x_1} \frac{g}{l} \sin x_1 dx_1 + \frac{1}{2} x_2^2$$

- If $R=0$ then E will be constant, so $\frac{dE}{dt} = 0$ (stable)
- If $R>0$, then $\frac{dE}{dt} < 0$ (asymptotically stable)

In case of the simple pendulum the Lyapunov function can be written as:

$$V(x) = \frac{g}{l} (1 - \cos x_1) + \frac{1}{2} x_2^2$$

We can see that $V(x)$ will always be positive so it satisfies the first condition and the derivative would be:

$$\dot{V}(x) = \frac{dV}{dx} \frac{dx}{dt} = \begin{bmatrix} \frac{dV}{dx_1} & \frac{dV}{dx_2} \end{bmatrix} \begin{bmatrix} f_1(x_1, x_2) \\ f_2(x_1, x_2) \end{bmatrix} = \begin{bmatrix} \frac{g}{l} \sin x_1 & x_2 \end{bmatrix} \begin{bmatrix} x_2 \\ -\frac{g}{l} \sin x_1 \end{bmatrix} = 0$$

So V satisfies both conditions. It can be seen that both functions V and E have the same properties and lead to the same conclusions about the behavior of the system, so either of them can be used.

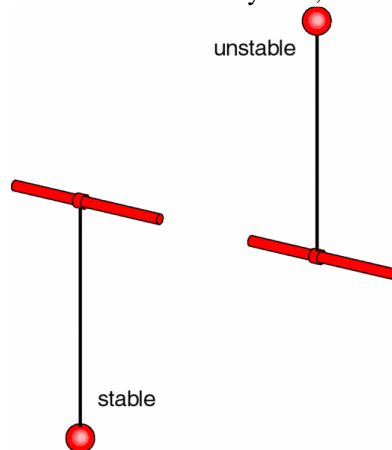


Figure 22 - Pendulum in different phases. the system will be attracted to a stable behavior

3.2 Bifurcations

A change of the qualitative behaviour of the system is called bifurcation. In mathematics it is the study of changes in the qualitative or topological structure of a given system. Crossing the boundary of stability only indicates a bifurcation point and the type of the bifurcating solutions. But it doesn't tell how and how many new solutions bifurcate or disappear in a bifurcation point. Also an attractor becoming unstable does not mean exactly that it disappears. It may be still there but unstable and coexisting with the new attractors.

A bifurcation occurs when a small smooth change to the parameter values (the bifurcation parameters) of a system causes a sudden 'qualitative' or topological change in its behavior. Bifurcations occur in both continuous systems and discrete systems.

Bifurcation phenomenon is closely related to chaos and usually its analysis is developed considering local and global bifurcations. Local bifurcations are developed in a small region of phase space, usually, near to an equilibrium point. On the other hand, global bifurcation is non-local. There are many different forms of bifurcations depending on the dynamical systems characteristics. The formation of Smale horseshoe is a common type of global bifurcation. Local bifurcation of a dynamical system may be analyzed from its normal form, $\dot{x} = f(x; \mu)$, $x \in \mathbb{R}^n$, $\mu \in \mathbb{R}^P$, where μ represents system parameters or bifurcation parameters.

An abstract mathematical definition could be:

A fixed point $(x, \mu) = (0, 0)$ of a one-parameter family of one-dimensional vector fields is said to undergo a bifurcation at $\mu = 0$ if the flow for μ near zero and x near zero is not qualitatively the same as the flow near $x = 0$ at $\mu = 0$.

3.2.1 Bifurcation Diagrams

Bifurcation diagrams represent the stroboscopically sampled variable values under the slow quasi-static increase of some system parameter (Thompson & Stewart, 1986). These diagrams allow a global analysis of the parameter changes in the system response (Machado *et al.*, 2004). Figure 12 shows some typical bifurcation diagrams obtained from the logistic map. In this particular system, the route to chaos is represented by period doubling cascades. Enlargement of regions of bifurcation diagrams shows the process of bifurcation until the accumulation point is reached. After that, the system presents a chaotic response. Besides, it is important to notice that there are periodic windows inside chaotic regions.

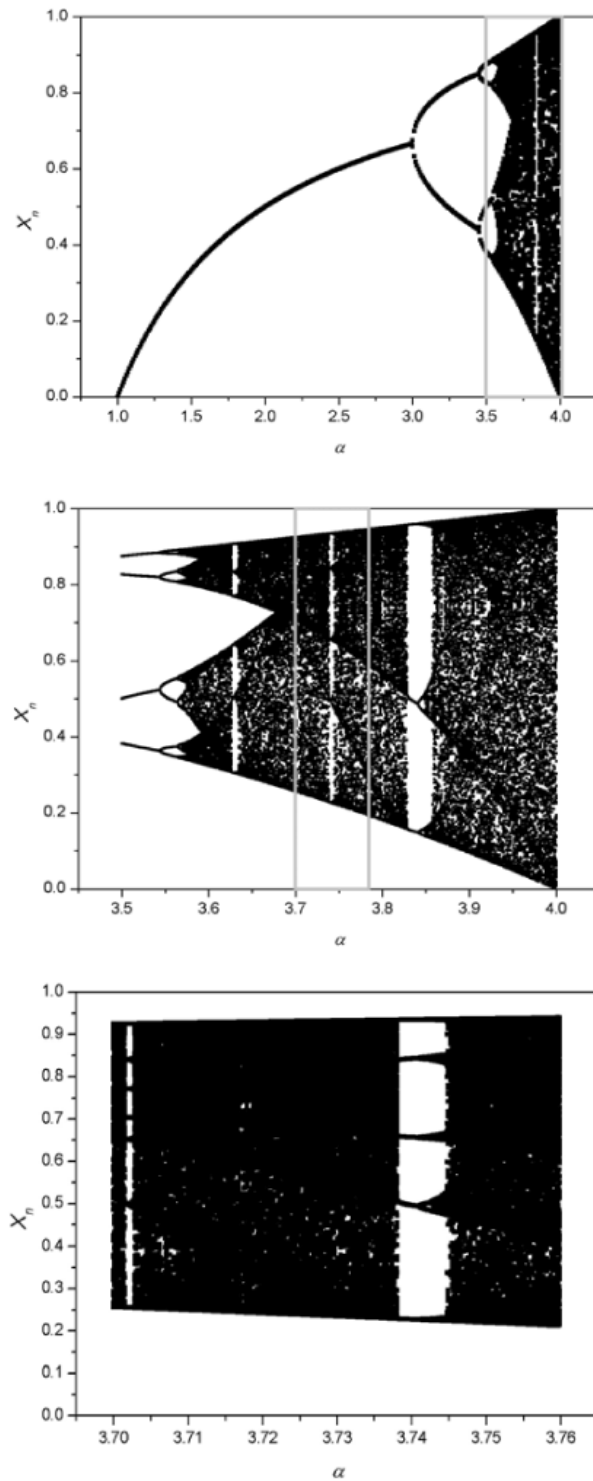


Figure 12. Bifurcation diagrams.

Figure 23 - Bifurcations diagrams of the logistic Map. This is a period doubling cascade way to chaos. Notice the periodic windows inside the regions of chaos, this is a classic characteristic of chaos, periodicity emerging from nowhere and disappearing again

Subregions within the bifurcation diagram look remarkably similar to each other and to the diagram as a whole. This self-similarity was shown to repeat itself at ever finer resolutions. Such behavior is characteristic of geometric entities called fractals and is quite common in iterated mappings. Interestingly enough, the distance between successive bifurcation points λ_n shrinks geometrically in such a fashion that the ratio of the intervals δ , approaches a constant value as n approaches infinity.

$$\delta = \frac{\lambda_n - \lambda_{n-1}}{\lambda_{n+1} - \lambda_n}$$

This constant, called Feigenbaum's constant, crops up repeatedly in self-similar figures and has an approximate value of :

4.669201609102990671853203820466201617258185577475768632745651343004134330211314
7371386897440239480138171659848551898151344086271420279325223124429888908908599449354
6323671341153248171421994745564436582379320200956105833057545861765222207038541064674
9494284981453391726200568755665952339875603825637225

Feigenbaum's constant can be used to predict when chaos will arise in such systems before it ever occurs. Not only does Feigenbaum's constant reappear in other figures, but so do many other characteristics of the bifurcation diagram. In fact, remarkably similar diagrams can be generated from any smooth, one-dimensional, non-monotonic function when mapped on to itself. A circle, ellipse, sine, or any other function with a local maximum will produce a bifurcation diagram with period-doublings whose ratios approach " δ ". Together with a second constant " α ", the scaling factor " δ " demonstrates universality previously unknown in mathematics: metrical universality. The behaviour of the quadratic map is typical for many dynamical systems.

The constant α reflects the scaling of the dependent variable, where smaller replicas of the system response successively appear with each bifurcation.

$$\alpha = \lim_{n \rightarrow \infty} \frac{d_n}{d_{n+1}}$$

Where d_n is the value of the nearest cycle element to 0 in the 2^n cycle. The value of α asymptotically converges to 2.5029, and this value allows prediction of the size of the system response with each bifurcation.

In general bifurcations can be classified based on the mechanisms that create them

- Local Bifurcations due to an attractor losing stability and one or more different attractors may become stable
- Global bifurcations due to manifolds interplay (multiple attractors)
- Bifurcations due to non-smoothness

3.2.2 Local Bifurcations

A local bifurcation occurs when a parameter change causes the stability of an equilibrium (or fixed point) to change. By looking at the eigenvalues at the local linearization we can define an area on the complex plane within which if the eigenvalues are located, the attractor is stable. In the time-continuous case, this stability area is the half-plane left of the imaginary axis, whereas in the time-discrete case it is the unit circle around the origin

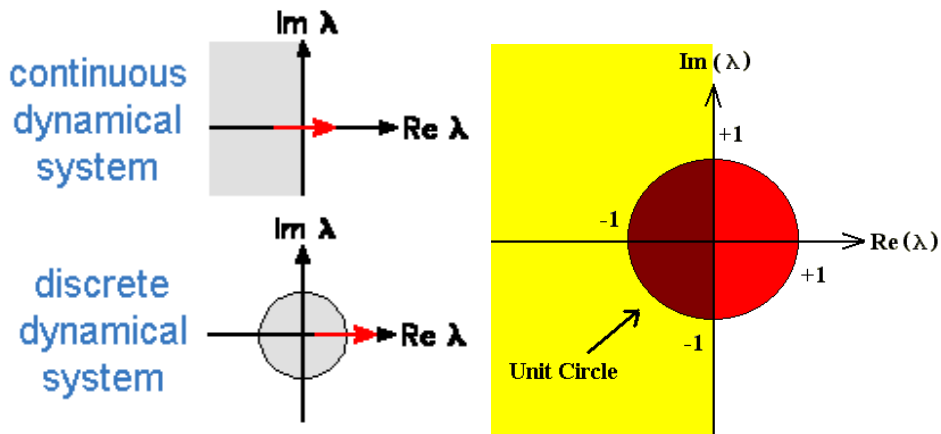


Figure 24 - boundaries of stability in the complex plane defined by the eigenvalues in discrete and continuous systems

Two things can happen:

- Eigenvalues becoming positive for flows
- Eigenvalues becoming greater than the unit circle for maps (slope becomes < -1 period doubling, slope becomes $> +1$ saddle node for 1D maps)

So the attractor will become unstable if the eigenvalues cross the imaginary axis for continuous systems or if the eigenvalues go out of the unit circle for discrete systems. Depending on the type of eigenvalues and the direction they cross the boundaries different types of bifurcations occur. Below we see the generic forms of those types of bifurcations.

The phase space variable is u . The control parameter is μ . The bifurcation point is at $\mu = 0$. The direction of motion in the one-dimensional phase space is shown by arrows. Stable (unstable) fixed points are drawn as red solid (dotted) lines. The normal forms are shown in blue. The term *codimension* counts the number of control parameters for which fine tuning is necessary to get such a bifurcation

saddle-node bifurcation

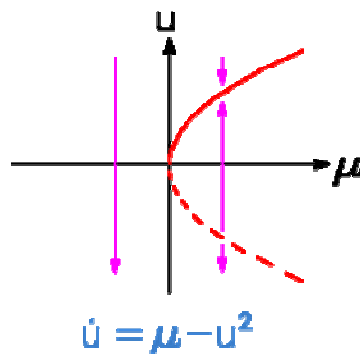


Figure 25 - The generic case of a saddle-node bifurcation

A saddle-node bifurcation. The minima and maxima of μ as a function of the curve length denote saddle-node bifurcations where a stable fixed point annihilates with an unstable one (a saddle in more than one dimension). A combination of a minimum and a maximum lead to the phenomenon of bistability where in a certain interval of the control parameter, two stable attractors exist with an unstable one in-between. When the interval of bistability is left the attractor disappears in a saddle-node bifurcation, and the system suddenly jumps to another attractor.

transcritical bifurcation

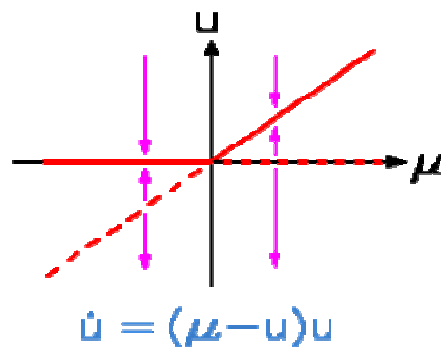


Figure 26 - the generic case of a transcritical bifurcation

The transcritical bifurcation occurs when in the combined space of phase space and controlparameter space two different manifolds of fixed points cross each other. At the crossing point the fixed points exchange their stability property. That is, the unstable fixed point becomes stable and vice versa. Note, that beyond the bifurcation point the number of fixed points has not changed contrary to saddle-node bifurcation where two fixed points appear or disappear. A transcritical bifurcation is not a generic bifurcation in a phase space with more than one dimension because it is unlikely that two lines cross each other in a space with more than two dimensions.

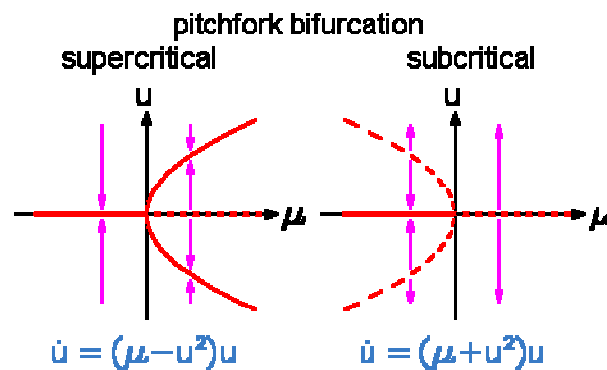


Figure 27 - The generic case of a pitchfork bifurcation

Pitchfork bifurcations are possible in dynamical systems with an inversion or reflection symmetry. That is, an equation of motion that remains unchanged if one changes the sign of all phase space variables (or at least for one). An example is the undriven pendulum. Usually, such a system has a symmetric fixed point (or limit cycle). Pitchfork bifurcations are the generic bifurcations when such a symmetric solution changes its stability. The bifurcating solution does not have the full symmetry of the equation of motion. This phenomenon is called broken symmetry. A solution with a broken symmetry does not occur in isolation because the broken symmetry applied onto such a solution generates a new solution where the same symmetry is broken. All such solutions build a family. Therefore, always *two* fixed points with a broken symmetry bifurcate at once in a pitchfork bifurcation. Both are either stable (supercritical pitchfork bifurcation) or unstable (subcritical pitchfork bifurcation)

The bifurcation diagrams of a Hopf and a period doubling bifurcation are similar to the diagram of a pitchfork bifurcation. That is, the bifurcating periodic or quasiperiodic solution is either stable (supercritical bifurcation) or unstable (subcritical bifurcation). Again, a broken symmetry is responsible for this similarity. Here, it is the invariance of the dynamical system against translations in time.

Examples

Saddle node bifurcation

We are considering the next map due to its simplicity to study the saddle node bifurcation. The equation is:

$$x_{n+1} = a - x_n^2$$

The location of the fixed points can be found by setting $x_{n+1} = x_n$. The equation becomes:

$$x_n^* = a - (x_n^*)^2$$

The roots would be the positions. The roots are:

$$x_{1,2}^* = -\frac{1 \pm \sqrt{1 + 4a}}{2}$$

To find the stability of the fixed points again we look at the slope (derivative) at each point. At $a = -\frac{1}{4}$ there is only one fixed point $x_n^* = \frac{1}{2}$ with slope $\frac{dx_{n+1}}{dx_n} = -2x_n = 1$, so it is stable. Two new fixed points begin to exist beyond the parameter value of $a = -\frac{1}{4}$, One stable and one unstable with opposite slopes. This is called a saddle-node bifurcation or tangent bifurcation. It happens on the logistic map also when the periodic windows come into existence.

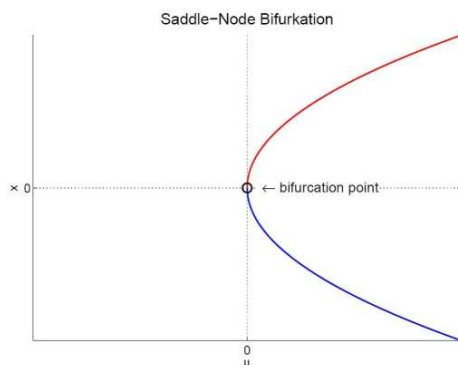


Figure 28 - The axes are placed so that the bifurcating point is at the center, two new fixed points are born, one stable and one unstable

Transcritical bifurcation

This bifurcation can be studied in the logistic map and it happens when $\mu=1$. The 2 fixed points $x_1^* = 0$, $x_2^* = 1 - \frac{1}{\mu}$, exchange stability at $\mu=1$. This can be seen by looking the slopes:

$$\text{at } x_1^* = 0 \Rightarrow \frac{dx_{n+1}}{dx_n} = \mu \text{ and at } x_2^* = 1 - \frac{1}{\mu} \rightarrow \frac{dx_{n+1}}{dx_n} = 2 - \mu$$

These points are existing all through but exchange stability at $\mu=1$

Pitchfork bifurcation

Another type of bifurcation can be demonstrated on the following map. The equation is:

$$x_{n+1} = (1 + \mu)x_n - x_n^3$$

The fixed points would be located where $x_{n+1} = x_n$. So we can find them by solving:

$$x_n^* = (1 - \mu)x_n^* - (x_n^*)^3$$

There are 3 fixed points:

$$x_1^* = 0, \quad x_2^* = \sqrt{\mu}, \quad x_3^* = -\sqrt{\mu}$$

We can check their stability by looking the slope. The slope in general would be:

$$\frac{dx_{n+1}}{dx_n} = (1 - \mu) - 3x_n^2$$

And by replacing each fixed point into the equation of slope we can conclude that x_0^* will be stable for for $-2 < \mu < 0$. At $\mu=0$ the slope at that point becomes greater than 1 and x_0^* becomes unstable, then 2 new points are born because x_2^* and x_3^* become real. And we can see from the slope that both are stable for $0 < \mu < 1$.

This looks like a period doubling bifurcation but here x_0^* became unstable when the slope became greater than one instead less than -1 and 2 stable period-1 orbits became stable, not 1 period-2 orbit.

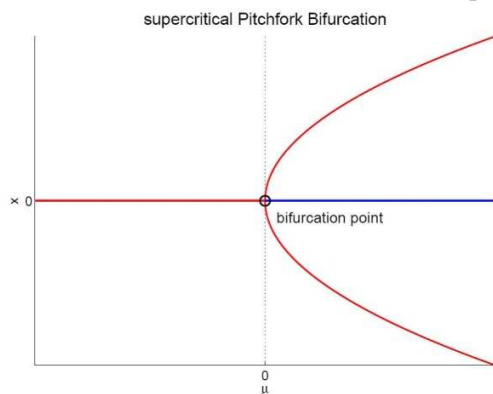


Figure 29 - One fixed point loses stability and two stable fixed points are born

3.2.3 Global Bifurcations

Global bifurcations occur when 'larger' invariant sets, such as periodic orbits, collide with equilibria. This causes changes in the topology of the trajectories in the phase space which cannot be confined to a small neighborhood, as is the case with local bifurcations. In fact, the changes in topology extend out to an arbitrarily large distance (hence 'global').

in cases of multiple attractors local linearization is not enough. To study these bifurcations some kind of tracking of the manifolds outside the local linearization must be done. There are 2 ways:

For unstable manifolds we can keep track of an initial condition starting on the manifold inside the local linearization area and watch it as the system evolves. The iterations will fall onto the manifold.

For stable manifolds we can't do that directly because the initial conditions will converge. But we can do it backwards if the map is invertible.

Three particular things might happen caused by interplay of stable and unstable manifolds :

- Boundary crisis (stable attractor crosses basin of attraction)
- Interior crisis (chaotic attractor crosses basin of attraction)
- Fractal basin boundary (manifolds cross)

The attractor loses stability after a boundary crisis, becomes bigger after interior crisis or a fractal nature is embedded to its geometry if manifold cross. The later is the way of chaos to create information in natural systems.

By studying the behaviour of fixed points and their manifolds we can make some conclusions

- Attractors lie on unstable manifolds (attracting behaviour)
- Stable manifolds form the basin boundary (repelling behaviour)
- Manifolds cannot intersect themselves (physically impossible)
- Manifolds can cross each other and one crossing means infinite crossings afterwards.

Applying these backwards we can say that if there are 2 attractors there should be a saddle fixed point one on each side of its unstable manifold. So saddles are the cornerstone of complicated dynamics.

Most bifurcations in natural systems can be analyzed by studying simpler less-dimensional discrete systems using the following techniques.

Centre manifold theorem:

Conclusions about dynamics and stability of a n-dimensional system can be made by studying a system with dimensions exactly the number of eigenvalues with 0 real part . the space associated with these eigenvalues is called centre manifold.

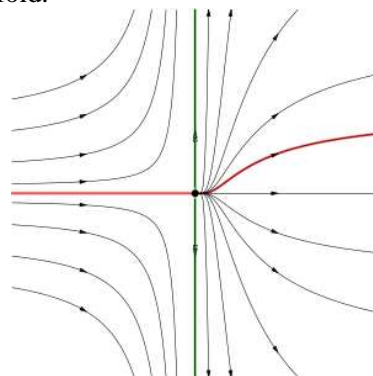


Figure 30 - Stable manifold represented with green

It helps to reduce the dimensionality of the phase space. The centre manifold theorem says, the dynamics can be projected onto the centre manifold without losing any significant aspect of the dynamics. Thus, the dynamics near a bifurcation can be described by an effective dynamics in a less-dimensional

subspace. Hopf-bifurcations need a two-dimensional phase space. This is exactly the minimum dimension for limit cycles in continuous dynamical systems and for quasiperiodic orbits in discrete dynamical systems. Period-doubling bifurcations need only a one-dimensional phase space.

Transformation to normal form:

The dynamics projected onto the centre manifold can be transformed to so-called normal forms by a nonlinear transformation of the phase space variables. The method of normal forms provides a way of finding a coordinate system in which the dynamical system takes the “simplest” form. Three important characteristics should become apparent.

- The method is local in the sense that the coordinate transformations are generated in a neighborhood of a known solution. The known solution will be a fixed point. However, when we develop the theory for maps, the results will have immediate applications to periodic orbits of vector fields by considering the associated Poincaré map.
- In general, the coordinate transformations will be nonlinear functions of the dependent variables. However, the important point is that the second-order transformations are found by solving a sequence of *linear* problems.
- The structure of the normal form is determined entirely by the nature of the linear part of the vector field

Centre manifold example

Suppose a system with equations:

$$\begin{aligned}\dot{x} &= ax^2 + xy - xy^2 \\ \dot{y} &= -y + bx^2 + x^2y\end{aligned}$$

There is one equilibrium point located at (0,0). the jacobian of this system would be

$$J = \begin{bmatrix} 3ax^2 + y - y^2 & x - 2xy \\ 2bx + 2xy & -1 + x^2 \end{bmatrix}$$

and at (0,0) it becomes:

$$J \text{ at } (0,0) = \begin{bmatrix} 0 & 0 \\ 0 & -1 \end{bmatrix}$$

So the eigenvalues are:

$$\lambda_1 = 0 \text{ and } \lambda_2 = -1$$

The eigenvectors are:

$$[A - \lambda I][x] = [0] \xrightarrow{\text{yields}}$$

$$\begin{bmatrix} 1 & 0 \\ 0 & 0 \end{bmatrix} \begin{bmatrix} x \\ y \end{bmatrix} = \begin{bmatrix} 0 \\ 0 \end{bmatrix} \text{ for } \lambda_1$$

So the associated eigenvector is $x = 0$, which is the vertical axis and

$$\begin{bmatrix} 1 & 0 \\ 0 & -1 \end{bmatrix} \begin{bmatrix} x \\ y \end{bmatrix} = \begin{bmatrix} 0 \\ 0 \end{bmatrix} \text{ for } \lambda_2$$

So the associated eigenvector is $y = 0$, which is the horizontal axis.

We can see that the eigenvector associated with λ_2 is stable but we cannot conclude about the eigenvector associated with λ_1 .

To find the center manifold we set $y = h(x)$ for $|x|$ small and separate the eigenvalues :

$$\begin{aligned}\dot{x} &= Ax + f(x, h(x)) \\ \dot{y} &= Bh(x) + g(x, h(x))\end{aligned}$$

But also

$$\dot{y} = \frac{d}{dt}h(x) = \frac{dh}{dx} \frac{dx}{dt} = \dot{h}(x)[Ax + f(x, h(x))]$$

So these can be written as:

$$\dot{h}(x)[Ax + f(x, h(x))] - Bh(x) - g(x, h(x)) = 0$$

And this can be expressed as some function :

$$N(h(x)) = 0$$

The above is the equation of the center manifold for small oscillations. If we look at the original equations $h(x)$ could be any function but it will be approximated by the series $h(x) \approx h_2x^2 + h_3x^3 + \dots + \text{Higher order terms}$. Higher order terms can be ignored for small oscillations, so:

$$h(x) = h_2x^2 \text{ and } \dot{h}(x) = 2h_2x$$

If we replace in N we get:

$$2h_2x[ax^3 + h_2x^3 - h_2^2x^5] + h_2x^2 - bx^2 + h_2x^4 = 0$$

We need only the lowest term to be zero so $h_2x^2 - bx^2 = 0 \Rightarrow h_2 = b$, so h will be:

$$h(x) = bx^2 + \text{Higher order terms} = bx^2 \text{ for small } |x|$$

In the whole process Higher order terms are ignored because we talk about small oscillations. By replacing to the original equation we get:

$$\dot{x} = ax^3 + bx^3 + \text{Higher order terms} \approx (a + b)x^3$$

So the system will be stable as long as $a + b > 0$. So even if linearization failed we were able to pinpoint the behavior.

3.2.4 Non smooth maps

The systems described above are everywhere differentiable. Bifurcations may also occur in systems governed by two different sets of equations (not everywhere differentiable) When a fixed point crosses the boundary, the eigenvalues take a discrete jump. These bifurcations are called border collision bifurcations.

These systems are called nonsmooth. for example there is a large number of systems with some kind of switch interaction.

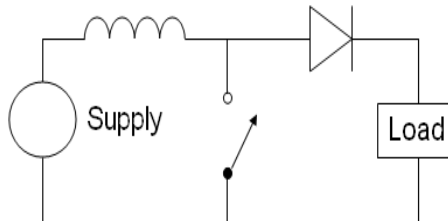


Figure 31 - A simple switch system. every system that contains a switch is considered nonlinear.

These systems have to be discretized in order to be studied by a Poincare section. they are represented as:

$$\dot{x} = \begin{cases} f_1(x), & \text{if } x \in R_1 \\ f_2(x), & \text{if } x \in R_2 \end{cases}$$

These bifurcations can be studied by using local linearization before and after collision and some coordinate transformations to obtain the piecewise linearized map which is an easy way to see how a fixed point changes by crossing the border (primary partitioning).

Three things may happen:

- Stable fixed point remains stable
- A pair or more fixed points is born
- A stable fixed point becomes unstable

These bifurcations look similar to those of smooth systems but here the cause is different.

3.3 Applications

The Lorenz equation

The most famous attractor is undoubtedly the Lorenz attractor, a three dimensional object whose body plan resembles a butterfly or a mask. The Lorenz attractor, named for its discoverer Edward N. Lorenz, arose from a mathematical model of the atmosphere.

Imagine a rectangular slice of air heated from below and cooled from above by edges kept at constant temperatures. This is our atmosphere in its simplest description. The bottom is heated by the earth and the top is cooled by the void of outer space. Within this slice, warm air rises and cool air sinks. In the model as in the atmosphere, convection cells develop, transferring heat from bottom to top.

The equations of the system are :

$$\begin{aligned}\dot{x} &= \sigma(x - y) \\ \dot{y} &= -xz + rx - y \\ \dot{z} &= xy - bz\end{aligned}$$

The state of the atmosphere in this model can be completely described by three time-evolving variables

- x the convective flow
- y the horizontal temperature distribution
- z the vertical temperature distribution

with three parameters describing the character of the model itself

- σ the ratio of viscosity to thermal conductivity
- r the temperature difference between the top and bottom of the slice
- b the width to height ratio of the slice

To study the system we must find the equilibrium points where we have good understanding of the behavior. For this example we set $b = -\frac{8}{3}$ and $\sigma = -10$ and let r vary. There are 3 equilibrium points:

$$A = (0, 0, 0), \quad B = (\sqrt{b(r-1)}, \sqrt{b(r-1)}, r-1), \quad C = (-\sqrt{b(r-1)}, -\sqrt{b(r-1)}, r-1)$$

We can see that if $r < 1$ the Eq.Point becomes imaginary, but the position must be real number so the Eq.Points B and C do not exist until r reaches 1. A exist all the time.

To understand more we have to look at the stability of A,B and C. So we obtain the the jacobian metrics which is the local linearization at each point. In general the metrics would be:

$$J = \begin{bmatrix} -\sigma & \sigma & 0 \\ -z + r & -1 & -x \\ y & x & -b \end{bmatrix}$$

At A=(0,0,0) this becomes:

$$J \text{ at } (0,0,0) = \begin{bmatrix} -10 & 10 & 0 \\ r & -1 & 0 \\ 0 & 0 & -8/3 \end{bmatrix}$$

There are 3 associated eigenvalues: $\lambda_1 = -\frac{8}{3}$, $\lambda_2 = -\frac{11+\sqrt{81+40r}}{2}$, $\lambda_3 = -\frac{11-\sqrt{81+40r}}{2}$

So λ_1 will always be stable but λ_2 and λ_3 depend on r. for $r=1$ λ_2 is at 0 and λ_3 is at -11 so both are stable but λ_2 is on the border of stability and instability. For $r > 1$ it will cross the boundary so the Eq.Point will become unstable but it will still exist because the eigenvalues are real.

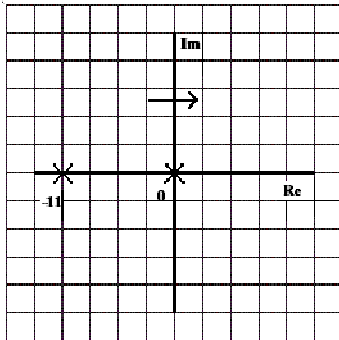


Figure 32 - At $r = 1$ the eigenvalue crosses the stability boundary and the fixed point becomes unstable

So at $r=1$ A became unstable and B,C came to existence. A became unstable in the direction of the eigenvalue that crossed the boundary. To understand how this expansion evolves we must check the stability of the B and C to see if they are attracting or repeling fixed points. Because they are symmetric we can check one of them and apply the conclusions to the other too. By Applying the above procedure we can see that the eigenvalues will be :

$$\lambda_1 = \text{real and negative} , \quad \lambda_2, \lambda_3 = \text{complex conjugates with negative real part}$$

From these we can conclude that the points B and C will be stable because they are attracting due to the negative real parts, with a spiral behavior due to the complex eigenvalues. The spirals are trapped in a complex plane defined by the real and imaginary part of complex eigenvalues.

This is a clear example (and one of the first ones) of the difference between linear and non-linear dynamics. In the first case if a stable Eq. point lose stability the system collapses. In the non-linear case the system jumps from a stable behavior to another stable behavior. In the Lorenz example this can be seen as the A point becomes unstable and 2 new Eq. points are born and stable.

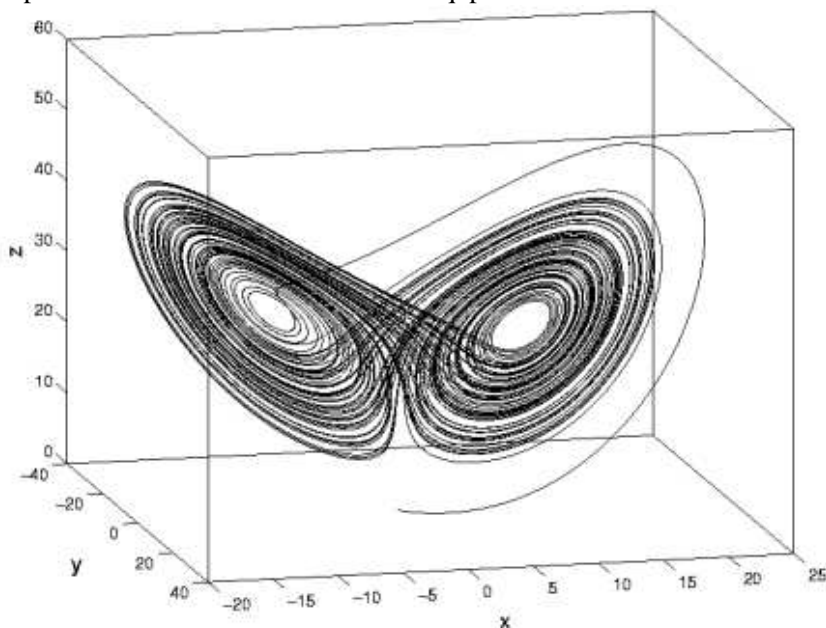


Figure 33 - The famous Lorenz attractor. The butterfly effect was named due to the similarity of this attractor to butterfly wings

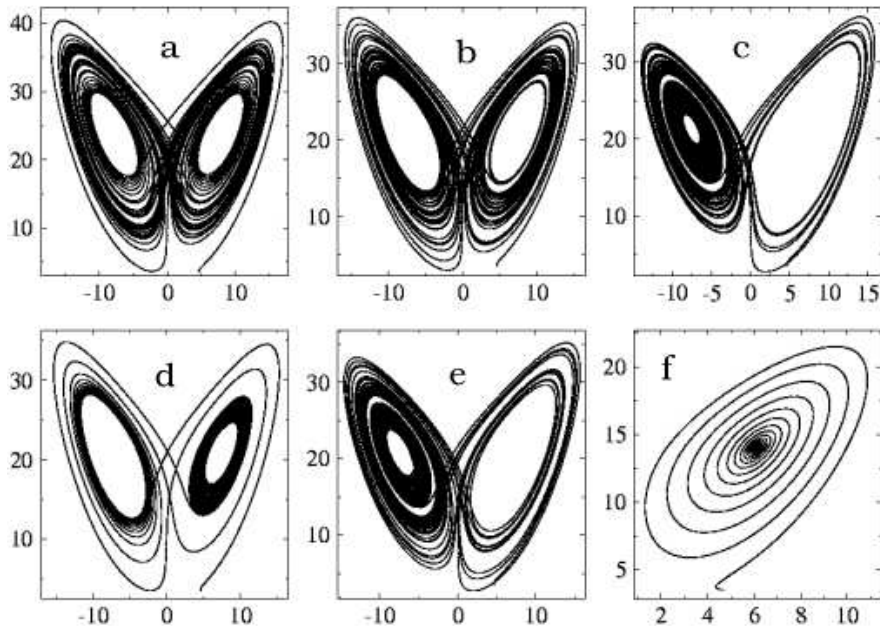


Figure 34 - Different perspectives of the Lorenz attractor at different stages of evolution

Increasing r further the parameter will cause mixing in the orbits. This is the famous Lorenz attractor (x, z) phase portrait for several asymptotic dynamics. (a) strange attractor; (b), (c), (d) and (e) asymptotic fixed point dynamics via chaotic transient; (f) fixed point

Logistic Map

The simple logistic equation is a formula for approximating the evolution of an animal population over time. Many animal species are fertile only for a brief period during the year and the young are born in a particular season. For this reason, the system might be better described by a discrete difference equation than a continuous differential equation, obtained by placing a Poincaré section in the original flow. Since not every existing animal will reproduce (a portion of them are male after all), not every female will be fertile, not every conception will be successful, and not every pregnancy will be successfully carried to term; the population increase will be some fraction of the present population.

The equation is:

$$x_{n+1} = \mu x_n (1 - x_n)$$

where " μ " is the growth rate or fecundity

In this example the period doubling bifurcation mechanism is demonstrated.

The position of the fixed points would be where $x_{n+1} = x_n$, so we can locate them by solving:

$$x_n^* = \mu x_n^* (1 - x_n^*)$$

The fixed points are at 0 and $1 - \frac{1}{\mu}$.

For different values of μ we get sequences of points that will either converge or diverge to these points. Because this map can be visualized it is easier to look at the plot

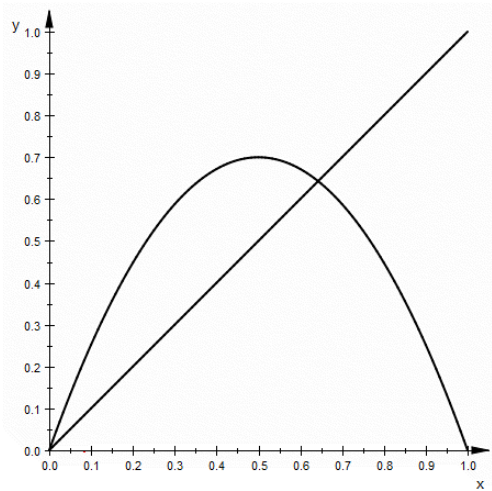


Figure 35 - Relation of the current with the next state. Fixed points are located on the 45 degree line at the point where it intersects with the graph of the map

The fixed points of the map lie on the 45 degree line because that's where $x_{n+1} = x_n$. The height of the curve depends on the value of μ . So we can see that changing μ will move the fixed point on the curve.

Here it also easy to see the convergence of different orbits by taking steps between the curve and the 45 degree line. It is clear from the plot that the condition of convergence is the slope of the map at that point to be less than 1. So we can check the stability of the equilibrium point by looking at the derivative at that point.

The derivative in general would be:

$$\frac{dx_{n+1}}{dx_n} = \mu - 2\mu x_n$$

- For the fixed point at 0 the slope is $\frac{dx_{n+1}}{dx_n} = \mu$. It only depends in μ , so it will be stable for $0 < \mu < 1$, and the orbits will converge here.
- For the fixed point at $\mu - \frac{1}{\mu}$ the slope is $\frac{dx_{n+1}}{dx_n} = 2 - \mu$. This point will be stable for $1 < \mu < 3$ and orbits will start converge here .

So period 1 is stable for $0 < \mu < 3$, but after 3 both points will become unstable so period-1 will become unstable.

For values greater than 3, the obrits start to converge to 2 new points. This implies a period doubling bifurcation. We can find the location of the new fixed points by setting $x_{n+2} = x_n$, and check if period-2 is stable.

$$x_{n+1} = \mu x_n (1 - x_n)$$

$$x_{n+2} = \mu x_{n+1} (1 - x_{n+1})$$

If we replace we get:

$$x_{n+2} = \mu(\mu x_n (1 - x_n)) (1 - (\mu x_n (1 - x_n)))$$

And the positions of the fixed points will be the solutions of this equation:

$$x_n^* = \mu(\mu x_n^*(1 - x_n^*)) \left(1 - (\mu x_n^*(1 - x_n^*))\right)$$

This is 4th order polynomial equation but we already know 2 roots which are the previous fixed points because the fixed points of period 1 are also fixed points of period 2, there are still there but unstable. If we take out the 2 roots then the polynomial becomes 2nd order and can be solved easier. So the above equation becomes:

$$x_{n+2} = x_n(1 - \mu + \mu x_n)(1 + \mu - \mu x_n - \mu^2 x_n + \mu^2 x_n^2)$$

And the 2 new roots are:

$$x_{1,2}^* = \frac{1 + \mu \pm \sqrt{\mu^2 - 2\mu - 3}}{2\mu}$$

These are the locations of the fixed points of period-2 orbit and we can see that they exist only for $\mu > 3$. Now we can check the stability of period-2 orbit by checking the slope of at the 2 new fixed points.

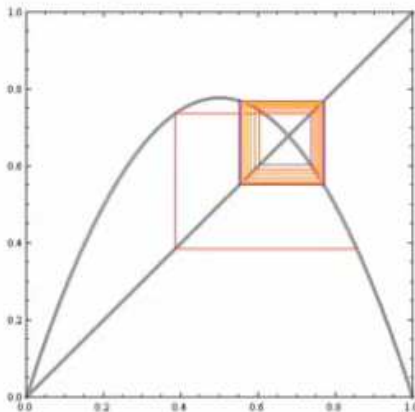


Figure 36 - the orbit settles into two new fixed points as the parameter is increased

We don't need to check the slope at each point separately, we can just look at the product of the 2 slopes to see if period-2 is stable. This is easier than doing it separately for all points. It can be written as

$$\frac{df}{dx} = \frac{df}{dg} \frac{dg}{dx} \xrightarrow{\text{yields}} f''(x) = f'(f(x))f'(x)$$

Where f is x_{n+2} and g is x_{n+1} . From that we can see that period-2 will be stable.

Again by looking at the plot for x_n and x_{n+2} we can see that easier. For values greater than 3 the curve bends and the intersections with the 45 degree line are doubling. More and more bends occur as we keep increasing μ .

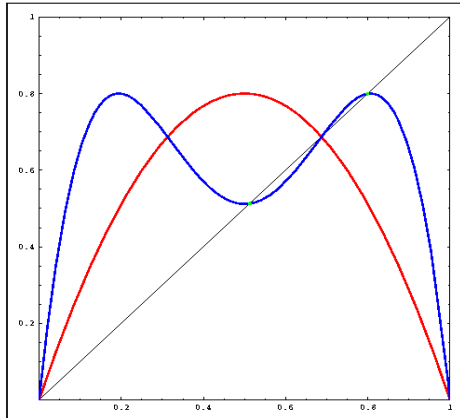


Figure 37 - Plot of the current state with the second iterate

This is called a period doubling cascade that ultimately leads to chaos and the mechanism for that is the period doubling bifurcations. In this example period doubling bifurcations happen due to the change of the parameter causing the slope become negative and destabilize the fixed point. But at that point 2 new fixed points are born, both stable and with slope 1.

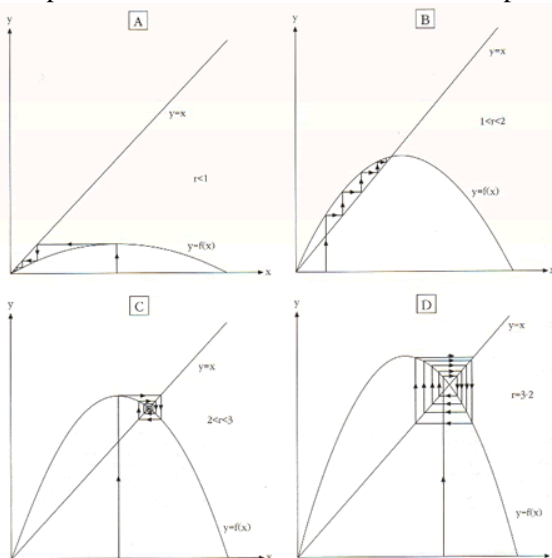


Figure 38 - Orbits for different parameter values and initial values. the height of the curve depends on μ , initial conditions are the starting points from the horizontal axis.

Henon map

The map was introduced by Michel Hénon as a simplified model of the Poincaré section of the Lorenz model. For the canonical map, an initial point of the plane will either approach a set of points known as the Hénon strange attractor, or diverge to infinity. The Hénon attractor is a fractal, smooth in one direction and a Cantor set in another. It is one of the most studied examples of dynamical systems that exhibit chaotic behavior.



Figure 39 - the graph produced by placing a Poincaré section to the Lorenz attractor. The result is a fractal object

The equations are:

$$x_{n+1} = A - x_n^2 + B y_n$$

$$y_{n+1} = x_n$$

The fixed points can be found where $\begin{cases} x_{n+1} = x_n \\ y_{n+1} = y_n \end{cases}$, so their location would be the solutions of the equations:

$$x^* = A - (x^*)^2 + B y^*$$

$$y^* = x^*$$

If we set $B = 0.4$ and let A vary the equations become:

$$(x^*)^2 + 0.6x^* - A = 0$$

$$y^* = x^*$$

There are 2 fixed points at the positions:

$$x_{1,2}^* = -0.3 \pm \sqrt{0.09 + A}$$

$$y_{1,2}^* = x_{1,2}^*$$

Their existence depends on A so we can see that they do not exist for $A < -0.09$. After that we can check their stability by looking at the eigenvalues obtained by the Jacobian (instead of slope that was the case for 1D). To make calculations easier we can check the stability at $A = 0$. So in general the Jacobian would be:

$$J = \begin{bmatrix} -2x^* & 0.4 \\ 1 & 0 \end{bmatrix}$$

And the eigenvalues would be:

$$\lambda_{1,2} = -x^* \pm \sqrt{(x^*)^2 + 0.4}$$

By replacing $x_{1,2}^*$ we can find the associated eigenvalues at those points:

$$\text{for } \begin{bmatrix} x_1^* \\ y_1^* \end{bmatrix} = \begin{bmatrix} 0 \\ 0 \end{bmatrix}, \rightarrow \lambda_{1,2} = \pm\sqrt{0.4}$$

$$\text{for } \begin{bmatrix} x_2^* \\ y_2^* \end{bmatrix} = \begin{bmatrix} -0.6 \\ -0.6 \end{bmatrix}, \rightarrow \lambda_{1,2} = 0.6 \pm \sqrt{0.76}$$

In the first case the eigenvalues are inside the unit circle so $\begin{bmatrix} x_1^* \\ y_1^* \end{bmatrix}$ is stable. In the case of $\begin{bmatrix} x_2^* \\ y_2^* \end{bmatrix}$, one eigenvalue is inside and one outside of the unit circle, so this is unstable.

This is the the equivelant saddle node bifurcation in 2D systems. Here two new fixed points are born, one stable and another unstable when A reaches -0.09 from the negative side. By increasing A further the eigenvalues of the stable fixed point will move towards -1 and finally become unstable.

To check the stability of the period 2 orbit we check the second itterate of the map:

$$x_{n+2} = A - x_{n+1}^2 + 0.4y_{n+1}$$

$$y_{n+2} = y_{n+1}$$

$$\begin{bmatrix} x_{n+2} = A - x_{n+1}^2 + 0.4y_{n+1} \\ y_{n+2} = y_{n+1} \end{bmatrix} \rightarrow \begin{bmatrix} x_{n+2} = A - (A - x_n^2 + By_n)^2 + 0.4x_n \\ y_{n+2} = A - x_n^2 + By_n \end{bmatrix}$$

This is a 4th order polyonimal but we allready have the 2 roots as previous fixed points. And if we calculate we can see that there are 2 new fixed points which are stable.

As a conclusion we can see that when eigen values are become exactly one, approaching from the positive side, a saddle node bifurcation occurs and 2 new fixed points one stable and onother unstable are born. If they become 1 from the negative side the 2 fixed points will come closer and when they collide and dissappear. In both cases eigenvalues after +1 do not exist but they can become less than -1.

Rossler map

Some of the Rössler attractor's elegance is due to two of its equations being linear; setting $z = 0$, allows examination of the behavior on the x,y plane

Type equation here.

The stability in the x,y plane can then be found by calculating the eigenvalues of the Jacobian $\begin{pmatrix} 0 & -1 \\ 1 & a \end{pmatrix}$, which are:

$$\lambda_{1,2} = a \pm \frac{\sqrt{a^2 - 4}}{2}$$

From this, we can see that when $0 < a < 2$, the eigenvalues are complex and both have a positive real component, making the origin unstable with an outwards spiral on the x,y plane. Now consider the z plane behavior within the context of this range for a . So long as x is smaller than c , the c term will keep the orbit close to the x,y plane. As the orbit approaches x greater than c , the z -values begin to climb. As z climbs, though, the $-z$ in the equation for dx / dt stops the growth in x .

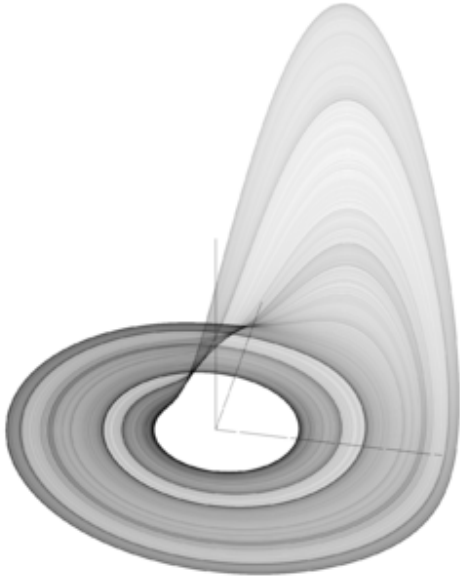


Figure 40 - The rossler attractor in 3D

In order to find the fixed points, the three Rössler equations are set to zero and the (x,y,z) coordinates of each fixed point were determined by solving the resulting equations. This yields the general equations of each of the fixed point coordinates:

$$x = \frac{c \pm \sqrt{c^2 - 4ab}}{2}$$

$$y = -\left(\frac{c \pm \sqrt{c^2 - 4ab}}{2a}\right)$$

$$z = \frac{c \pm \sqrt{c^2 - 4ab}}{2a}$$

This in turn can be used to show the actual fixed points for a given set of parameter values

$$\left(\frac{c + \sqrt{c^2 - 4ab}}{2}, \frac{-c - \sqrt{c^2 - 4ab}}{2a}, \frac{c + \sqrt{c^2 - 4ab}}{2a}\right)$$

$$\left(\frac{c - \sqrt{c^2 - 4ab}}{2}, \frac{-c + \sqrt{c^2 - 4ab}}{2a}, \frac{c - \sqrt{c^2 - 4ab}}{2a}\right)$$

One of these fixed points resides in the center of the attractor loop and the other lies comparatively removed from the attractor.

The stability of each of these fixed points can be analyzed by determining their respective eigenvalues and eigenvectors. Beginning with the Jacobian:

$$\begin{pmatrix} 0 & -1 & -1 \\ 1 & a & 0 \\ z & 0 & x - c \end{pmatrix}$$

The eigenvalues can be determined by solving the following cubic:

$$-\lambda^3 + \lambda^2(\alpha + x - c) + \lambda(ac - ax - 1 - z) + x - c + az = 0$$

For the centrally located fixed point, Rössler's original parameter values of $a = 0.2, b = 0.2,$ and $c = 5.7$ yield eigenvalues of $\lambda_1 = 0.097 + 0.995i, \lambda_2 = 0.097 - 0.995i, \lambda_3 = -5.687$

The magnitude of a negative eigenvalue characterizes the level of attraction along the corresponding eigenvector. Similarly the magnitude of a positive eigenvalue characterizes the level of repulsion along the corresponding eigenvector. The eigenvectors corresponding to these eigenvalues are:

$$v_1 = \begin{pmatrix} 0.707 \\ -0.072 + 0.703i \\ 0.004 + 0.0007i \end{pmatrix}, v_2 = \begin{pmatrix} 0.707 \\ -0.072 - 0.703i \\ 0.004 - 0.0007i \end{pmatrix}, v_3 = \begin{pmatrix} 0.168 \\ -0.028 \\ 0.985 \end{pmatrix}$$

These eigenvectors have several interesting implications. First, the two eigenvalue/eigenvector pairs (v_1 and v_2) are responsible for the steady outward slide that occurs in the main disk of the attractor. The last eigenvalue/eigenvector pair is attracting along an axis that runs through the center of the manifold and accounts for the z motion that occurs within the attractor.

Chapter 4 - Fractals

4.1 Introduction

The mathematics behind fractals began to take shape in the 17th century when a mathematician and philosopher Gottfried Leibniz considered recursive self-similarity (although he made the mistake of thinking that only the straight line was self-similar in this sense).

It was not until 1872 that a function appeared whose graph would today be considered fractal, when Karl Weierstrass gave an example of a function with the non-intuitive property of being everywhere continuous but nowhere differentiable. In 1904, Helge von Koch, dissatisfied with Weierstrass's abstract and analytic definition, gave a more geometric definition of a similar function, which is now called the Koch curve. Waclaw Sierpiński constructed his triangle in 1915 and, one year later, his carpet. The idea of self-similar curves was taken further by Paul Pierre Lévy, who, in his 1938 paper *Plane or Space Curves and Surfaces Consisting of Parts Similar to the Whole* described a new fractal curve, the Lévy C curve. Georg Cantor also gave examples of subsets of the real line with unusual properties—these Cantor sets are also now recognized as fractals.

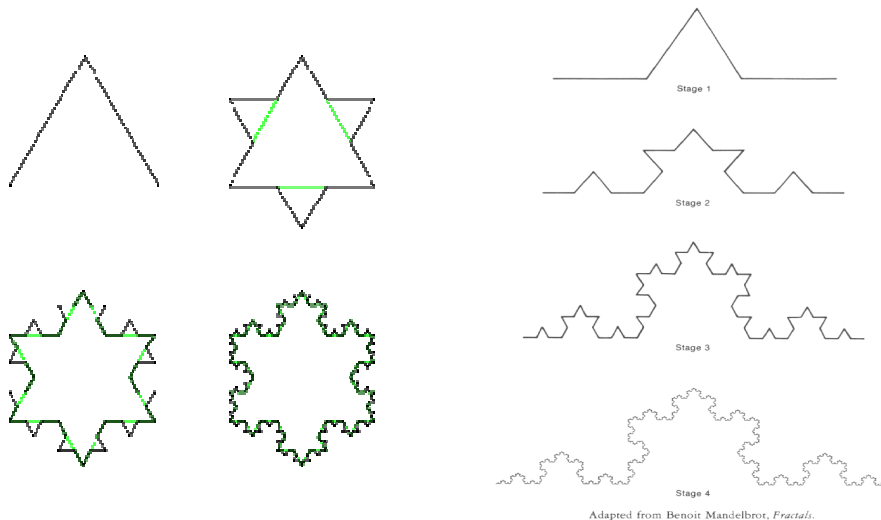
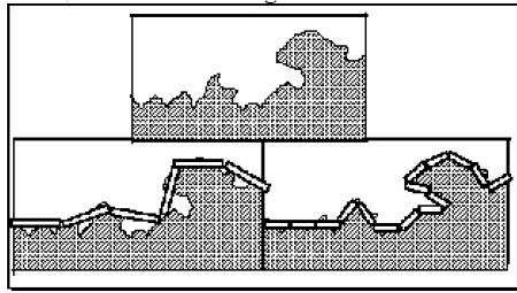


Figure 41 - different fractal objects. koch triangle, koch flake and koch line. all based on the same reapeative procedure

Iterated functions in the complex plane were investigated in the late 19th and early 20th centuries by Henri Poincaré, Felix Klein, Pierre Fatou and Gaston Julia. Without the aid of modern computer graphics, however, they lacked the means to visualize the beauty of many of the objects that they had discovered.

In the 1960s, Benoît Mandelbrot started investigating self-similarity in papers such as *How Long Is the Coast of Britain? Statistical Self-Similarity and Fractional Dimension*, which built on earlier work by Lewis Fry Richardson. Finally, in 1975 Mandelbrot coined the word "fractal" to denote an object whose Hausdorff–Besicovitch dimension is greater than its topological dimension. He illustrated this mathematical definition with striking computer-constructed visualizations. These images captured the popular imagination; many of them were based on recursion, leading to the popular meaning of the term "fractal".



Measuring the length of a coastline using rulers of varying lengths.

Figure 42 - The problem of measuring the coast line of England as introduced by B. Mandelbrot

If one tries to measure it there will be errors due to curves that define lines smaller than the scale of measurement. If we keep decreasing the scale the error will be smaller but always there will be more curves appearing. Each time we decrease the measure unit the length becomes bigger. As $\text{scale} \rightarrow 0$ the $\text{length} \rightarrow \text{Infinity}$. This defines an object with infinite length enclosing a finite area of the space (the sea in this case). Other example is the Koch curve and Koch flake

In general fractals have to do with geometry. And geometry deals with objects and with spaces. An n -dimensional object can be placed into a n -dimensional or greater space. Normal objects that we imagine and study like a triangle are idealized objects and cannot be found anywhere in nature. The spaces containing these shapes are also idealized (the distance between two points is defined as a line).

In the beginning of 20th century other spaces were introduced. Einstein used a curved space to describe the gravitational field in his general theory of relativity. But objects remained idealized.

Fractal geometry was developed to study objects and spaces that are not idealized and often is called geometry of nature because it deals with high complexity objects.

The difference between idealized and natural curves is that for idealized curves we assume that as we look closer and closer at smaller sections of the curve the more it resembles a straight line so the derivative can be calculated if we plot. But for natural lines that assumption is not true, they are continuous non differentiable objects.

The concepts of idealized objects will not help our understanding of these objects. A way to do that is by studying the dimension of an object or in other words how it "fills" space.

A fractal often has the following features:

- It has a fine structure at arbitrarily small scales.
- It is too irregular to be easily described in traditional Euclidean geometric language.
- It is self-similar (at least approximately or stochastically).
- It has a Hausdorff dimension which is greater than its topological dimension (although this requirement is not met by space-filling curves such as the Hilbert curve).
- It has a simple and recursive definition.
- Natural objects are fractals
- The concept of infinite surfaces enclosing finite volumes

The character of the space also matters because it shows how the objects behave in relation with the space they are embedded in.

Four common techniques for generating fractals are:

- Escape-time fractals – (also known as "orbits" fractals) These are defined by a formula or recurrence relation at each point in a space (such as the complex plane). Examples of this type are the Mandelbrot set, Julia set, the Burning Ship fractal, the Nova fractal and the Lyapunov fractal. The 2d vector fields that are generated by one or two iterations of

escape-time formulae also give rise to a fractal form when points (or pixel data) are passed through this field repeatedly.

- Iterated function systems – These have a fixed geometric replacement rule. Cantor set, Sierpinski carpet, Sierpinski gasket, Peano curve, Koch snowflake, Harter-Heighway dragon curve, T-Square, Menger sponge, are some examples of such fractals.
- Random fractals – Generated by stochastic rather than deterministic processes, for example, trajectories of the Brownian motion, Lévy flight, fractal landscapes and the Brownian tree. The latter yields so-called mass- or dendritic fractals, for example, diffusion-limited aggregation or reaction-limited aggregation clusters.
- Strange attractors – Generated by iteration of a map or the solution of a system of initial-value differential equations that exhibit chaos.

Fractals can also be classified according to their self-similarity. There are three types of self-similarity found in fractals:

- Exact self-similarity – This is the strongest type of self-similarity; the fractal appears identical at different scales. Fractals defined by iterated function systems often display exact self-similarity. For example, the Sierpinski triangle and Koch snowflake exhibit exact self-similarity.
- Quasi-self-similarity – This is a looser form of self-similarity; the fractal appears approximately (but not exactly) identical at different scales. Quasi-self-similar fractals contain small copies of the entire fractal in distorted and degenerate forms. Fractals defined by recurrence relations are usually quasi-self-similar. The Mandelbrot set is quasi-self-similar, as the satellites are approximations of the entire set, but not exact copies.
- Statistical self-similarity – This is the weakest type of self-similarity; the fractal has numerical or statistical measures which are preserved across scales. Most reasonable definitions of fractal trivially imply some form of statistical self-similarity. (Fractal dimension itself is a numerical measure which is preserved across scales.) Random fractals are examples of fractals which are statistically self-similar. The coastline of Britain is another example; one cannot expect to find microscopic Britains (even distorted ones) by looking at a small section of the coast with a magnifying glass.

Possessing self-similarity is not the sole criterion for an object to be termed a fractal. Examples of self-similar objects that are not fractals include the logarithmic spiral and straight lines, which do contain copies of themselves at increasingly small scales. These do not qualify, since they have the same fractal dimension as topological dimension.

4.2 Fractal dimension

Normally and based on common sense we think dimension as an integer. In general in order to measure something you also need fractions of integers. Also a distinction should be made between space dimension and object dimension. Dimension of an object and dimension of an embedding space are two different things. The dimension of the embedding space is the degrees of freedom.

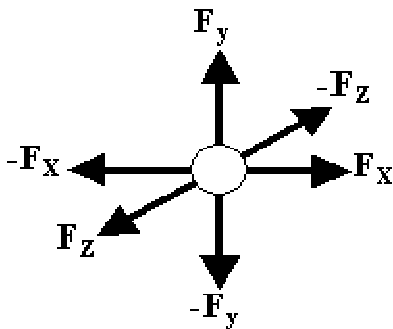


Figure 43 - The up-down, right-left and in-out movements represent 3 degrees of freedom or a 3-dimensional space.

So for an 1 dimensional space there is 1 degree of freedom, for a 2 dimensional space 2 degrees, for a 3 dimensional space 3 degrees etc...Because the degrees are integers, the dimension of spaces have an integer value. But that is not always true for objects. Because an object is embedded into a space its dimension must be understood by terms of "filling" the space.

This object is embedded in a 2d space. To understand how it fills the space we divide the space into smaller boxes and count the boxes it fills(integer). If we further divide these boxes the object covers more boxes.

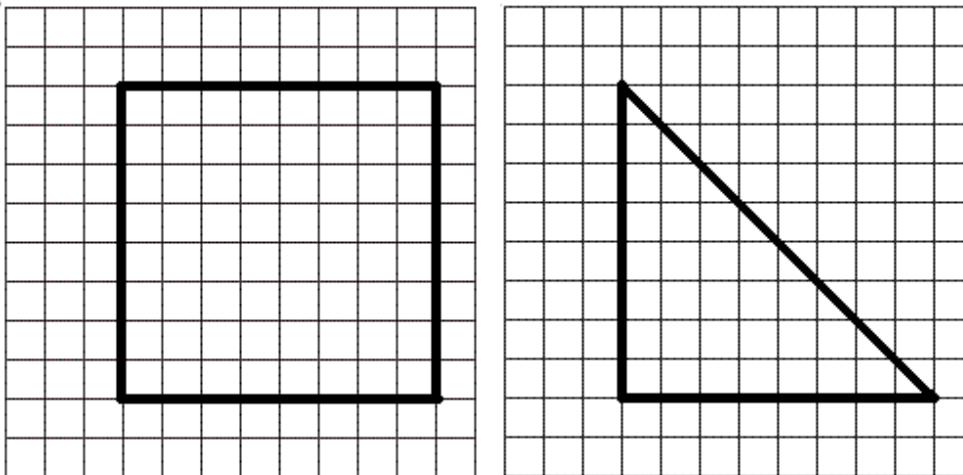


Figure 44 - dimension can be obtained by placing objects on a grid and applying box-counting

If N is the number of boxes it covers and x the length of the box side then the relation is:

$$N(x) = \left(\frac{1}{x}\right)^2 \text{ for a square}$$

We can apply the same procedure to a triangle. The boxes that are half covered are counted as 1.

$$N(x_1) = \frac{1}{2} \left(\frac{1}{x_1}\right)^2$$

For the triangle this number will not be equal to half of the one calculated for the square, it will be a little bigger because some squares are half but counted as 1. But as we divide the boxes further to infinity these numbers converge.

$$\text{So } \frac{1}{2}N(x) < N(x_1) \text{ initially but as } x_1 \rightarrow 0, \quad N(x_1) \rightarrow \frac{1}{2}N(x)$$

Same for a circle :

$$N(x_2) = \frac{\pi}{4} \left(\frac{1}{3}\right)^2$$

$$\text{And } \frac{\pi}{4}N(x) < N(x_2) \text{ initially but as } x_2 \rightarrow 0, \quad N(x_2) \rightarrow \frac{\pi}{4}N(x)$$

Notice that $N(x)$ remains independent as we become more accurate and for the above cases the number converges to 2.

In general

$$N(x) = k \left(\frac{1}{x}\right)^2 \text{ as } x \rightarrow 0$$

This function converges to a number that is an integer equal to the dimension of the space for idealized objects.

Further analyzing this, we can extract 2 because we know these are 2-dimensional objects. We assume infinite accuracy so we have

$$N(x) = k \left(\frac{1}{x}\right)^2 \text{ becomes } 2 = \frac{\ln N(x)}{\ln \frac{1}{x}} - \frac{\ln k}{\ln \frac{1}{x}}$$

The second part becomes 0 as $x \rightarrow 0$ so

$$d = \frac{\ln N(x)}{\ln \frac{1}{x}}$$

this gives the dimension of any object. This can be applied to natural objects too.

So the concept of dimension is at what number the relationship converges as $x \rightarrow 0$.

But in natural objects the number will always converge to a non integer number. This is called fractional dimension, so fractals are objects with fractional dimension. For n -dimensional spaces this number will converge to a number between $n-1$ and n if the object is a fractal. Only idealized objects take exactly the dimension of the space. for example the dimension of a cube in a 3-dimensional space converges to 3 as $x \rightarrow 0$.

This number shows the differences of a natural object compared to an idealized. In other words it shows how curved, bended, twisted etc the object is. Usually these differences are ignored for simplicity but in nonlinear systems we can not afford this simplification because there is sensitive dependence on initial conditions and orbits that are not idealized but have all kinds of twists and bends.

4.3 Mandelbrot sets and julia sets

The first connection between fractals and differential equations was made by Benoit mandelbrot who studied and popularized the mandelbrot set. The Mandelbrot set is a particular mathematical set of points, whose boundary generates a distinctive and easily recognisable two-dimensional fractal shape. The set is closely related to the Julia set (which generates similarly complex shapes)

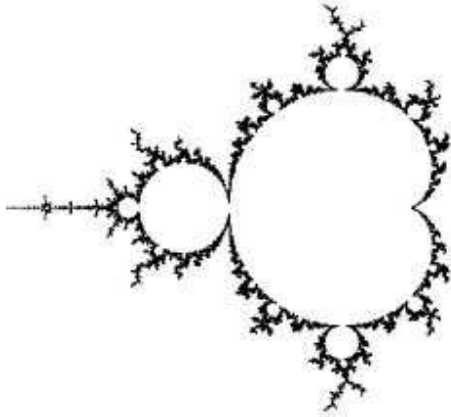


Figure 45 - The famous Mandelbrot Set, an object of infinite Complexity embedded into it

Notice that 2-dimensional map becomes easier to use if we use complex numbers using the two part as dimensions of one point.

So the system

$$x_{n+1} = f(x_n)$$

$$y_{n+1} = f(y_n)$$

becomes:

$$z_{n+1} = f(z_n)$$

In a simple system the equation might be :

$$z_{n+1} = z_n^2 + C$$

Where c the parameter

So knowing c and starting from z_n we get z_{n+1} . this shows that the behavior of the system depends only on c. For some values of C the iterations go to infinity while for some others they remain bounded. C is also a complex number so it can be represented easily as a point in the complex plane. we can take a set of points within which all iterations remain bounded. If we try to visualize that we get a fractal object called mandelbrot set.

For each of these points there is a region in the state space that if Initial conditions are in the orbit remains bounded. If we try to visualize that we also get a fractal object called julia set. Essentially the julia set is the basin of attraction and it can be constructed for every value of the parameter. so every point in the mandelbrot set corresponds to a different julia set . mandelbrot set has infinite points so it is an infinite complicated object. Obtaining the dimension of this object can be done but is a bit complicated.

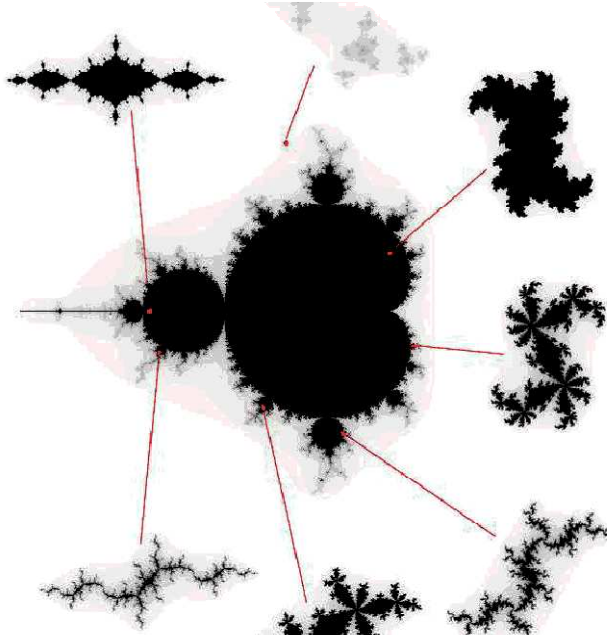


Figure 46 - Each point in the mandelbrot set reveals a coresponding Julia set

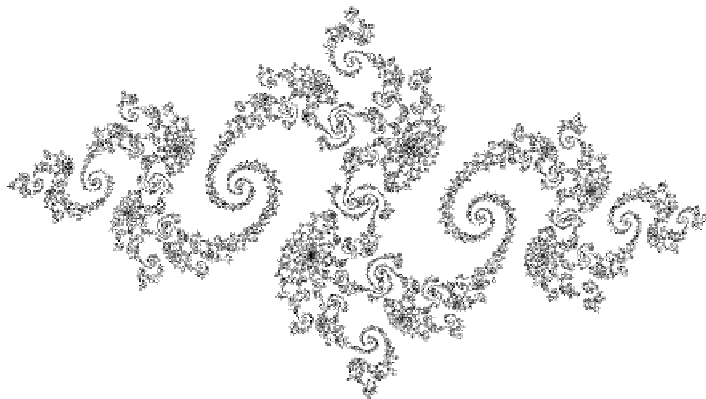


Figure 47 - Example of a julia set extracted from the mandelbrot set. It is also a fractal object of infinite complexity

4.4 Cantor sets and Sierpinsky sets

Cantor set

The Cantor set was introduced by German mathematician Georg Cantor in 1883. It is a set of points lying on a single line segment that has a number of remarkable properties like fractal dimension. This object was created using a repeating procedure so we can say that there are also some procedures that can create fractals. Through consideration of it, Cantor and others helped lay the foundations of modern general topology, although Cantor himself defined the set in a general, abstract way and mentioned the ternary construction in passing, as an example of a more general idea of a perfect set that is nowhere dense. The procedure to create a Cantor set is the following.

- Take a line between 0 and 1
- Divide it into 3 equal parts
- Remove the middle part

If we apply the same to the lines that are created after infinite steps we get a set of points called Cantor set. We can check if this object is a fractal by looking in its dimension:



Figure 48 - The procedure of creating a Cantor set. The first five iterations are illustrated

To make things easier initially we set the scale length to $x=1/3$. The scale will be referred to as box counting. So initially we need 3 boxes

After first iteration we need 2 boxes so:

$$D = \frac{\ln 2}{\ln 3}$$

Which is a fractional number. For the second iteration the box length will be $1/9$, so we need 4 boxes. Again:

$$D = \frac{\ln 2}{\ln 3}$$

As we change scaling further we notice that the dimension doesn't change. So at the last step where there will be points the dimension will also be $\frac{\ln 2}{\ln 3}$. So we can conclude that this is indeed a fractal object due to its fractional dimension.

Sierpinski set

Sierpinski set is also a fractal object named after the Polish mathematician Waclaw Sierpiński who described it in 1915. With the same logic similar procedures like the one used to create Cantor sets can be applied also to n-dimensional objects. In case of 2 dimensions it can be applied to a square.

- Take a square with side length 1

- Divide it into 9 equal squares
- Remove the middle part

If we apply the same to the squares that are created after infinite steps we get a set of points called Sierpinsky set. We can check if this object is a fractal also by looking in its dimension:

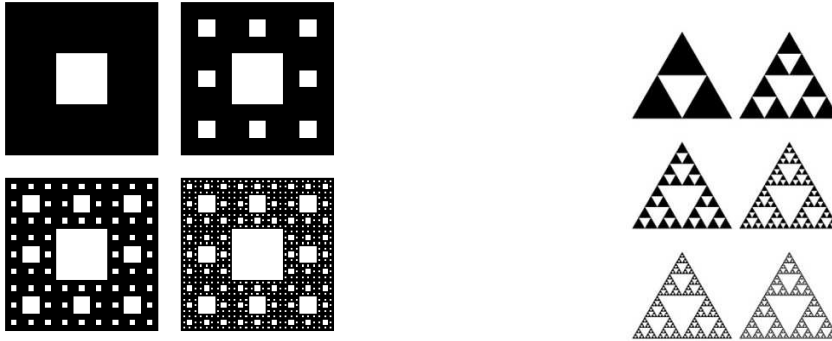


Figure 49 - The Sierpinski's set, created by applying the same procedure used to create cantor sets. Here applied to squares and triangles.

Again here the length x is chosen to be $1/3$ in the first step so we need 8 boxes.

$$D = \frac{\ln 8}{\ln 3}$$

which is a fractional number between 1 and 2. For the 2nd step $x=1/9$ so we need 64 boxes

$$D = \frac{\ln 64}{\ln 9} = \frac{\ln 8}{\ln 3}$$

Here also the dimension is invariable and fractional as we take steps to infinity. So the Sierpinsky set is also a fractal object due to its fractal dimension. There are similar procedures for 3 dimensional objects like the Sierpinsky triangle and Sierpinsky cube. So there are simple procedures that allow us to create fractals in any dimensional space.

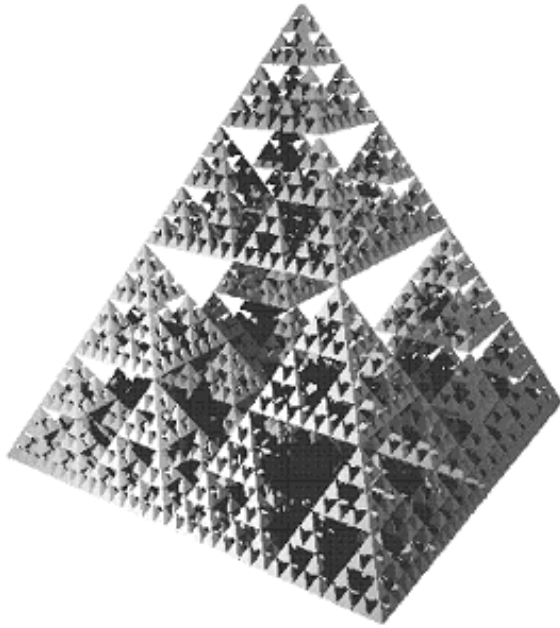


Figure 50- Sierpinski Pyramid

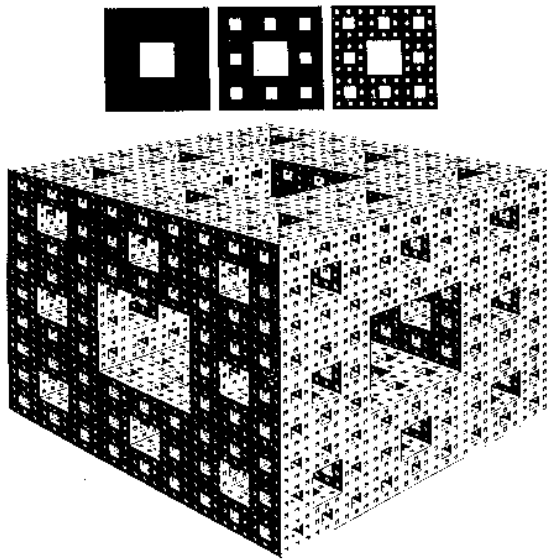


Figure 51 - Sierpinski cube

Chapter 5 - Statistic Analysis of chaotic attractors

5.1 Introduction

Chaotic attractors are non periodic bounded orbits in the state space. so the frequency cannot be used to characterize that kind of orbits. other kind of measures of characterizing a strange attractors have been studied over the last years, the main and most commonly used are the density of the orbit, the dimension of the attractor and the lyapunov exponents. All of these methods are based on statistical analysis techniques.

5.2 Density

Based on the fact that chaotic orbits cover large part of the state space (ergodic orbits) a statistical analysis of the density of the orbit can be made to characterize the orbit.

This is done by dividing the state space into squares or bins and see where the points fall after some iterations. Some bins will be more populated than others. So the orbit will be more dense for the corresponding values of the parameter. this is related to the probability of finding the state in each box. Using a computer is easy to count the number of points.

So the density function is defined as:

$$\int_0^1 D = \frac{\text{number of iterates in the box}}{\text{total number of iterations}}$$

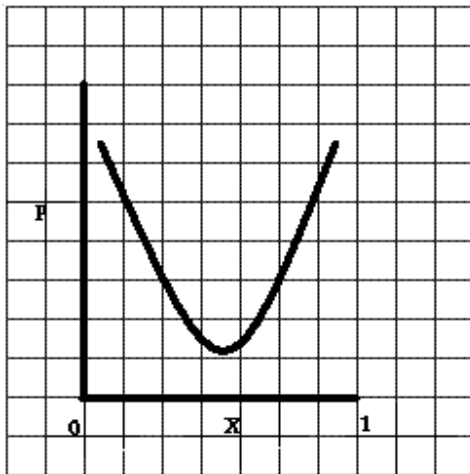


Figure 52 - The density function for the logistic map

So even in a chaotic orbit the average value is determined by the density. The same can be applied and to n-dimensional maps. This density function will be different for different initial conditions but ultimately as iterations go to infinity it converges to a certain function which will have the property that if you iterate the map again will result to the same density function. This function is called invariant density function.

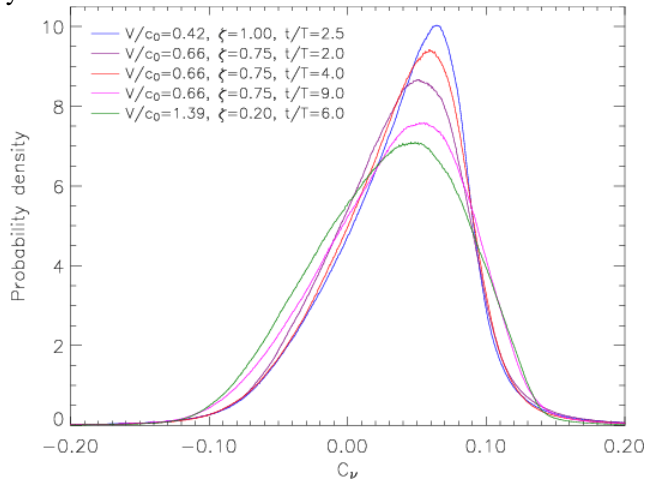


Figure 53 - Density functions for different initial conditions

In some classes of systems (piecewise Linear systems – markov maps) we can obtain the density function mathematically using a Birkhoff’s ergodic theorem.

This theorem is proved by Birkhoff that says that in ergodic system (systems with large part of state space covered) the 2 densities are the same. Starting from any initial condition and giving the system finite time to evolve the orbit will visit every box (time average = ensemble average).

So given an initial condition a function will start mapping to another function and so on. Then we can define an operator (Frobenius – Perron) by which these functions change. If we apply this operator to the invariant density function it will give the same function. So the invariant density is the fixed point of that operator.

$$AP_n(x) \rightarrow P_{n+1}(x) \text{ and invariant density } P_n(x) \text{ is the fixed point of } A$$

This operator can be calculated if we think in terms of slope. As we take iterations the density function maps to another density function and so on. So the density in a box will increase or decrease depending on the slope (or the Jacobian) of the density function. We can write for an 1-dimensional system for example:

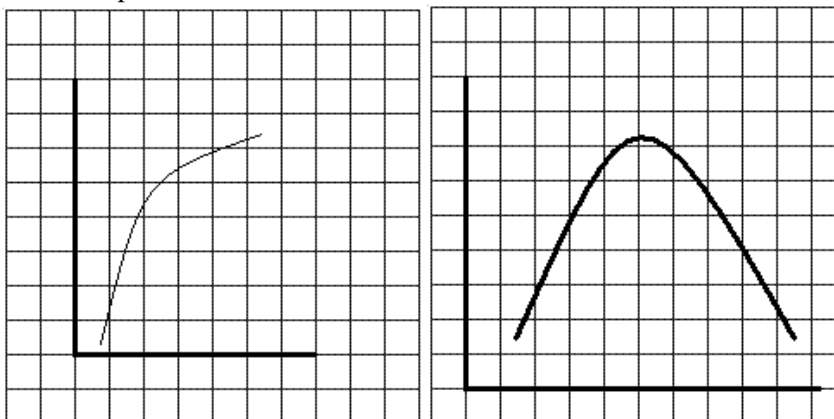


Figure 54 - If the graph has curves, density function has to be written as a summation

$$P(x_{n+1}) = \frac{P(x_n)}{\frac{dy}{dx}}, \text{ at } x_n$$

But if the we have a curve we must write it as a summation.

$$P_{n+1}(y, y + Dy) = \dots + \dots + \dots$$

This is operator is defined for each box seperately and is a function, starting from any initial condition and watching how density function evolves under the application of the operator we can see that it converges to the invariant density function operator.

Markov map example

In this example the density function can be calculated mathematically. The equations of this map are:

$$x_{n+1} = x_n + \frac{1}{3}, \quad \text{for } 0 \leq x_n \leq \frac{2}{3}$$

$$x_{n+1} = 3 - 3x_n, \quad \text{for } \frac{2}{3} \leq x_n \leq 1$$

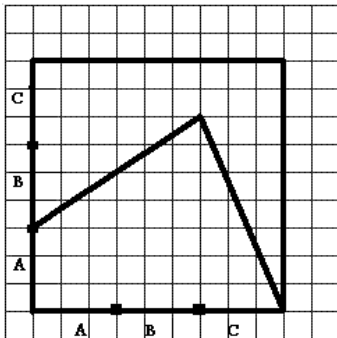


Figure 55 - The Markov Map

This system will experience chaotic behavior if there is expotensial divergence of nearby orbits (expansion). That depends on the slope (since this is an 1-D map).

For the first section the slope is < 1 so there will be no expansion but for the second section there is expansion since the slope there is > 1 . This means that there can be no periodic orbit since the product of those 2 slopes will allways be > 1 . so if a bounded orbit exists it must be a chaotic orbit (ergodic) and the density theorem can be applied to find the invariant density. The density for each part will be:

$$\rho_{n+1}(A) = \frac{\rho_n(C)}{3}$$

$$\rho_{n+1}(B) = \frac{\rho_n(A)}{1} + \frac{\rho_n(C)}{3}$$

$$\rho_{n+1}(C) = \frac{\rho_n(B)}{1} + \frac{\rho_n(C)}{3}$$

Here we have on the left side the next itterate expressed as a product of the probenius operator and a density function.

This can be expressed in metrics form as (assuming same density everywhere because we are looking for the invariant density):

$$\begin{bmatrix} P_{n+1}^*(A) \\ P_{n+1}^*(B) \\ P_{n+1}^*(C) \end{bmatrix} = \begin{bmatrix} 0 & 0 & \frac{1}{3} \\ 1 & 0 & \frac{1}{3} \\ 0 & 1 & \frac{1}{3} \end{bmatrix} \begin{bmatrix} P_n^*(A) \\ P_n^*(B) \\ P_n^*(C) \end{bmatrix}$$

In order to obtain the density function $\begin{bmatrix} P_{n+1}^*(A) \\ P_{n+1}^*(B) \\ P_{n+1}^*(C) \end{bmatrix}$ must be equal to $\begin{bmatrix} P_n^*(A) \\ P_n^*(B) \\ P_n^*(C) \end{bmatrix}$. This is true for the

eigenvector with eigenvalue 1. Then the equations can be written as:

$$P^*(C) = 3P^*(A)$$

$$P^*(B) = 2P^*(A)$$

And in addition for normalization

$$\frac{1}{3}(P^*(A) + P^*(B) + P^*(C)) = 1$$

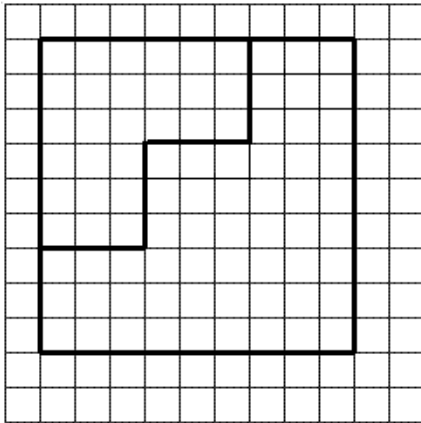
Which results to :

$$P^*(A) = \frac{1}{2}$$

$$P^*(B) = 1$$

$$P^*(C) = \frac{3}{2}$$

So the density function will be:



5.3 Fractal Dimension

Another way to characterise an attractor is to obtain its dimension. There are many specific definitions of fractal dimension. The most important theoretical fractal dimensions are the Rényi dimension, the Hausdorff dimension and packing dimension. Practically, there are 2 ways widely used to obtain the fractal dimension, due to their ease of implementation:

- Box counting
- Correlation dimension

Box counting can be applied easily on 2 d systems but in 3d systems correlation dimension is easier to use. The main difference is that correlation dimension also takes into account the density of the orbit.

In the box counting method the number of boxes covering the point set is a power law function of the box size:

$$D = \frac{\ln N}{\ln \frac{1}{E}} = \frac{\log_2 N}{\log_2 \frac{1}{E}}$$

Where N is the number of self-similar structures of linear size E needed to cover the whole structure.

Then correlation dimension is

$$C(r) = \frac{\text{The number of pairs in the orbit that their distance is less than } r}{\text{The total number of pairs in the orbit}} =$$

$$= \frac{\#\{\text{pairs}(\omega_1, \omega_2) : \omega_1, \omega_2 \in S_n, |\omega_1 - \omega_2| < r\}}{\#\{\text{pairs}(\omega_1, \omega_2) : \omega_1, \omega_2 \in S_n\}}$$

This converges to a value very close to the fractal dimension and that deviation is due to density taken into account. Also it can easily be done by a computer.

As we change a parameter an orbit may become more chaotic. This deviation can be measured by watching how correlation dimension changes.

The 2 dimensions will become equal if the density is the same everywhere on the orbit.

5.4 Lyapunov exponent

A quantitative measure of the sensitive dependence on the initial conditions is the Lyapunov exponent. It is the rate of divergence (or convergence) of two trajectories starting in the same neighbourhood. The number of Lyapunov exponents in a system is equal to the dimension of the phase space, one for each eigenvector (in linear systems eigenvalues are the same everywhere, thus we can predict accurately with the Newtonian model). These exponents have been used as the most useful dynamical diagnostic tool for chaotic system analysis and can also be used for the calculation of other invariant quantities as the attractor dimension. The signs of these exponents provide a qualitative picture of the system's dynamics. The existence of positive Lyapunov exponents defines directions of local instabilities in the system dynamics and any system containing at least one positive exponent presents chaotic behavior. A response with more than one positive exponent is called as hyperchaos (Savi & Pacheco, 2002; Franca & Savi, 2003; Machado *et al.*, 2003).

Lyapunov exponents are important because they determine the prediction horizon. Qualitative predictions are impossible for a time interval beyond this horizon. It is given by $\ln \frac{\varepsilon}{\lambda_{max}}$, where ε is the error of the measurement of the initial state. Lyapunov exponent can be obtained in similar ways for continuous and discrete systems. This works if we have already obtained the equations of the system, not in experimental situations. But if we apply rescaling it might work.

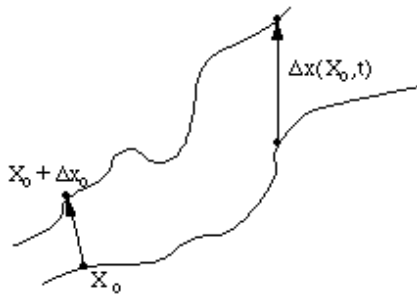


Figure 56 - Two nearby orbits will diverge expotensially in chaotic systems

Consider two points in a space, X_0 and $X_0 + \Delta x_0$, each of which will generate an orbit in that space using some equation or system of equations. These orbits can be thought of as parametric functions of a variable that is something like time. If we use one of the orbits a reference orbit, then the separation between the two orbits will also be a function of time. Because sensitive dependence can arise only in some portions of a system (like the logistic equation), this separation is also a function of the location of the initial value and has the form $\Delta x(X_0, t)$. In a system with attracting fixed points or attracting periodic points, $\Delta x(X_0, t)$ diminishes asymptotically with time. If a system is unstable, like pins balanced on their points, then the orbits diverge exponentially for a while, but eventually settle down. For chaotic points, the function $\Delta x(X_0, t)$ will behave erratically. It is thus useful to study the mean exponential rate of divergence of two initially close orbits.

The determination of Lyapunov exponents of dynamical system with an explicitly mathematical model, which can be linearized, is well-established from the algorithm proposed by Wolf *et al.* (1985). On the other hand, the determination of these exponents from time series is quite more complex. In essence, there are two different classes of algorithms: Trajectories, real space or direct method (Wolf *et al.*, 1985; Rosenstein *et al.*, 1993; Kantz, 1994); and perturbation, tangent space or Jacobian matrix method (Sano & Sawada, 1985; Eckmann *et al.*, 1986; Brown *et al.*, 1991; Briggs, 1990; Krueel *et al.*, 1993).

In order to understand the idea related to the determination of Lyapunov exponents consider a D -sphere of states that is transformed by the system dynamics in a D -ellipsoid. Lyapunov exponents are related to the expanding and contracting nature of different directions in phase space. The evaluation of the divergence of two nearby orbits is done considering the relation between the initial D -sphere and the D -ellipsoid (Figure 10). This variation may be expressed by: $d(t) = d_0 b^t$, where d is the diameter and b is a reference basis. The parameter l is called as Lyapunov exponent and when it is negative or vanishes, trajectories do not diverge. On the other hand, when the exponent is positive, indicates that trajectories diverges, characterizing chaos.

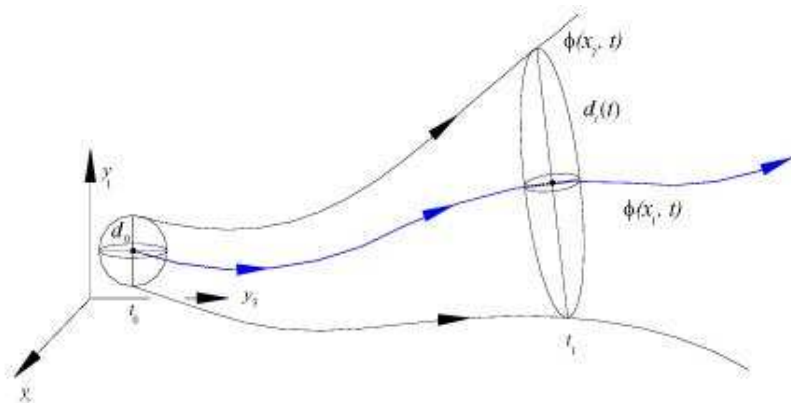


Figure 57 - The error ball decomposes to an ellipsoid, renormalization has to be made to estimate the lyapunov exponents

In chaotic situations, there is a local exponential divergence of nearby orbits so proper algorithms are necessary in order to evaluate Lyapunov exponents (Wolf 1985, Parker & Chua 1989). These algorithms evaluate the average of this divergence considered in different points of the trajectory. Hence, when the distance $d(t)$ becomes large, it is defined a new $d_0(t)$ in order to evaluate the divergence, as follows:

$$\lambda = \frac{1}{t_n - t_0} \sum_{k=1}^n \log_b \left(\frac{d(t_k)}{d_0(t_{k-1})} \right)$$

The attractor dimension may be evaluated from the Lyapunov spectrum considering the Kaplan-Yorke conjecture (Kaplan & Yorke, 1983).

For $\lambda < 0$, the orbit attracts to a stable fixed point or stable periodic orbit. Negative Lyapunov exponents are characteristics of dissipative or non-conservative systems. Such systems exhibit asymptotic stability. The more negative the exponent, the greater the stability. Fixed points with $\lambda = -\infty$ are called superstable fixed points. For instance in the critically damped oscillator when the system heads towards its equilibrium point as quickly as possible.

For $\lambda = 0$, the orbit is a neutral fixed point or an eventually fixed point. A Lyapunov exponent equal to 0 indicates that the system is in some sort of steady state mode. A physical system with this exponent is conservative. Such systems exhibit Lyapunov stability. For example in the case of two identical simple harmonic oscillators with different amplitudes, because the frequency is independent of the amplitude, a Poincaré section of the two oscillators would be a pair of concentric circles. The orbit in this situation would maintain a constant separation.

For $\lambda > 0$, the orbit is unstable and chaotic. Nearby points no matter how close will diverge to any arbitrary separation. All neighborhoods in the phase space will eventually be visited (ergodic system). These points are unstable. For discrete system the Poincaré section will look like television snow. This does not exclude a pattern or an organization behind the chaos. For a continuous system the phase space would be a tangled sea of wavy lines like spaghetti. A physical example can be found in the Brownian motion. Although the system is deterministic, there is no order to the orbit that ensues.

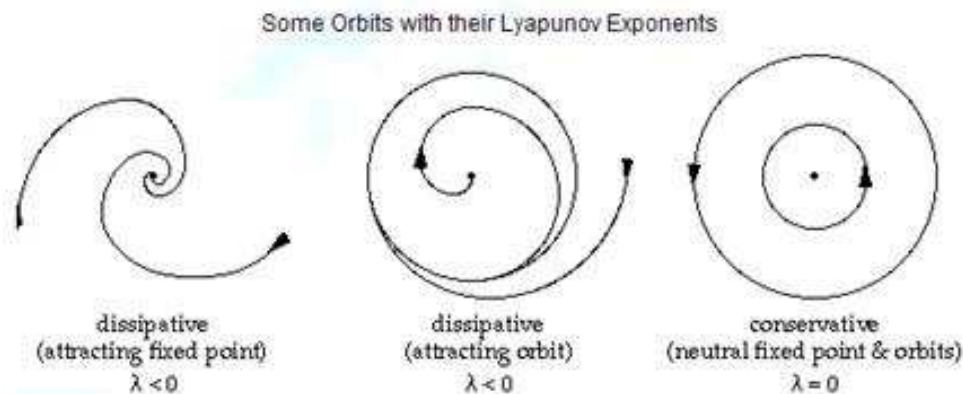


Figure 58 - Lyapunov Exponents used to estimate behavior

Example

Consider two orbits, a reference orbit and a test orbit, separated at time t_0 by a small phase space distance d_0 . We will use the test orbit as a means of calculating the value of the maximum Lyapunov exponent. Under evolution of the equations of motion, the two orbits may (or may not) separate. If the motion is chaotic, the orbits will, by definition, separate at an exponential rate. The maximum Lyapunov exponent λ is a measure of this rate of separation:

$$\lambda = \lim_{t \rightarrow \infty} \frac{1}{t - t_0} \ln \frac{d(t)}{d_0}$$

In practice, we cannot afford the luxury of infinitely long integrations, so we instead calculate the instantaneous maximum Lyapunov exponent.

$$\lambda(t) = \frac{1}{t - t_0} \ln \frac{d(t)}{d_0}$$

Another practical problem is that, for chaotic orbits, the distance between reference and test particles $d(t)$, quickly saturates. Hence we must periodically renormalize the orbit separation. We will leave the reference orbit alone and rescale the test orbit whenever the separation $d(t)$ has passed beyond a threshold value D . It is important that D be set small enough that it is still in the linear regime (i.e., the regime in which the linearized equations of motion are an accurate description). We define a rescaling parameter:

$$\alpha_1 = \frac{d(t_1)}{d(t_0)}$$

Where t_1 is the time at which $d(t) \geq D$. Then we can write:

$$\lambda_1 = \frac{1}{t_1 - t_0} \ln \frac{d_1}{d_0} = \frac{1}{t_1 - t_0} \ln \alpha_1$$

Where $\lambda_i = \lambda(t_i)$ and $d_i = d(t_i)$.

At this point, the test orbit is then rescaled. The rescaling of the test particle orbit is performed on the test - reference phase space distance vector. Whenever the distance $d(t)$ becomes greater than or equal to the threshold D , we scale the test particle distance from the reference particle by the factor $\frac{1}{\alpha_i}$ maintaining the current relative orientation between the two particles in phase space. The reference and test particle phase space vectors are

$$\vec{R} = \begin{pmatrix} x \\ y \\ z \\ v_x \\ v_y \\ v_z \end{pmatrix}_{ref} \quad \text{and} \quad \vec{r} = \begin{pmatrix} x \\ y \\ z \\ v_x \\ v_y \\ v_z \end{pmatrix}_{test}$$

We define $\vec{p} = \vec{r} - \vec{R}$. Then the adjustment to the test particle phase space coordinates at time t_i is

$$\vec{r}_i \leftarrow \vec{R}_i + \frac{\vec{p}_i}{\alpha_i}$$

Similarly, for successive threshold crossings and subsequent rescalings, we have:

$$\lambda_2 = \frac{1}{t_2 - t_0} \ln \frac{d_2 \alpha_1}{d_0} = \frac{1}{t_2 - t_0} \ln(\alpha_1 \alpha_2)$$

$$\lambda_3 = \frac{1}{t_3 - t_0} \ln \frac{d_3 \alpha_1 \alpha_2}{d_0} = \frac{1}{t_3 - t_0} \ln(\alpha_1 \alpha_2 \alpha_3)$$

... ..

The multiplicative factors $\alpha_1\alpha_2\alpha_3$ can be derived from the summation and we can conclude that the Lyapunov exponent is:

$$\lambda_n = \frac{1}{t_n - t_0} \sum_{i=1}^n \ln a_i$$

As long as the rescalings take place in the linear regime, this construction is valid. Notice that, in a computer, only the accumulating sum of the natural log of the a_i need be stored. In addition, the time intervals need not be evenly spaced

Chapter 6

Analysis of Chaotic Time Series

6.1 Introduction

In general, a dynamical system is analyzed from its mathematical model. An alternative approach to deal with the dynamical system response is based on the analysis of data derived from an experiment where not all state variables can be identified. But it might be possible to get a conclusion about the qualitative behavior of the system by analyzing a time series of one variable. Therefore a dynamical system may be analyzed either by a mathematical model or by a measured time series. The basic idea of the time series analysis is that a signal contains information about unobserved state variables, which can be used to predict the present state (Kantz & Schreiber, 1997, Franca & Savi, 2001).

A dynamical system may be analyzed either in time or in frequency domain. Spectrum techniques or Fourier transform establish a relationship between these two domains.

The Analysis is based around the idea of extracting mean square value and average value of that time series $x(t)$. These values remain stable even in chaotic orbits so they can be used to characterize them and also to calculate other usable measures. This leads to accurate conclusions about the qualitative behavior of the system in situations where the system has too many state variables to keep track of all of them. This is also very common in natural systems.

These values are:

- Mean square :

$$\psi_x^2 = \lim_{t \rightarrow \infty} \frac{1}{T} \int_0^T x^2(t) dt$$

- Average value:

$$\mu_x = \lim_{t \rightarrow \infty} \frac{1}{T} \int_0^T x(t) dt$$

6.2 Probability density function

An easy way to extract these values is to obtain the probability density function. An estimation is made considering the possibility for the value of the waveform to be in a defined area.

Supposing the orbit spends T_x time in the range $x \rightarrow \Delta_x$ so the probability of finding $x(t)$ in the range $x \rightarrow x + \Delta x$ is $\lim_{t \rightarrow \infty} \frac{T_x}{T}$ ($prob\{x < x(t) < x + \Delta x\}$)

so the probability density function will be :

$$P(x) = \lim_{\Delta x \rightarrow 0} \frac{prob\{x < x(t) < x + \Delta x\}}{\Delta x}$$

and using that we can find also the probability of finding the state between x_1, x_2

$$P(x) = \int_{x_1}^{x_2} P(x) dx$$

so the average can be calculated as

$$\mu_x = \int_{-\infty}^{+\infty} x P(x) dx$$

and mean square value can be calculated as

$$\psi_x^2 = \int_{-\infty}^{+\infty} x^2 P(x) dx$$

6.3 Auto correlation function

Another way to obtain these values is the auto correlation function, which shows how present state is correlated to its past and future. The auto correlation function is defined as:

$$R_x(\tau) = \lim_{T \rightarrow \infty} \frac{1}{T} \int_0^\tau x(t)x(t-\tau)dt$$

It is an even function so $R_x(-\tau) = R_x(\tau)$ and $R_x(0) > |R_x(\tau)| \forall \tau$ and we can see that $\psi_x^2 = R_x(0)$ and $\mu_x = \sqrt{R_x(\infty)}$

6.4 Frequency characteristics (Power Contained between two frequencies)

The frequency characteristics of the time series are very important in many practical cases like electrical engineering. Then it makes more sense to talk about the power spectrum and the average and square values can be extracted from the power spectrum which can be calculated easy via fourier transform

In these cases when we talk about the frequency we refer to the power contained between 2 frequencies f and $f+\Delta f$, because the wave form might be a composition of 2 or more frequencies. The power will be:

$$\psi_x^2(f, \Delta f) = \lim_{T \rightarrow \infty} \frac{1}{T} \int_0^T x^2(t, f, \Delta f) dt$$

The power spectrum can be obtained by reducing Δf to 0:

$$G_x(f) = \lim_{\Delta f \rightarrow 0} \frac{\psi_x^2(f, \Delta f)}{\Delta f}$$

This is a good way to visualize the power spectrum but usually we obtain it by the fourier transform:

$$x(f) = \int_{-\infty}^{\infty} x(t)e^{j2\pi ft} dt \text{ and } G_x(f) = |x^2(f)|$$

Often we can obtain the power spectrum from Sin transform too which can be applied only to even functions but since chaotic orbits are statistically even it works

So we can extract these values from the power spectrum as :

$$\mu_x = \sqrt{\int_{0^-}^{0^+} G(f)df} \text{ and } \psi_x^2 = \int_0^\infty G_x(f)df$$

The power spectrum is also can also be extracted from the auto correlation function via Convolution which in some cases is easier since the correlation function is the inverse fourier of the power spectrum.

$$\int_{-\infty}^{+\infty} |x^2(f)| e^{j2\pi ft} df = \int_{-\infty}^{+\infty} x(f)x(f)e^{j2\pi ft} dt = x(t) * x(t) \text{ (convolution)} = \int_{-\infty}^{+\infty} x(t)x(t - \tau)dt$$

This means that if you have the inverse transform for power spectrum you get the correlation function

6.5 Multiple time Series

In some cases we have many time series of finite length and we need to make conclusions for the behavior for infinite time. If we consider the probenius operator these time series will converge and based on this we can study the time series and make conclusions for infinite time under some conditions.

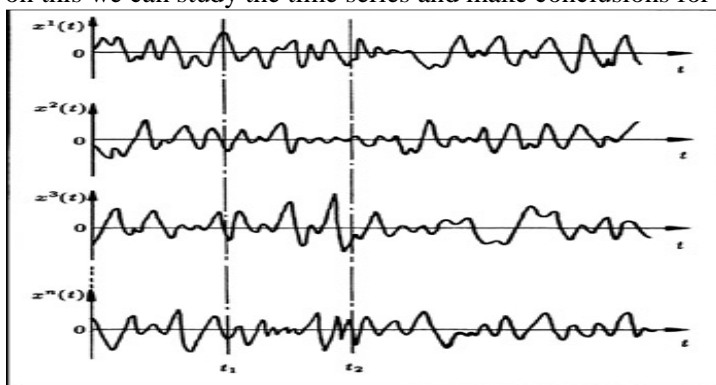


Figure 59 - Multiple time series used to make conclusions about qualitative behavior

This is based on density function. We divide the y axis into boxes of length $x + \Delta x$ so we can count the number of points M falling into each box (this is done by a computer easilly). If n is the number of time series the probability of finding a point of the time series in the range $x + \Delta x$ would be:

$$Prob(x < x(t) < x + \Delta x) = \frac{M}{n}$$

This can be defined for different t. if the probability function does not change over time then it is a stationary time series. If not, it is non-stationary.

If there is an attractor the time series will be non-stationary before the attractor and stationary after. But stationary time series can occur for different types of attractors (quasiperiodic, chaotic, etc..). so if the time series is stationary with non-periodic elements then it must be ergotic. Which implies that single time series over long time will become equal to multile time series over short time. It also implies a torus type state space, topological mixing and and quasiperiodic and chaotic orbits.

Many systems ralay on these principles

6.6 Delay coordinate embedding (State space reconstruction)

The state space reconstruction establishes that a scalar time series, $s(t)$, may be used to construct a vector time series that is topological equivalent to the original dynamics. The state space reconstruction needs to form a coordinate system to capture the structure of orbits in state space. The method of delay coordinates can be done using lagged variables, $s(t + t)$, where t is the time delay. Then, considering an experimental signal, $s(t)$, where $t = t_0 + (n - 1) D_e$ with $n = 1, 2, 3, \dots, N$, it is possible to use a

collection of time delays to create a vector in a D_e -dimensional space, $u(t)$, which represents the reconstructed dynamics of the system.

$$u(t) = \{s(t), s(t + \tau), \dots, s(t + (D_e - 1)\tau)\}^T$$

The method of delays was first proposed by Ruelle and Packard and then by Takens and Sauer. Its use has become popular for dynamical reconstruction, and the choice of the delay parameters, t - time delay, and D_e - embedding dimension, is an important task related to this procedure. Among many possibilities to define the delay parameters (Franca & Savi, 2001) one could mention the average mutual information method to determine time delay (Fraser, 1989) and the method of false nearest neighbors to estimate embedding dimension (Kennel., 1992).

There are cases where the system has too many state variables to observe and we cannot keep track of all of them. Although it is possible to make a representative model of the system by having access only to a few variables.

The logic is that if the model behaves as the actual system then we can predict accurately the behavior so the model is representative even if it has come through only 1 variable.

The procedure used to obtain the model is called delay coordinate embedding. A 1-dimensional time series becomes 2-dimensional by inserting a delay $x(t - \tau)$

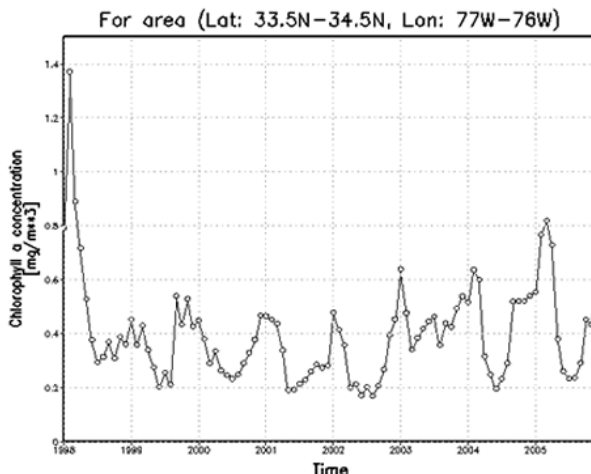


Figure 60 - Concentrations in fluids can be monitored by one time series. Very useful in Chemistry

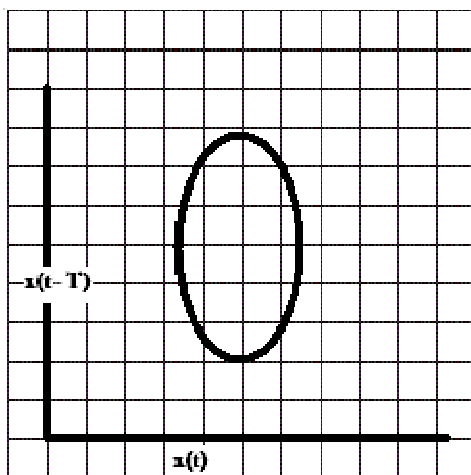


Figure 61 - Plot of the time series with the delayed one. If it is not smooth (i.e. a circle) or if there are intersections, more delays have to be inserted.

By plotting $x(t - \tau)$ and $x(t)$ we can now distinguish in a way where the next state will be and we can see if there is a closed loop in the system (Periodicity). This is independent from τ because the topological character of the orbit remains the same (it becomes rounder for bigger τ). We usually set τ by experimenting.

Looking at the delay plot we can now predict by applying simple analogies if every point is unique. (there is not a crossing in the orbit). If there is an intersection the dimension has to be increased further in order to predict accurately. This is done with the same logic by inserting another delay $x(t - 2\tau)$. Now the system is 3-dimensional and the intersection should be eliminated, If not we can repeat until we can predict accurately.

The system model created this way will be representative if for each point in the initial orbit there is a point in the representative orbit. Taken's theorem proves that this will be true as long as for the n -dimensional system that we are trying to represent, $2n+1$ dimensions are chosen. This guarantees that each point will map to a unique point.

6.7 Chaos Control

Chaos control is an important task related to natural rhythms. This control is associated with many regulatory mechanisms that control the dynamics of living systems.

The mechanisms of chaos control were understood by the pioneer work of Ott (1990) which propose the well-know OGY approach (a tribute to the authors Ott-Grebogi-Yorke). Essentially, chaos control is based on the richness of responses of chaotic behavior. A chaotic attractor has a dense set of unstable periodic orbits (UPOs) and the system often visits the neighborhood of each one of them. Besides, chaotic response has sensitive dependence on initial condition, which implies that the system's evolution may be altered by small perturbations. Therefore, chaos control may be understood as the use of tiny perturbations for the stabilization of an UPO embedded in a chaotic attractor, which makes this kind of behavior to be desirable in a variety of applications, since one of these UPO can provide better performance than others in a particular situation.

The control of chaos can be thought as a two-stage process. The first stage is composed by the identification of UPOs and is named as "learning stage" (Gunaratne, 1989). After the UPOs identification, one can proceed to the next stage of the control process that is the desired orbit stabilization, which can be done by different forms (Pereira-Pinto, 2004). The OGY approach considers a discrete system with a map form, $x_{n+1} = f(x_n, p)$ where p is a control accessible parameter. This is equivalent to a parameter dependent map associated with a general surface, usually a Poincaré section. Let $x_{f+1} = f(x_f, 0)$ denote the unstable fixed point on this section corresponding to an orbit in the chaotic attractor that one wants to stabilize. The control idea is to monitor the system dynamics until the neighborhood of this point is reached. After that, a proper small change in the parameter p causes the next state x_{n+1} to fall into the stable direction of the fixed point. This procedure may be understood as a stabilization of a sphere over a saddle, as it is schematically shown in Figure below.

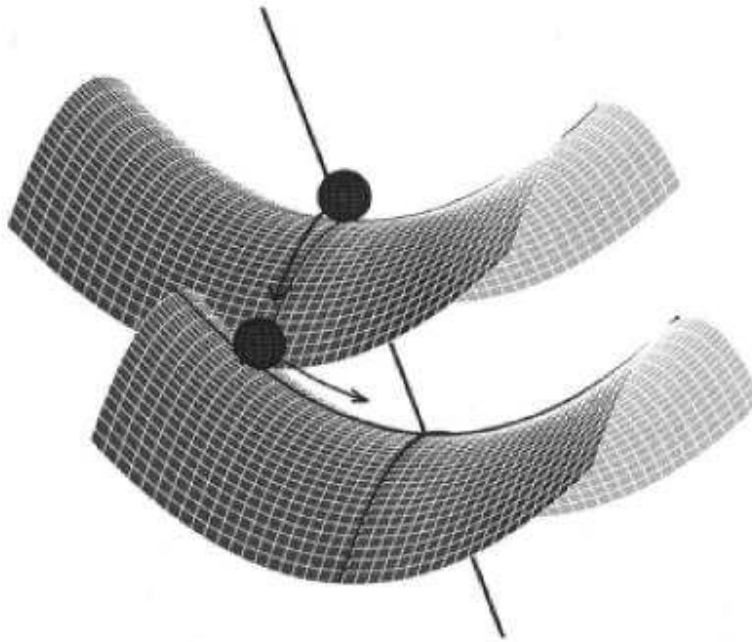


Figure 62 - The OGY control method represented schematically.

In order to find the proper variation in the control parameter, p , it is considered a linearized version of the dynamical system near the equilibrium point.

$$\delta\xi_{i+1} \approx A\delta\xi_i + w\delta p_i$$

where, $dx_n = x_n - x_f$, $dp_n = p_n - p_0$, $D_x f(x_f, p_0)$ and $w = df/dp(x, p_0)$

The OGY method can be employed even in situations where a mathematical model is not available (Pereira-Pinto, 2005). Under this situation, all parameters can be extracted from time series analysis. The Jacobian A and the sensitivity vector w can be estimated from time series using a least-square fit method as described in Auerbach *et al.* (1987) and Otani & Jones (1997).

Chapter 7 – System Representation

7.1 Introduction

It has been said that whereas linearity is a specification of a field of activity, nonlinearity is a nonspecification and its field is unbounded. In nature, nonlinearity is the rule rather than the exception, while linearity is a simplification adopted for analysis. Most practical systems used for control are essentially nonlinear, and in many applications, particular in the area of chaos, it is the nonlinear rather than the linear characteristics that are most used. Signals found in the physical world are also far from conforming to linear models. Indeed, the complex structure of dynamic systems makes it almost impossible to use linear models to represent them accurately. Nonlinear models are designed to provide a better mathematical way to characterize the inherent nonlinearity in real dynamic systems, although we may not be able to take all their physical properties into account. We will focus on other nonlinear techniques than modeling, which may provide more useful perspectives.

For most real-world practical applications, there are advantages to using nonlinear models to characterize the nonlinear relationships. Mathematical models may be expressed in the form of difference or differential equations. Depending on the given engineering problem and the circumstances, one mathematical model may be better suited than another.

In general, nonlinear representations can be classified into three types: (1) system input-output representation, (2) state-space representation, and (3) model-free representation. The first type considers the input-output behavior of a system without considering any internal variations. The second type focuses on both internal and external performance of the system, and the last type focuses on the representation of nonlinear systems that cannot be handled by the other two approaches.

7.2 Input-Output System Representation

Nonlinear system representation means the characterization of nonlinear systems using nonlinear mathematical models. In fact, nonlinear models may be considered as a tool for explaining the nonlinear behavior patterns in terms of a set of easily understood elements. The input-output representation approach for describing a given nonlinear system is:

$$y(t) = f(u)$$

where $y(t)$ refers to the system output, $u(t)$ refers to the system input, the independent variable t is time, and the f denotes a mathematical relationship describing the nonlinear behavior: the system yields the output $y(t)$ when the system has a input $u(t)$.

Generally, the nonlinear mapping f is very complicated, and there is no single technique suitable for the analysis of all nonlinear behaviors. In order to appreciate the complexity associated with nonlinear systems, it is best first to review the relative simplicity associated with linear systems. The main reason is that dynamic system analysis relies heavily on linear models, due to their comprehensiveness and the availability of well-developed linear system theories.

A system is called a linear system if it satisfies

$$f(au_1 + bu_2) = af(u_1) + bf(u_2)$$

Note two important features. One is that the sum of inputs results in the sum of the responses to the individual inputs, and the other is that a multiple of an input results in the same multiple of the corresponding output. An electric circuit containing a capacitor and a resistor is a common example used for explication.

A dynamic system is called *anticipatory* or *noncausal* if its outputs depend on the past, present, and future values of its inputs. A system is called *nonanticipatory* or *causal* if its outputs depend only on the past and present values of its inputs. We say that a system is *time-invariant* if its properties are invariant to a shift of time.

7.3 Nonlinear Differential Algebraic Representaion

The specification of the modeling problem for a linear system is simplified by the fact that it is easy to parametrize the response via a defined coordinate system. This fact enables us to reduce the problem of constructing a standard model from an input-output relation to a linear-algebra expression. In the nonlinear case, there is no such global coordinate system. Usually we have to be cautious in defining what we mean by the problem data. We cannot simply assume the system response to be as simple as an infinite sequence of functions or an impulse function.

The first step in constructing a nonlinear model is the development of a differential representation for describing the system input-output behavior. Clearly, there are a number of ways in writing differential equations that describe the behavior of different dynamic systems. There is no single one of them which is preferable in all circumstances. In general, the result depends on the familiarity of the investigator with a particular method to determine the form of the differential equations. One particularly convenient method of characterizing the behavior of a nonlinear system is by

$$\dot{y} = f[y(t), u(t), t], \quad (1)$$

where $u(t)$ is the system input, $y(t)$ is the system output, and f is an arbitrary nonlinear function. There are several reasons for the importance of this differential algebraic form of the system equations. Apart from the notational simplicity, one can deal with all systems by means of a compact notation instead of having to write a system of simultaneous differential equations. Also, this representation is the one that most modern literature in the theory of differential equations makes use of.

It is natural to represent the output in terms of the input as a series expansion

$$y(t) = h_0(t) + \int_0^t h_1(t, s_1)u(s_1)ds_1 + \int_0^t \int_0^{s_1} h_2(t, s_1, s_2)u(s_2)u(s_1)ds_2ds_1 + \dots \quad (2)$$

where the real-valued function of n variables $h_i(t_1, t_2, \dots, t_n)$, $i = 0, 1, 2, \dots$ is equal to zero if any $t_i < 0$, that is to say, the system is causal. Obviously the system is not linear, and it is a time-invariant system if $h_i(t_1, t_2, \dots, t_n) = \dot{h}_i(t_1 - t_2, \dots, -t_n)$. Formally the above expansion is a generalization of the linear-variation-of-constants formula. Clearly, this type of modeling problem for nonlinear systems may be expressed as follows:

Given a sequence of input-output pairs, find a canonical model whose input-output behavior generates the series of impulse functions $h_i, i = 0, 1, 2, \dots$

The modeling process is rather straightforward if there are no further hypotheses on the analytic behavior of f in equation (1) and there is a suitable definition of the canonical model. In general the problem is unsolvable, but the following theorem provides conditions under which the expansion exists and is unique:

If the nonlinear relationship f in Equation (1) is an analytic vector field and the equation has a solution on $[0, T]$ with $y(0) = h_0(0)$, then the input-output behavior of the equation has a unique representation expressed by the series expansion (2) on $[0, T]$.

Now it is quite clear that the condition of analyticity of the defining vector field is essential. The reason is clear: analyticity forces a certain type of rigidity upon the system, namely, the system behavior is determined by its response in an arbitrarily small open set. Fortunately, it is a property possessed by all systems defined by sets of algebraic equations.

7.4 State Space Representation

A state-space representation is usually used for describing physical systems. If the state of a system is known, then any output or quantity of interest with respect to certain performance indices can be achieved. To determine the state of a system as a function of time, we need a set of equations to relate the inputs state of the system. One approach for obtaining that set of equations is to consider each state variable as an output, to be determined via an n^{th} -order differential or difference equation. Using the state-space approach, we will be able to write n first-order differential or difference equations for the n state variables of the system. In general they will be coupled equations, that is, they will have to be solved simultaneously. For nonlinear systems, these first-order equations will be nonlinear ones. One advantage of the state-space representation is that once the first-order equations are solved, complete knowledge of the system behavior is obtained. All outputs are algebraic functions of the state variables. No further solution of a differential or difference equation is needed. The input-output behavior of a nonlinear system can be characterized by first-order differential or difference equations:

$$\dot{x}(t) = f[x(t), u(t)]$$

$$y(t) = g[x(t), u(t)]$$

Or

$$x(k + 1) = f[x(k), u(k)]$$

$$y(k) = g[x(k), u(k)]$$

where x are the internal states of the system, u are the inputs, y are the outputs and $f: n \times m \rightarrow n$, $g: n \times q \rightarrow q$. While the inputs and outputs of a system are generally the tangible physical data, it is the state variables that assume the dominant role in this formulation. It is possible that quantities that are not of interest will lead to an unnecessarily complicated problem.

A major difficulty in dealing with nonlinear equations is that the existence and the uniqueness of solutions, even in a local sense, cannot be taken for granted. As a matter of fact, there does not exist any general methodology to determine the nonlinear relations f and g . Instead, various simplified nonlinear models are widely used in practical engineering applications. The so-called bilinear model is among these.

Now let us look at the discrete-time nonlinear model. It is assumed that the initial state is $x(0) = 0$, and that $f(0, 0) = 0$ and $g(0, 0) = 0$. Then the functions $f(x, u)$ and $g(x, u)$ can be represented using a Taylor series about $x = u = 0$ of order sufficient to permit calculating the polynomial input-output representation to the degree desired:

$$x(k + 1) = \sum_{i,j=0}^N F_{ij} x^i(k) u^j(k)$$

$$y(k) = \sum_{i,j=0}^N G_{ij} x^i(k) u^j(k)$$

where $x^i = x \times x \times \dots \times x$ (i factors) and F_{ij} , G_{ij} are the standard Kronecker products. Just as in the continuous time case, the crucial requirement is that the kernels through order N corresponding to Eq. (48) should be identical to the kernels through order N corresponding to Eq. (47).

7.5 Nonlinear representation by using neural networks

Conventional model-based theoretical methods have dominated nonlinear-representation research over the last few decades. These methods depend on a mathematical characterization of the monitored

system. The main disadvantage of such approaches is that they are very sensitive to the selection of model type, modeling errors, parameter variations, and measurement noise. The success of model-based representation approaches is heavily dependent upon the quality of the models as well. For most practical nonlinear physical systems, it is often very difficult, if not impossible, to describe them by sufficiently simplified analytical models. In view of these, there is great interest in developing a robust and less model-dependent methodology for representing a complex nonlinear dynamic system. To avoid the difficulties experienced in the classical nonlinear system modeling, neural-network-based nonlinear system modeling methods appeared to be an appealing alternative. The rationale behind this approach lies in the fact that a multilayer neural network with an appropriate nonlinear activation function can approximate any nonlinear relationship.

In using neural networks for nonlinear system modeling, their nonlinear functional approximation capability can be enhanced by using higher-order architectures. The distinctive aspects of this network are that the parameters of the hidden layer, such as the weights and the thresholds, are selected randomly and independently in advance. The parameters of the output layer are learned using simple quadratic optimization, whereas under conventional approaches all parameters need to be learned using complicated nonquadratic optimization.

Many types of neural networks have been developed for tackling different problems, but two types have received the most attention in recent years:

- multilayer feedforward neural networks and
- recurrent networks.

Multilayer feedforward networks have proved extremely successful in pattern recognition problems, and recurrent networks for dynamical system modeling and time-series forecasting. A multilayer network is a network of neurons organized in the form of layers. A typical form of a multilayer network is one, in which an input layer of source nodes projects onto the hidden layer composed of hidden neurons. The output of the hidden neurons then projects onto an output layer. In general, one hidden layer is adequate to handle most engineering problems. The nonlinear activation function of the hidden neurons, which is generally sigmoidal, is chosen to intervene between the external input and the network output. For hidden neurons to be useful in modeling nonlinear systems, they must be sufficiently numerous. Though there has been much research on determining the optimal number of hidden neurons, there is no straightforward rule for doing so. When the number of hidden neurons reaches a certain threshold, the overall performance will not be significantly affected by small further increases. In this respect, the design criterion is rather loose. The source nodes of the network supply corresponding elements of the activation pattern (input vector), which constitute the input signals applied to the neurons in the hidden layer. The set of output signals of the neurons in the output layer of the network constitutes the overall response of the network to the activation pattern supplied by the source nodes at the input layer.

A neural network is said to be *fully connected* when every node in each layer of the network is connected to every other node in the adjacent forward layer. We say that the network is *partially connected* if some of the links are missing. Evidently, fully connected networks are relatively complex, but they are usually capable of much better functional approximation. A form of partially connected multilayer network of particular interest is the *locally connected network*. In practice, the specialized structure built into the design of a connected network reflects prior information about the characteristics of the activation pattern being classified.

Network training and adjustment

As multilayer feedforward neural networks have become generally recognized as a suitable architecture for representing unknown nonlinearities in dynamic systems, numerous algorithms for training the networks on the basis of observable input-output information have been developed by many researchers. In the next example, a training algorithm for neural networks called the cumulant-based weight-decoupled extended Kalman filter is described. Third-order cumulants are employed to define output errors for the network training. By this means, Gaussian disturbances or non-Gaussian noises with symmetric probability density function among the output signals can be rejected in the cumulant domain.

Thus we can obtain clean neural network output information for nonlinear mapping implementation. The weight-decoupled extended Kalman filter training algorithm is applied because it provides faster convergence (learning rate) than other training algorithms. This feature is very important for neural-network-based analysis of nonlinear dynamic systems.

The summary of the notation used in the network learning algorithm:

- The index i refers to different layers in the network, where $1 \leq i \leq M$, and M is the total number of layers (including the hidden and output layers) in the network.
- The index j refers to different neurons in the i^{th} layer, where $1 \leq j \leq n_i$, and n_i is the neuron number of the i^{th} layer.
- The index s refers to different neurons in the $(i - 1)^{th}$ layer, where $1 \leq s \leq n_{i-1} + 1$.
- The index v refers to different neurons in the output layer, where $1 \leq v \leq n_M$.
- The iteration index k refers to the k^{th} training pattern (example) presented to the network.
- The symbol $w_{js}^i(k)$ denotes the synaptic weight connecting the output of neurons in the $(i - 1)^{th}$ layer to the input of neuron j in the i^{th} layer at iteration k .
- The learning-rate parameter of the weight $w_{js}^i(k)$ at iteration k with respect to the v^{th} output error is denoted by $\eta_{js}^i(k)$
- The symbol $e_v(k)$ refers to the error signal between the target output and the actual output at the output of neuron v in the output layer at iteration k .
- The symbol $h_{js}^i(k)$ denotes the derivative of the output error $e_v(k)$ at iteration k with respect to the weight $w_{js}^i(k - 1)$ at iteration $k - 1$.
- The symbol $p_{js}^i(k)$ denotes the variance of the estimated weight $w_{js}^i(k)$ at iteration k .
- The symbol $a_v(k)$ refers to the central adjustment parameters for the output of neuron v in the output layer at iteration k .
- Suppose the network output is corrupted by a Gaussian noise $\{n_v(k)\}$ at iteration k . Then the symbol $r_v(k)$ denotes the variance of $\{n_v(k)\}$.
- The symbol $y(k)$ refers to the target output of the network, $N(w(k - 1), u(k))$ refers to the actual output of the network, its weight matrix is $w(k - 1)$ at iteration $k - 1$, and the network input at iteration k is $u(k)$.

The training mechanism can be described by the following:

$$w_{js}^i(k) = w_{js}^i(k - 1) + \sum_{v=1}^{n_M} \eta_{jsv}^i(k) h_{jsv}^i(k) e_v(k)$$

$$\eta_{js}^i(k) = p_{js}^i(k - 1) a_v(k)$$

$$p_{js}^i(k) = \left(1 - \sum_{v=1}^{n_M} \eta_{jsv}^i(k) [h_{jsv}^i(k)]^2 \right) p_{js}^i(k - 1)$$

$$a_v(k) = \frac{1}{r_v(k) + \sum_{i=1}^M \sum_{j=1}^{n_i} \sum_{s=1}^{n_{i-1}+1} [h_{jsv}^i(k)]^2 p_{js}^i(k - 1)}$$

$$e_v(k) = \left[\text{Cum}_3[y(k) - N(\omega(k - 1), u(k))] \right]^2$$

$$h_{js}^i(k) = \frac{de_v(k)}{dw_{js}^i(k - 1)}$$

where Cum_3 denotes the third-order cumulant operation

$$Cum_3[f] = m_3[f] - 3m_1[f]m_2[f] + 2(m_1[f])^3$$

With

$$m_3[f] = E[f(k)f(k+m)f(k+n)] \approx \frac{1}{pp} \sum_{pp} f(k)f(k+m)f(k+n)$$

$$m_2[f] = E[f(k)f(k+m)] \approx \frac{1}{pp} \sum_{pp} f(k)f(k+m)$$

$$m_1[f] = E[f(k)] \approx \frac{1}{pp} \sum_{pp} f(k)$$

A number of network initialization procedures have been developed for general feedforward networks. These algorithms are based on linear-algebraic methods to determine the optimal initial weights. With the optimal initial weights, the initial network error is much smaller, thus speeding up the overall training procedure. Here, a conventional randomized-weight initialization procedure is presented:

- Weights are initialized as random numbers with normal distribution, typically in the range of ± 0.1 .
- We initialize the matrices $P_i(k): \{p_{js}^i(k)\}$ and $R(k): \{r_v(k)\}$ as $P_i(0) = 100.0I$ and $R(0) = I$, where I refers to the unit matrix.

Thereafter, the cumulant-based weight-decoupled extended Kalman filter algorithm can be applied to train the neural network on which the nonlinear representation is based.

A *recurrent* neural network differs from a multilayer feedforward neural network in that it has at least one feedback loop, which represents the dynamical characteristics of the network. For example, a recurrent network may consist of a single layer of neurons with each neuron feeding its output signals back to the inputs of all the other neurons. In this structure, there are no *self-feedback* loops in the network. Selffeedback refers to a situation where the output of a neuron is fed back to its own input. The feedback connections originate from the hidden neurons as well as the output neurons. The presence of feedback loops has a profound influence on the learning capability of the network and on its dynamical performance. Moreover, the feedback loops involve the use of special branches composed of unit-delay elements, which result in nonlinear dynamical behavior by virtue of the nonlinear nature of the neurons. Nonlinear dynamics plays a key role in the storage function of a recurrent network.

The Hopfield network is a typical recurrent network that is well known for its capability of storing information in a dynamically stable configuration. It was Hopfield's paper in 1982, elaborating the remarkable physical capacity for storing information in a dynamically stable network, that sparked off the research on neural networks on the eighties. One of the most fascinating findings of his paper is the realization of the associative memory properties. This has now become immensely useful for pattern recognition.

Physically, the Hopfield network operates in an unsupervised fashion. Thus, it may be used as a content addressable memory or as a computer for solving optimization problems of a combinatorial kind. The classical traveling-salesman problem is a typical example. Koch applied Hopfield networks to the problem of vision. There has been other work on depth computation and on reconstructing and smoothing images.

In tackling a combinatorial optimization problem we are facing a discrete system that has an extremely large but finite number of possible solutions. The task is to find one of the optimal solutions through minimizing a cost function, which provides a measure of system performance. The Hopfield network requires time to converge to an equilibrium condition. The time required depends on the problem

size and the possible stability problem. Hence it is never used online unless special-purpose hardware is available for its implementation.

The operational procedure for the Hopfield network may be summarized as follows:

- *Storage (Learning)*. Let $\varepsilon_1, \varepsilon_2 \dots \varepsilon_p$ denote a known set of N -dimensional memories. Construct the network by using the outer-product rule to compute the synaptic weights of the network as

$$w_{ji} = \begin{cases} \frac{1}{N} \sum_{\mu=1}^p \varepsilon_{\mu,j} \varepsilon_{\mu,i}, & \text{for } j \neq i \\ 0, & \text{for } j = i \end{cases}$$

Where w_{ji} is the synaptic weight from neuron i to neuron j . The elements of the vector $\varepsilon_{\mu} = \pm 1$. Once they are determined, the synaptic weights are kept fixed.

- *Initialization*. Let X denote an unknown N -dimensional input vector presented to the network. The algorithm is initialized by setting

$$s_j(n+1) = \text{sgn} \left(\sum_{i=1}^N w_{ji} s_i(n) \right)$$

Repeat until the state vector s remains unchanged.

- *Outputting*. Let s_f denote the fixed point (stable state) computed at the end of step 3. The resulting output vector y of the network is

$$y = s_f$$

It is clear that a neural network is a massively parallel-distributed network that has a natural capacity for storing experimental knowledge and making it available for use.

The primary characteristics of knowledge representation are twofold: what information is actually made explicit, and how the information is physically encoded. In real-world applications of intelligent machines, neural networks represent a special and versatile class of modeling techniques that are significantly different from conventional mathematical models. Neural networks also offer a convenient and reliable approach for the modeling of highly nonlinear multiinput-multioutput systems.

Bibliography

- Stephen Wiggins, Texts in applied Mathematics, *Introduction to Applied Nonlinear Dynamical Systems and Chaos*, Springer, second edition
- Alfredo Medio, and Marji Lines, *Nonlinear Dynamics , A Primer*, Cambridge University Press, 2003
- A. Wolfe, J. B. Swift, H. L. Swinney, and J. A. Vastano, *Determining Lyapunov exponents from a time series*, 1985
- B. Mandelbrot, *The Fractal Geometry of Nature*. New York: Freeman, 1982
- P. Grassberger and I. Procaccia, Characterization of strange attractors. *Phys. Rev. Letters*, 1983
- Packard, J. P. Crutchfield, J. D. Farmer, and R. S. Shaw, Geometry from a time series. *Phys. Rev. Letters* 1980
- Benettin, L. Galgani, A. Giorgilli, and J.-M. Strelcyn, Lyapunov characteristic exponents for smooth dynamical systems: A method for computing all of them, 1980
- D. Holton and R. M. May, Distinguishing chaos from noise. In *The Nature of Chaos*, Chap.7, Oxford University Press, 1993
- W. Liebert and H. G. Schuster, Proper choice of the time delay for the analysis of chaotic time series. *Phys. Letters*, 1989
- R. Noack, F. Ohle, and H. Eckelmann, Construction and analysis of differential equations from experimental time series of oscillatory systems, 1992
- E. Ott and M. Spano, Controlling chaos. *Phys. Today* May, 1995
- Stephen H. Strogatz, *Studies in Nonlinearty, Nonlinear Dynamics and Chaos, With Applications to physics, biology, chemistry and engineering*, Perseus Books
- James Gleich, *Chaos, A new Science*
- R. Kabala, K.spingarn, L. Tesfatsion, A new differential Equation method for finding the peron root of a positive matrix, 1980
- Holger Schanz, Marc-Felix Otto, Roland Ketzmerick, and Thomas Dittrich, *Classical and Quantum Hamiltonian Ratchets*, *Physical Review Letters*, july 2001
- Moritz Hiller, Tsampikos Kottos, and T. Geisel. Complexity in parametric Bose-Hubbard Hamiltonians and structural analysis of eigenstates, , *Physical Review Letters*, June 2006
- T. Geisel, R. Ketzmerick, and G. Petschel, Metamorphosis of a cantor Spectrum Due to Classical Chaos, *Physical Review Letters*, December 1991
- Sven Jahnke^{1,2*}, Raoul-Martin Memmesheimer³ and Marc Timme, How chaotic is the balanced state, frontiers in computational neuroscience, November 2009
- Holger Schanz, Phase-Space Correlations of Chaotic Eigenstates, *Physical Review Letters*, april 2005
- Stefan Großkinsky, Marc Timme, and Björn Naundorf, Universal Attractors of Reversible Aggregate-Reorganization Processes, *Physical Review Letters*, June 2002
- Nonlinear Dynamics and systems theory, An international journal of research and survey
- Li and Yorke, "Period three implies chaos", 1975
- Zonghua Liu, Chaotic Time Series Analysis, review article, 2010
- Murray Frank, Thanasis Stengos, Chaotic Dynamics in economic time-series, journal of economic surveys, Vol. 2, No. 2, 1988
- Francesco camastra, and alessandro Vinciarelli, Intristic Dimension Estimation of Data: An approach based on grassberger-Procaccia's algorithm, *Neural Processing Letters*, 2001
- MA Hong-guang, HAN Chong-zhao, Selection of Embedding Dimension and Delay Time in Phase Space Reconstruction, *Front. Electr. Electron. Eng. China*, 2006
- J.P. Eckmann, S. Oliffson Kamphorst, D. Ruelle, S.Ciliberto, Liapunov Exponents from time series, *Physical Review Letters*, 1986
- A.M. Albano, P.E. Rapp, A. Passamante, Kolmogorov-Smirnov test Distinguishes attractors with similar dimensions, *Physical review*, July 1995
- Peter Grassberger, and Itamar Procaccia, Characterization of strange attractors, *Physical Review Letters*, January 1981

- Peter Grassberger, and Itamar Procaccia, Measuring the strangeness of attractors, *Physica 9D*, 1983
- J.G.Caputo, P. Atten, Metric Entropy: An Experimental means for characterizing and quantifying Chaos
- P. Bryant, R. Brown, H.D.I Abarbanel, Lyapunov exponents from observed time series, *Physical review letters*, September 1990
- P.Grassberger, Itamar Procaccia, Estimation of the Kolmogorov entropy from a chaotic signal, *physical review letters*, October 1983
- A.M. Albano, J.Muench, C.Schwartz,A.I.Mees, P.E.Rapp, Singular value decomposition and the grassberger-procaccia algorithm, *physical review letters*, September 1988
- H.G. Schuster, S.Martin, W. Martienssen, New Method for determining the largest Liapunov exponent of simple nonlinear systems, *Physical review letters*, may 1986
- Ph. Holmes, Ninety plus thirty years of nonlinear dynamics, 2005
- Bruce Henry, Nigel Lovell, and Fernando Camacho, nonlinear dynamics time series analysis
- P. Grassberger, Itamar Procaccia, Measuring the strangeness of strange attractors, *Physica 9D*, May 1983
- R.Kalaba, K. Spingarn, L. Tesfatsion, Variational Equations for the eigenvalues and eigenvectors of nonsymmetric matrices, *Journal of optimization theory and applications*, Vol.33, January 1981
- C. E. Shannon, *Mathematical Theory of Communication*, 1948
- K. Josic, Invariant Manifolds and Synchronization of Coupled Dynamical Systems, *Physical Review Letters*, April 1998
- E. McSharry, Leonard A. Smith, Consistent nonlinear dynamics: identifying model inadequacy, *Physica D*, January 2004
- J.H. Liu, A first course in the qualitative theory of differential equations, James Madison University, Pearson Education, Inc, 2003
- Mario di Bernardo,C. Budd, A. Champneys, P. Kowalczyk, Bifurcation and chaos in piecewise smooth dynamical systems, theory and applications, Springer
- Ewa Skubalska-Rafajłowicz, A new method of estimation of the box-counting dimension of multivariate objects using space-filling curves, 2005
- N.H.Packard, J.P. Crutchfield, J.D. Farmer, R.S. Shaw, Geometry from a Time Series, *Physical Review Letters*, 1979
- D. E. Thompson, *Design Analysis: Mathematical Modeling of Nonlinear Systems*, New York, Cambridge Univ. Press, 1999
- J. L. Casti, *Nonlinear System Theory*, Orlando, Academic Press, 1985
- P. N. Paraskevopoulos, A. S. Tsirikos, K. G. Arvanitis, A new orthogonal series approach to state space analysis of bilinear systems, *IEEE Trans. Automat. Control*, 1994.
- S. Chen, S. A. Billings, Representation of nonlinear systems: the NARMA model, *Int. J. Control*, 1989
- I. J. Leontaritis, S. A. Billings, Input-output parametric models for non-linear systems, deterministic non-linear systems, *Int. J. Control*, 1985.
- J. J. Hopfield, Learning algorithm and probability distributions in feed-forward and feed-back networks, *Proc. Nat. Acad. Sci.*, 1987
- K. Hornik, M. Stinchcombe, H. White, Multilayer feedforward networks are universal Approximators, *Neural Networks*, 1989
- H.-Z. Tan, T. W. S. Chow, Blind identification of quadratic nonlinear models using neural networks with higher-order cumulants, *IEEE Trans. Ind. Electron*, 2000
- J. Y. F. Yam, T. W. S. Chow, A weight initialization method for improving training speed in feedforward neural network, *Neurocomputing*, 1999.
- J. Y. F. Yam, T. W. S. Chow, C. T. Leung, A new method in determining initial weights of feedforward neural networks for training enhancement, *Neurocomputing*, 1997.
- J. J. Hopfield, Neural networks and physical systems with emergent collective properties, *Proc. Nat. Acad. Sci. U.S.A.*, 1982
- H.-Z. Tan, Y. Fang, T. W. S. Chow, Wiener models identification based on the higher-order cumulants and orthogonal wavelet neural networks, 1999
- Guckenheimer, J. & Holmes, *Nonlinear Oscillations, Dynamical Systems and Bifurcations of*

Vector Fields, Springer, NY, 1983.

D. Puthankattil Subha, Paul K. Joseph, Rajendra Acharya, Choo Min Lim, EEG Signal Analysis: A Survey, Springer, 2008

Ewa Skubalska-Rafajlowicz, A new method of estimation of the box-counting dimension of multivariate objects using space-filling curves, Nonlinear Analysis, 2005

Παράρτημα Α

Solution of linear differential equations

we want to solve differential equation of the form

$$\dot{x} = Ax \quad (1)$$

with an initial condition x_0 at time t_0

Theorem: if we can find any two linearly independent solutions (one is a constant multiple of the other).

$$x = x_1(t), \quad y = y_1(t) \quad \text{and} \quad x = x_2(t), \quad y = y_2(t) \quad (2)$$

then the general solution of the system of equations (1) starting from any given initial condition is

$$\begin{aligned} x &= c_1 x_1(t) + c_2 x_2(t) \\ y &= c_1 y_1(t) + c_2 y_2(t) \end{aligned} \quad (3)$$

where the constants c_1 and c_2 are given by the initial condition.

Notice that in (1), A operates on the vector x to give the vector \dot{x} . Generally the derived vector is different from the source vector, both in magnitude and direction.

Eigenvector: special directions in the state space such that if the vector x is in that direction, the resultant vector \dot{x} also lies along the same direction. It only gets stretched or squeezed.

Eigenvalue: the factor by which any eigenvector expands or contracts when it is operated on by the matrix A.

When the matrix A operates on the vector x and if x happens to be an eigenvector, then we can write

$$Ax = \lambda x$$

where λ is the eigenvalue. This yields

$$(A - \lambda I)x = 0$$

where I is the identity matrix of the same dimension as A. this condition would be satisfied if the determinant

$$|A - \lambda I| = 0$$

thus

$$\begin{aligned} \begin{vmatrix} A_{11} & A_{12} \\ A_{21} & A_{22} \end{vmatrix} - \begin{vmatrix} \lambda & 0 \\ 0 & \lambda \end{vmatrix} &= 0 \\ (A_{11} - \lambda)(A_{22} - \lambda) - A_{12}A_{21} &= 0 \\ \lambda^2 - (A_{11} + A_{22})\lambda + (A_{11}A_{22} - A_{12}A_{21}) &= 0 \end{aligned}$$

this is called the characteristic equation, whose roots are the eigenvalues. Thus, for a 2x2 matrix one gets a quadratic equation - which in general yields 2 eigenvalues.

finding eigenvectors: by the definition of eigenvector

$$Ax = \lambda_1 x$$

$$(A - \lambda_1 I)x = 0$$

$$\begin{bmatrix} A_{11} - \lambda_1 & A_{12} \\ A_{21} & A_{22} - \lambda_1 \end{bmatrix} \begin{bmatrix} x \\ y \end{bmatrix} = 0$$

this leads to the 2 equations

$$(A_{11} - \lambda_1)x + A_{12}y = 0 \quad (4)$$

$$A_{21}x + (A_{22} - \lambda_1)y = 0$$

these two equations always turn out to be identical.

Summary

Eigenvalues are obtained by solving the equation

$$|A - \lambda I| = 0$$

and the eigenvectors are obtained, for each real eigenvalue from the equation

$$(A - \lambda I)x = 0$$

Using eigenvectors to solve Differential Equations

The definition of eigenvector tells us that if an initial condition is located on an eigenvector, then the \dot{x} vector remains along the same eigenvector and therefore the whole solution also remains along the eigenvector.

The equation (4) may yield 3 different types of results

1. eigenvalues real and distinct
2. eigenvalues complex conjugate
3. eigenvalue real and equal

Let λ_1 and λ_2 be eigenvalues, v_1 and v_2 be eigenvectors. If we place an initial condition on v_1 then

$$\dot{x} = Av_1 = \lambda_1 v_1$$

Dynamics is constrained along the eigendirection. This is like a 1D differential equation

$$\dot{x} = \lambda x$$

whose solution is

$$x(t) = e^{\lambda t} x_0$$

therefore the solution of the differential equation $\dot{x} = \lambda_1 v_1$ along the eigendirection is

$$x_1(t) = e^{\lambda_1 t} v_1$$

Similarly, for any initial condition placed along v_2 we have another solution

$$x_2(t) = e^{\lambda_2 t} v_2$$

therefore the general solution can be constructed as

$$x(t) = e^{\lambda_1 t} v_1 + e^{\lambda_2 t} v_2 \quad (5)$$

Example

Let the system Equations be given by

$$\dot{x} = \begin{bmatrix} \dot{x} \\ \dot{y} \end{bmatrix} = \begin{bmatrix} -4 & -3 \\ 2 & 3 \end{bmatrix} \begin{bmatrix} x \\ y \end{bmatrix} \quad (6)$$

the matrix A has eigenvalues $\lambda_1 = 2$ and $\lambda_2 = -3$. For λ_1 , the eigenvector is given by $2x = -y$. To choose any point on the eigenvector, set $x = 1$. This gives $y = -2$. Thus

$$v_1 = \begin{bmatrix} 1 \\ -2 \end{bmatrix}$$

For this initial condition the solution is

$$x_1(t) = e^{2t} \begin{bmatrix} 1 \\ -2 \end{bmatrix}$$

similarly for $\lambda_2 = -3$ the eigenvector is $x = -3y$. To choose a point on this eigenvector take $x = 3$. This gives $y = -1$. Thus the second eigenvector becomes

$$v_2 = \begin{bmatrix} 3 \\ -1 \end{bmatrix}$$

and the solution along the eigenvector becomes

$$x_2(t) = e^{-3t} \begin{bmatrix} 3 \\ -1 \end{bmatrix}$$

Hence the general solution of the system of differential equation is

$$x(t) = c_1 e^{2t} \begin{bmatrix} 1 \\ -2 \end{bmatrix} + c_2 e^{-3t} \begin{bmatrix} 3 \\ -1 \end{bmatrix}$$

where the constants c_1 and c_2 are to be determined by the initial condition.

For example, if the initial condition is $(1,1)$ at $t = 0$, then this equation gives

$$c_1 \begin{bmatrix} 1 \\ -2 \end{bmatrix} + c_2 \begin{bmatrix} 3 \\ -1 \end{bmatrix} = \begin{bmatrix} 1 \\ 1 \end{bmatrix}$$

solving, we get $c_1 = -\frac{4}{5}e^{2t}$ and $c_2 = \frac{3}{5}$. Thus the solution of the differential equation with this initial condition is

$$x(t) = -\frac{4}{5}e^{2t} \begin{bmatrix} 1 \\ -2 \end{bmatrix} + \frac{3}{5}e^{-3t} \begin{bmatrix} 3 \\ -1 \end{bmatrix}$$

or, in terms of the individual coordinates

$$x(t) = -\frac{4}{5}e^{2t} + \frac{9}{5}e^{-3t}, \quad y(t) = \frac{8}{5}e^{2t} - \frac{3}{5}e^{-3t}$$

Eigenvalues complex conjugate

Complex eigenvalues always occur as complex conjugate pairs. If $\lambda = \sigma + j\omega$ is an eigenvalue then $\bar{\lambda} = \sigma - j\omega$ is also an eigenvalue. let v be an eigenvector corresponding to the eigenvalue $\lambda = \sigma + j\omega$. This is a complex-valued vector. It is easy to check that \bar{v} , the conjugate of the vector v , is associated with the eigenvalue $(\sigma - j\omega)$.

Though complex-valued eigenvectors cannot represent any specific direction in the real-valued state space, their physical significance derives from the fact that the eigenvector equation $Av = \lambda v$ holds.

This allows us to obtain a solution as

$$x_1(t) = e^{\lambda t} v \quad (7)$$

Here the left hand side is a real-valued function and the right hand side is a complex-valued, expressible in the form $(P + jQ)$ which is a linear combination of the functions P and Q.

therefore the real part and the imaginary part must individually be solutions of the differential equation. This allows us to write two real-valued solutions from which the general solution can be constructed.

--

Let us illustrate this with the system of equations

$$\begin{aligned} \dot{x} &= \sigma x - \omega y \\ \dot{y} &= \omega x + \sigma y \end{aligned} \quad (8)$$

for which the eigenvalues are $\sigma \pm j\omega$. For $\lambda = \sigma + j\omega$ the eigenvector equation is

$$\begin{bmatrix} -j\omega & -\omega \\ \omega & -j\omega \end{bmatrix} \begin{bmatrix} v_1 \\ v_2 \end{bmatrix} = \begin{bmatrix} -j\omega v_1 & -\omega v_2 \\ \omega v_1 & -j\omega v_2 \end{bmatrix} = \begin{bmatrix} 0 \\ 0 \end{bmatrix}$$

Thus the eigenvector direction is given by $v_1 = jv_2$. To choose a specific eigenvector, we take $v_1 = 1$, so that $v = [j, 1]^T$ is an eigenvector.

Thus a complex-valued solution is

$$\begin{aligned} x(t) &= e^{(\sigma+j\omega)t} \begin{bmatrix} j \\ 1 \end{bmatrix} = e^{\sigma t} (\cos \omega t + j \sin \omega t) \begin{bmatrix} j \\ 1 \end{bmatrix} = \\ &= e^{\sigma t} \begin{bmatrix} j \cos \omega t - \sin \omega t \\ \cos \omega t + j \sin \omega t \end{bmatrix} = e^{\sigma t} \left[\begin{pmatrix} -\sin \omega t \\ \cos \omega t \end{pmatrix} + j \begin{pmatrix} \cos \omega t \\ \sin \omega t \end{pmatrix} \right] \quad (9) \end{aligned}$$

which is a linear combination of the real part and the imaginary part. Hence the two linearly independent real-valued solutions are

$$e^{\sigma t} \begin{pmatrix} -\sin \omega t \\ \cos \omega t \end{pmatrix} \text{ and } e^{\sigma t} \begin{pmatrix} \cos \omega t \\ \sin \omega t \end{pmatrix}$$

therefore the general solution is

$$x(t) = c_1 e^{\sigma t} \begin{pmatrix} -\sin \omega t \\ \cos \omega t \end{pmatrix} + c_2 e^{\sigma t} \begin{pmatrix} \cos \omega t \\ \sin \omega t \end{pmatrix} \quad (10)$$

The other eigenvalue supplies no new information, as it is the complex conjugate of the first one.

As a final check, one can differentiate $x(t)$ and $y(t)$ from (10) to obtain back (8), which would imply that (10) is a really solution for (8).

The case of imaginary roots is a special case of this solution where $\sigma = 0$. Thus the solutions for imaginary eigenvalues $\lambda = \pm j\omega$ are

$$\begin{aligned} x(t) &= -c_1 \sin \omega t + c_2 \cos \omega t \\ y(t) &= c_1 \cos \omega t + c_2 \sin \omega t \quad (11) \end{aligned}$$

Here also, the values of c_1 and c_2 have to be obtained from the initial condition.

To illustrate, let an initial condition be (1,0), Substituting this value of x at $t = 0$ in (11) we get $c_1 = 0$ and $c_2 = 1$. Thus the trajectory is given by

$$x(t) = \cos \omega t \text{ and } y(t) = \sin \omega t$$

Thus each state variable follows a sinusoidal variation, while $y(t)$ lags behind $x(t)$ by $\frac{\pi}{2}$.

Eigenvalues are real and equal

We have only one real-valued eigenvector v associated with the eigenvalue λ . So we have only one solution

$$x_1(t) = e^{\lambda t} v$$

In this case the rule is to look for a second solution of the form

$$x_2(t) = e^{\lambda t} \begin{bmatrix} A_1 + A_2 t \\ B_1 + B_2 t \end{bmatrix} \quad (12)$$

so that the general solution is

$$x(t) = c_1 e^{\lambda t} \begin{bmatrix} v_1 \\ v_2 \end{bmatrix} + c_2 e^{\lambda t} \begin{bmatrix} A_1 + A_2 t \\ B_1 + B_2 t \end{bmatrix} \quad (13)$$

Example

Let

$$\begin{aligned} \dot{x} &= 3x - 4y \\ \dot{y} &= x - y \end{aligned} \quad (14)$$

Here both the eigenvalues are equal to 1. For this eigenvalue the eigenvector equation is $x = 2y$, so that an eigenvector $v = [2, 1]^T$. Thus one nontrivial solutions is

$$x_1(t) = e^t v$$

we now seek another solution of the form (12) with $\lambda = 1$ substituting this into (14) we get

$$\begin{aligned} (A_1 + A_2 t + A_2) e^t &= 3(A_1 + A_2 t) e^t - 4(B_1 + B_2 t) e^t \\ (B_1 + B_2 t + B_2) e^t &= (A_1 + A_2 t) e^t - (B_1 + B_2 t) e^t \end{aligned}$$

this reduces to

$$\begin{aligned} (2A_1 - A_2 - 4B_1) + (2A_2 - 4B_2)t &= 0 \\ (A_1 - 2B_1 - B_2) + (A_2 - 2B_2)t &= 0 \end{aligned}$$

Since these equations must hold independent of t , each term in the above equations must be zero. Hence

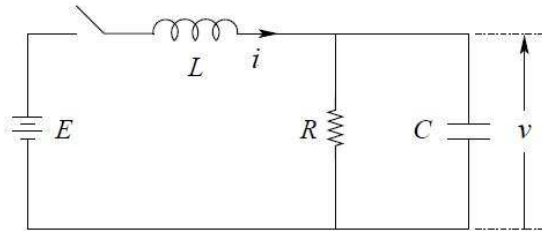
$$\begin{aligned} (2A_1 - A_2 - 4B_1) &= 0, & (A_1 - 2B_1 - B_2) &= 0 \\ (2A_2 - 4B_2) &= 0, & (A_2 - 2B_2) &= 0 \end{aligned}$$

solving these, we have $A_1 - 2B_1 = 1$, $A_2 = 2$, and $B_2 = 1$. since we can take any values of A_1 and B_1 satisfying these equations, we take $A_1 = 1$ and $B_1 = 0$. This gives another linearly independent solution of (14) as

$$x_2(t) = e^t \begin{bmatrix} 1 + 2t \\ t \end{bmatrix}$$

hence the general solution of (14) is

$$x(t) = c_1 e^t \begin{bmatrix} 2 \\ 1 \end{bmatrix} + c_2 e^t \begin{bmatrix} 1 + 2t \\ t \end{bmatrix}$$

Example


KCL gives:

$$i = i_R + i_C = \frac{u}{R} + C \frac{du}{dt} \quad \text{or} \quad \frac{du}{dt} = \frac{i}{C} - \frac{u}{RC}$$

KVL gives:

$$E = L \frac{di}{dt} + u \quad \text{or} \quad \frac{di}{dt} = \frac{E}{L} - \frac{u}{L}$$

In matrix form:

$$\begin{bmatrix} \dot{u} \\ \dot{i} \end{bmatrix} = \begin{bmatrix} -\frac{1}{RC} & \frac{1}{C} \\ -\frac{1}{L} & 0 \end{bmatrix} \begin{bmatrix} u \\ i \end{bmatrix} + \begin{bmatrix} 0 \\ \frac{1}{L} \end{bmatrix} E$$

The second order equation can be obtained in terms of u or i . Differentiating the first equation,

$$\frac{d^2u}{dt^2} = \frac{1}{C} \frac{di}{dt} - \frac{1}{RC} \frac{du}{dt} = \frac{1}{LC} (E - u) - \frac{1}{RC} \frac{du}{dt} \quad \text{or,} \quad \frac{d^2u}{dt^2} + \frac{1}{RC} \frac{du}{dt} + \frac{1}{LC} u = \frac{1}{LC} E$$

We first take the homogenous part:

$$p_1, p_2 = -\frac{1}{2RC} \pm \frac{1}{2} \sqrt{\frac{1}{R^2C^2} - \frac{4}{LC}}$$

The critical value of the resistance is given by

$$\frac{1}{R^2C^2} = \frac{4}{LC} \quad \text{or,} \quad R_{cr} = \sqrt{\frac{L}{2C}}$$

The undamped ($R = 0$) natural frequency of oscillation

$$\omega_n = \frac{1}{\sqrt{LC}}$$

Now we mould the equation in the form

$$\ddot{u} + 2\zeta\omega_n\dot{u} + \omega_n^2 u = 0$$

Which demands that

$$2\zeta\omega_n = \frac{1}{RC} \quad \text{or,} \quad \zeta = \frac{1}{2R} \sqrt{\frac{L}{C}}$$

Notice that in this case we have to define ζ as $\frac{R_{cr}}{R}$.

Now let us look at it from the point of view of the homogenous first order equations $\dot{x} = Ax$:

$$\begin{bmatrix} \dot{u} \\ \dot{i} \end{bmatrix} = \begin{bmatrix} -\frac{1}{RC} & \frac{1}{C} \\ -\frac{1}{L} & 0 \end{bmatrix} \begin{bmatrix} u \\ i \end{bmatrix}$$

To calculate the eigenvalues, $|A - \lambda I| = 0$.

$$\begin{bmatrix} -\frac{1}{RC} & \frac{1}{C} \\ -\frac{1}{L} & 0 \end{bmatrix} - \begin{bmatrix} \lambda & 0 \\ 0 & \lambda \end{bmatrix} = 0 \text{ or, } \begin{bmatrix} -\frac{1}{RC} - \lambda & \frac{1}{C} \\ -\frac{1}{L} & -\lambda \end{bmatrix} = 0$$

This gives

$$\lambda^2 + \frac{1}{RC}\lambda + \frac{1}{LC} = 0$$

Which is the same equation as derived in the 2nd order case. Therefore the eigenvalues are the same as the roots of the characteristic equation.

$$\lambda_1, \lambda_2 = -\frac{1}{2RC} \pm \frac{1}{2} \sqrt{\frac{1}{R^2C^2} - \frac{4}{LC}}$$

In terms of ζ and ω_n the eigenvalues are:

$$\lambda_1, \lambda_2 = -\zeta\omega_n \pm \omega_n\sqrt{\zeta^2 - 1}$$

The eigenvalues will be real for $\zeta > 1$ and complex conjugate for $\zeta < 1$.

Now let $L=1H$, $C=1F$ and $R=0.25\Omega$, for which the eigenvalues are real : $\lambda_1 = -0.268$ and $\lambda_2 = -3.732$. Substituting the parameter values we have $\dot{x} = Ax$ as

$$\begin{bmatrix} \dot{u} \\ \dot{i} \end{bmatrix} = \begin{bmatrix} -\frac{1}{RC} & \frac{1}{C} \\ -\frac{1}{L} & 0 \end{bmatrix} \begin{bmatrix} u \\ i \end{bmatrix} = \begin{bmatrix} -4 & 1 \\ -1 & 0 \end{bmatrix} \begin{bmatrix} u \\ i \end{bmatrix}$$

First take $\lambda_1 = -0.268$ and calculate its corresponding eigenvector.

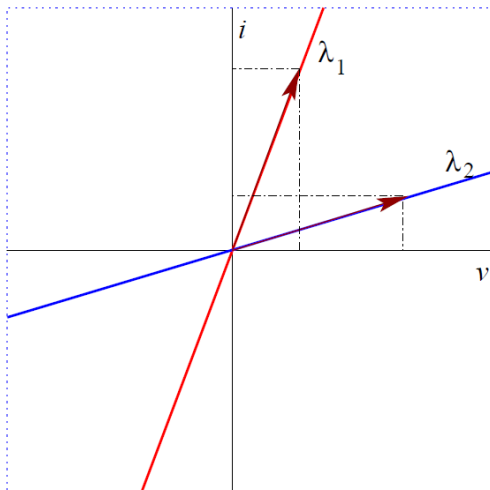
$$\begin{bmatrix} -4 + 0.268 & 1 \\ -1 & 0.268 \end{bmatrix} \begin{bmatrix} u \\ i \end{bmatrix} = \begin{bmatrix} 0 \\ 0 \end{bmatrix}$$

The two lines give

$$-3.732u + i = 0 \text{ and } -u + 0.268i = 0$$

These are identical equations, giving the eigenvector $u = 0.268i$. Similarly, for the other eigenvalue $\lambda_2 = -3.732$ we get the eigendirection $u = 3.732i$.

Now, we select specific (arbitrary) eigenvectors along the eigendirections. Choose $i = 1A$ and $u = 0.268V$ as the first eigenvector and $u = 1V$ and $i = 0.268A$ along the second.



The solution is straightforward obtained as

$$\begin{bmatrix} u \\ i \end{bmatrix} = c_1 e^{-0.268t} \begin{bmatrix} 0.268 \\ 1 \end{bmatrix} + c_2 e^{-3.732t} \begin{bmatrix} 1 \\ 0.268 \end{bmatrix}$$

c_1 and c_2 are to be obtained from the initial conditions.

Now take $L = 1H, C = 1F$ and $R = 1\Omega$ for which the eigenvalues are complex conjugate:

$$\lambda_{1,2} = -\frac{1}{2} \pm j \frac{\sqrt{3}}{2}$$

Substituting the parameter values we have $\dot{x} = Ax$ as

$$\begin{bmatrix} \dot{u} \\ \dot{i} \end{bmatrix} = \begin{bmatrix} -\frac{1}{RC} & \frac{1}{C} \\ \frac{1}{L} & 0 \end{bmatrix} \begin{bmatrix} u \\ i \end{bmatrix} = \begin{bmatrix} -1 & 1 \\ -1 & 0 \end{bmatrix} \begin{bmatrix} u \\ i \end{bmatrix}$$

First take $\lambda_{1,2} = -\frac{1}{2} \pm j \frac{\sqrt{3}}{2}$ and calculate its corresponding eigenvector.

$$\begin{bmatrix} -1 + \frac{1}{2} - j \frac{\sqrt{3}}{2} & 1 \\ -1 & \frac{1}{2} - j \frac{\sqrt{3}}{2} \end{bmatrix} \begin{bmatrix} u \\ i \end{bmatrix} = \begin{bmatrix} 0 \\ 0 \end{bmatrix}$$